The Geological Society of America
Field Guide 11
2008

Active tectonics of the eastern California shear zone

Kurt L. Frankel*†
School of Earth and Atmospheric Sciences, Georgia Institute of Technology, Atlanta, Georgia 30332, USA

Allen F. Glazner†
Department of Geological Sciences, University of North Carolina, Chapel Hill, North Carolina 27599, USA

Eric Kirby†
Department of Geosciences, Pennsylvania State University, University Park, Pennsylvania 16802, USA

Francis C. Monastero†
Geothermal Program Office, Naval Air Weapons Station, China Lake, California 93555, USA

Michael D. Strane†
Department of Geological Sciences, University of North Carolina, Chapel Hill, North Carolina 27599, USA,
and *William Lettis & Associates, Inc., 27220 Turnberry Lane, Suite 110, Valencia, California 91355, USA*

Michael E. Oskin†
Department of Geological Sciences, University of North Carolina, Chapel Hill, North Carolina 27599, USA

Jeffrey R. Unruh†
William Lettis & Associates, Inc., 1777 Bothelo Drive, Suite 262, Walnut Creek, California 94596, USA

J. Douglas Walker†
Department of Geology, University of Kansas, Lawrence, Kansas 66045, USA

Sridhar Anandakrishnan
Department of Geosciences, Pennsylvania State University, University Park, Pennsylvania 16802, USA

John M. Bartley
Department of Geology and Geophysics, University of Utah, Salt Lake City, Utah 84112, USA

Drew S. Coleman
Department of Geological Sciences, University of North Carolina, Chapel Hill, North Carolina 27599, USA

James F. Dolan
Department of Earth Sciences, University of Southern California, Los Angeles, California 90089, USA

Robert C. Finkel
Center for Accelerator Mass Spectrometry, Lawrence Livermore National Laboratory, Livermore, California 94550, USA

*kfrankel@gatech.edu
†Field trip leader

Frankel, K.L., Glazner, A.F., Kirby, E., Monastero, F.C., Strane, M.D., Oskin, M.E., Unruh, J.R., Walker, J.D., Anandakrishnan, S., Bartley, J.M., Coleman, D.S., Dolan, J.F., Finkel, R.C., Greene, D., Kylander-Clark, A., Morrero, S., Owen, L.A., and Phillips, F., 2008, Active tectonics of the eastern California shear zone, *in* Duebendorfer, E.M., and Smith, E.I., eds., Field Guide to Plutons, Volcanoes, Faults, Reefs, Dinosaurs, and Possible Glaciation in Selected Areas of Arizona, California, and Nevada: Geological Society of America Field Guide 11, p. 43–81, doi: 10.1130/2008.fld011(03).

Dave Greene
Department of Geosciences, Pennsylvania State University, University Park, Pennsylvania 16802 USA

Andrew Kylander-Clark
Department of Geological Sciences, University of North Carolina, Chapel Hill, North Carolina 27599, USA,
and *Department of Earth Sciences, University of California, Santa Barbara, California 93106, USA*

Shasta Marrero
Department of Earth and Environmental Science, New Mexico Institute of Mining and Technology, Socorro, New Mexico 87801, USA

Lewis A. Owen
Department of Geology, University of Cincinnati, Cincinnati, Ohio 45221, USA

Fred Phillips
Department of Earth and Environmental Science, New Mexico Institute of Mining and Technology, Socorro, New Mexico 87801, USA

ABSTRACT

The eastern California shear zone is an important component of the Pacific–North America plate boundary. This region of active, predominantly strike-slip, deformation east of the San Andreas fault extends from the southern Mojave Desert along the east side of the Sierra Nevada and into western Nevada. The eastern California shear zone is thought to accommodate nearly a quarter of relative plate motion between the Pacific and North America plates. Recent studies in the region, utilizing innovative methods ranging from cosmogenic nuclide geochronology, airborne laser swath mapping, and ground penetrating radar to geologic mapping, geochemistry, and U-Pb, $^{40}Ar/^{39}Ar$, and (U-Th)/He geochronology, are helping elucidate slip rate and displacement histories for many of the major structures that comprise the eastern California shear zone. This field trip includes twelve stops along the Lenwood, Garlock, Owens Valley, and Fish Lake Valley faults, which are some of the primary focus areas for new research. Trip participants will explore a rich record of the spatial and temporal evolution of the eastern California shear zone from 83 Ma to the late Holocene through observations of offset alluvial deposits, lava flows, key stratigraphic markers, and igneous intrusions, all of which are deformed as a result of recurring seismic activity. Discussion will focus on the constancy (or non-constancy) of strain accumulation and release, the function of the Garlock fault in accommodating deformation in the region, total cumulative displacement and timing of offset on faults, the various techniques used to determine fault displacements and slip rates, and the role of the eastern California shear zone as a nascent segment of the Pacific–North America plate boundary.

Keywords: faults, neotectonics, earthquakes, slip rates.

INTRODUCTION

The temporal and spatial constancy of fault loading and strain release rates is one of the most fundamental, unresolved issues in modern tectonics. In order to understand how strain is distributed in both time and space across plate boundaries slip rate and displacement data must be compared over a wide range of temporal and spatial scales, from very short-term (tens of years) geodetic data to longer-term (thousands to millions of years) geologic data and from individual fault segments (hundreds to thousand of meters) to entire fault zones (tens to hundreds of kilometers). Such data are critical to unraveling the complex behavior of lithospheric deformation along plate boundaries.

The eastern California shear zone is an ideal natural laboratory in which to study the spatial and temporal evolution of active plate boundary fault systems. As such, the region has been the focus of a number of field-based studies in recent years, each with the goal of unraveling the spatial and temporal histories of fault displacements and slip rates. Results of this research highlight the importance of the eastern California shear zone as a

major piece of the Pacific–North America plate boundary evolution puzzle.

The eastern California shear zone is an evolving component of the Pacific–North America plate boundary system (e.g., Faulds et al., 2005; Wesnousky, 2005). This region of predominantly right-lateral strike-slip faults is thought to accommodate ~20%–25% of total relative motion between the Pacific and North America plates (Bennett et al., 2003; Dixon et al., 2000, 2003; Dokka and Travis, 1990; Hearn and Humphreys, 1998; Humphreys and Weldon, 1994; McClusky et al., 2001; Thatcher et al., 1999). The area of active deformation extends northward from the eastern end of the Big Bend of the San Andreas fault near Palm Springs for ~500 km through the Mojave Desert and along the western edge of the Basin and Range east of the Sierra Nevada (Fig. 1).

In the Mojave Desert, south of the left-lateral Garlock fault, the eastern California shear zone comprises a 100-km-wide network of NNW–trending right-lateral faults. Geodetic data indicate that elastic strain is accumulating across this zone at a rate of 12 ± 2 mm/yr (Savage et al., 1990; Gan et al., 2000; McClusky et al., 2001; Miller et al., 2001; Peltzer et al., 2001). Seismological and paleoseismological data also indicate that this part of the eastern California shear zone releases strain at a relatively rapid rate; portions of several of these faults ruptured during the 1992 moment magnitude (M_w) 7.3 Landers and 1999 M_w 7.1 Hector Mine earthquakes. Moreover, paleoseismologic data indicate that these two earthquakes are part of an ongoing, ≥1000-yr-long seismic cluster (Rockwell et al., 2000). However, such evidence for rapid strain accumulation and release during the recent past is at odds with longer-term slip-rate data, which suggest that the long-term, cumulative slip rate across the Mojave part of the eastern California shear zone is much slower. Recent work in the Mojave section of the eastern California shear zone indicates the total long-term slip rate across this fault system is on the order of 5–7 mm/yr, or about half of the current rate of strain accumulation determined from space-based geodesy (Oskin and Iriondo, 2004; Oskin et al., 2006, 2007) These observations suggest a pronounced strain transient across the Mojave section of the eastern California shear zone.

The Garlock fault bisects the eastern California shear zone, forming a major geologic and physiographic boundary between the Mojave Desert and western Basin and Range (Fig. 1). This fault system began accommodating Pacific–North America plate boundary deformation in the middle to late Miocene and has long been recognized as a major tectonic feature in the region (Burbank and Whistler, 1987; Davis and Burchfiel, 1973; Loomis and Burbank, 1988; Monastero et al., 1997; Smith et al., 2002). Since the late Pleistocene, there has been at least 18 km of offset along the fault, yet little to no significant earthquake activity has occurred over at least the past ~300 yr (Carter, 1980; Dawson et al., 2003; McGill and Sieh, 1991). The Garlock fault is somewhat enigmatic in that nowhere does it appear to offset, or be offset by, NW-trending eastern California shear zone faults. A large question in eastern California shear zone tectonics remains as to how Pacific–North America plate boundary strain is transferred through, or around, the Garlock fault.

Nonetheless, displacement from the southern part of the eastern California shear zone in the Mojave Desert is funneled northward across the Garlock fault onto four main fault systems; the Owens Valley, Panamint Valley–Hunter Mountain–Saline Valley, Death Valley–Fish Lake Valley, and Stateline fault zones (Fig. 1). The only fault in the northern eastern California shear zone to experience significant seismic activity is the Owens Valley fault, which last ruptured in a M_w 7.6(?) earthquake near the town of Lone Pine in 1872 (Beanland and Clark, 1994). A series of down-to-the-NW normal faults transfer slip between the Owens Valley, Panamint Valley–Hunter Mountain–Saline Valley, and Death Valley–Fish Lake Valley faults (Fig. 1; Dixon et al., 1995; Lee et al., 2001a; Reheis and Dixon, 1996). In contrast to the strain transient south of the Garlock, the region-wide rate of dextral shear across these four faults appears to have remained constant at 9–10 mm/yr over late Pleistocene to recent time scales, although large uncertainties in geologic slip rates on the Owens Valley and Panamint Valley–Hunter Mountain–Saline Valley faults make the strain budget somewhat tentative (Bacon and Pezzopane, 2007; Bennett et al., 2003; Frankel et al., 2007a; Lee et al., 2001b; Oswald and Wesnousky, 2002).

Farther north, dextral motion between the Sierra Nevada block and North America is focused on two faults bounding the east and west sides of the White Mountains: the White Mountains fault zone to the west and the Fish Lake Valley fault zone to the east. Of these two, global positioning system (GPS) data suggest that the Fish Lake Valley fault system is storing at least 75% of the elastic strain accumulating in this region (Dixon et al., 2000). However, recent late Pleistocene slip rate studies on these two faults reveal a geologic versus geodetic rate discrepancy similar to that in the Mojave, whereby the White Mountains and Fish Lake Valley faults account for less than half of the region-wide rate of shear determined from GPS data (Bennett et al., 2003; Frankel et al., 2007b; Kirby et al., 2006).

Until recently, the total displacement on any of the major faults in the eastern California shear zone was thought to be only a few tens of kilometers (Burchfiel et al., 1987; Guest et al., 2007; Moore and Hopson, 1961; Niemi et al., 2001; Ross, 1962). However, the correlation of Jurassic and Cretaceous dikes, Cretaceous leucogranites, and a Devonian submarine channel across Owens Valley suggests that right-lateral deformation, in what is now the eastern California shear zone, is much greater than this and may have started as early as 83 Ma (Bartley et al., 2008; Glazner et al., 2005; Kylander-Clark, 2003; Kylander-Clark et al., 2005). The total dextral component of shear across Owens Valley serves as an important constraint on the timing, duration, and rate of strike-slip deformation throughout the region.

This field guide reviews some of the newest results bearing on displacement and slip rate histories for many of the faults in the eastern California shear zone. We begin with a discussion of temporal variations in rates of deformation across the Mojave Desert, then move on to Miocene to recent slip rate variations

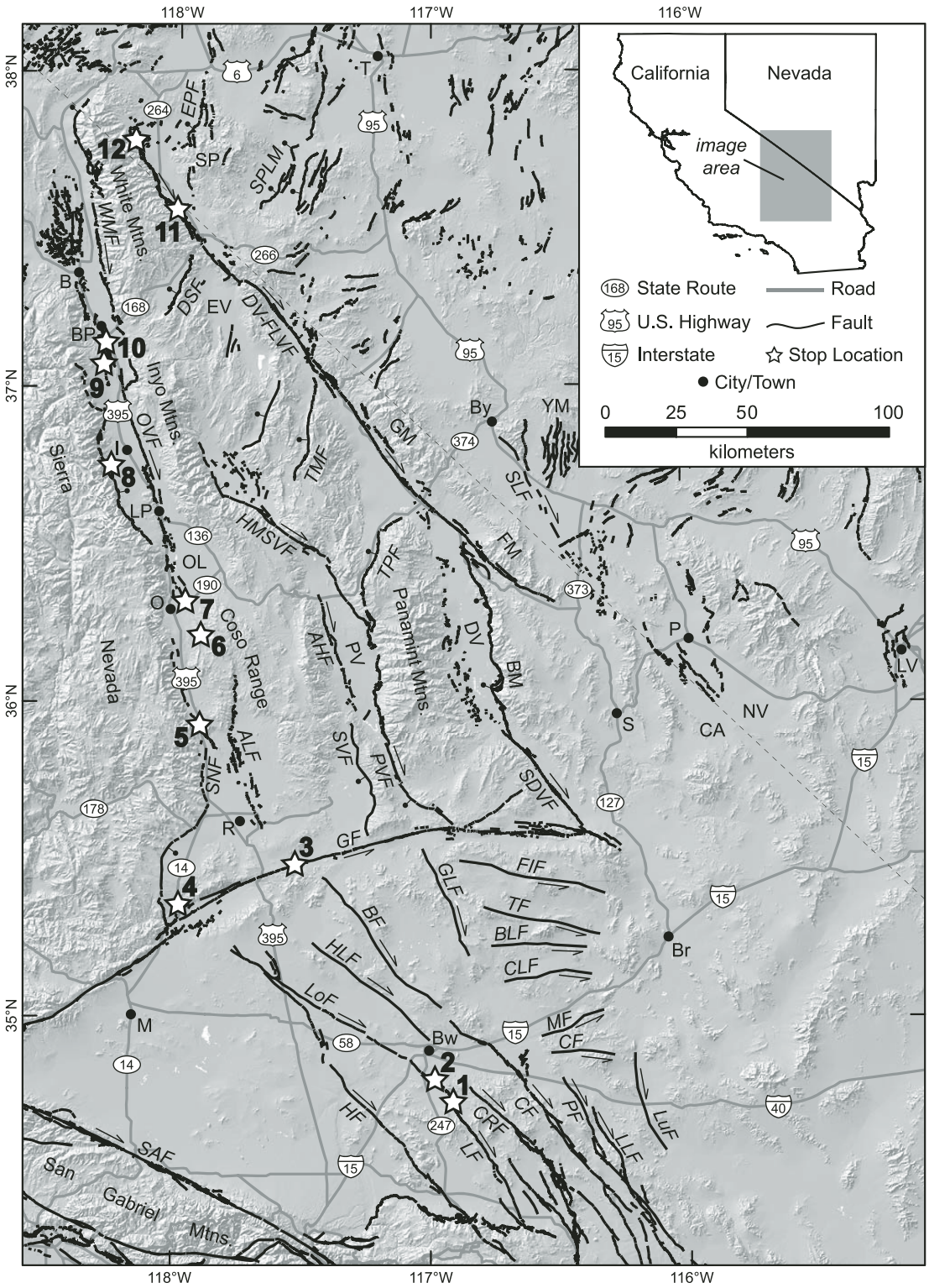

Figure 1. Shaded relief index map of Quaternary faults, roads, towns, and field trip stops in the eastern California shear zone. Most faults are from the U.S. Geological Survey Quaternary fault and fold database (http://earthquake.usgs.gov/regional/qfaults). Arrows indicate relative fault motion for strike slip faults. Bar and circle indicates the hanging wall of normal faults. Field trip stop location numbers are tied to site descriptions in the field guide section. AHF—Ash Hill fault; ALF—Airport Lake fault; B—Bishop; BF—Blackwater fault; BLF—Bicycle Lake fault; BM—Black Mountains; BP—Big Pine; Br—Baker; Bw—Barstow; By—Beatty; CA—California; CF—Cady fault; CLF—Coyote Lake fault; CoF—Calico fault; CRF—Camp Rock fault; DSF—Deep Springs fault; DV-FLVF—Death Valley–Fish Lake Valley fault; EPF—Emigrant Peak fault; EV—Eureka Valley; FIF—Fort Irwin fault; FM—Funeral Mountains; GF—Garlock fault; GFL—Goldstone Lake fault; GM—Grapevine Mountains; HF—Helendale fault; HLF—Harper Lake fault; HMSVF—Hunter Mountain–Saline Valley fault; I—Independence; LF—Lenwood fault; LLF—Lavic Lake fault; LoF—Lockhart fault; LP—Lone Pine; LuF—Ludlow fault; LV—Las Vegas; M—Mojave; MF—Manix fault; NV—Nevada; O—Olancha; OL—Owens Lake; OVF—Owens Valley fault; P—Pahrump; PF—Pisgah fault; PV—Panamint Valley; PVF—Panamint Valley fault; R—Ridgecrest; S—Shoshone; SAF—San Andreas fault; SDVF—southern Death Valley fault; SLF—Stateline fault; SPLM—Silver Peak–Lone Mountain extensional complex; SNF—Sierra Nevada frontal fault; SP—Silver Peak Range; T—Tonopah; TF—Tiefort Mountain fault; TMF—Tin Mountain fault; TPF—Towne Pass fault; WMF—White Mountains fault; YM—Yucca Mountain.

along the Garlock fault, followed by a history of faulting in Owens Valley spanning the past 83 m.y., and finish with a discussion of late Pleistocene slip rates and kinematics of the Death Valley–Fish Lake Valley fault system. The second part of the guidebook serves as a road log to 12 field sites that we feel provide an excellent representation of the Late Cretaceous to late Holocene deformational history of the eastern California shear zone.

ACTIVITY OF THE EASTERN CALIFORNIA SHEAR ZONE ACROSS THE CENTRAL MOJAVE DESERT: EXAMPLE OF THE LENWOOD FAULT

Paleoseismic records from southern California indicate clustering of earthquake activity over millennial time-scales on individual major faults (Garlock: Dawson et al., 2003; San Andreas: Weldon et al., 2004; San Jacinto: Rockwell et al., 2006) and across fault systems (Mojave eastern California shear zone: Rockwell et al., 2000; Los Angeles basin: Dolan et al., 2007). Understanding the origin of such clustered earthquake activity is clearly important for seismic hazard forecasts and also bears on understanding of fault strength and loading processes. Discrepancy between geologic slip rates and short-term loading measured from geodesy can indicate variation in the distribution of loading rate across a system of faults (e.g., Friedrich et al., 2003; Bennett et al., 2004). The Mojave Desert portion of the eastern California shear zone contains well-documented examples of such conditions. The sinistral Garlock fault is undergoing loading at less than half its well-established geologic slip rate of 5–7 mm/yr (McClusky et al., 2001; McGill and Sieh, 1993). Conversely, the Blackwater fault appears to be loading at a rate that is up to an order of magnitude faster than its geologic slip rate (Peltzer et al., 2001; Oskin and Iriondo, 2004).

New evidence from a comprehensive slip-rate investigation across the Mojave Desert section of the eastern California shear zone reveals that the geologic versus geodetic discrepancy exists system-wide (Oskin et al., 2006). New slip rates were determined from mapping of high-resolution airborne laser swath mapping (ALSM) topography and dating of offset features along six dextral faults that comprise the eastern California shear zone at ~34.7°N. From east to west these faults are the Helendale, Lenwood, Camp Rock, Calico, Pisgah-Bullion, and Ludlow (Fig. 1). Based on offset alluvial fans and mid-Quaternary basalt flows, the sum of fault slip-rates across the entire province is at most ~6 ± 2 mm/yr (Oskin et al., 2006). This geologic rate is only half the geodetic rate of 12 ± 2 mm/yr across the province (Sauber et al., 1994; Bennett et al., 2003) but is comparable to that expected from the paleoseismology of Rockwell et al. (2000). This rate discrepancy supports the conclusions of Peltzer et al. (2001) and Dolan et al. (2007) that strain accumulation alternates between different components of the southern California fault system, though the length- and time-scale of such alternation remains to be determined. Consistency of strain release rates measured over ~60 k.y. and ~650 k.y. on the Calico fault (Oskin et al., 2007) and the overall consistency between geologic rates and paleoseismicity suggests that the time-scale of loading variation is shorter than the ~5000 yr return period of Mojave eastern California shear zone earthquake clusters.

The Lenwood Fault

The Lenwood fault is a typical example of the active dextral faults that transect the Mojave Desert region. Total dextral slip on the northern Lenwood fault is only 1.0 ± 0.2 km, based on offset of the Lenwood anticline (Strane, 2007). This offset is consistent with ~1 km displacement of a 7.33 ± 0.12 Ma ($^{40}Ar/^{39}Ar$; A. Iriondo, unpublished data) basalt flow in the Fry Mountains by the southern Lenwood fault (Carleton, 1988). South of the Fry Mountains, the Old Woman Springs fault branches westward from the Lenwood fault. Both fault strands terminate southward at the foot of the San Bernardino Mountains. Similar bifurcations occur approaching southern terminations of other Mojave eastern California shear zone dextral faults (Fig. 1). Slip on the northernmost Lenwood fault diminishes into parasitic folding of the north limb of the Lenwood anticline (Dibblee, 1970) before reemerging as the Lockhart fault (Fig. 1). Geologic and geomorphic mapping of a 48 km^2 ALSM topographic survey by Strane (2007) defined both Miocene and late Quaternary stratigraphy and displacements. This field guide examines two sections of the northern Lenwood fault where Quaternary alluvial fan markers have been deposited across the fault and cut by subsequent dextral slip (Figs. 2 and 3).

Alluvial Fan Ages and Stratigraphy

Quaternary units are subdivided based upon three weathering-related, age-diagnostic criteria (Wells et al., 1987): (1) development of desert varnish and rubification (reddening) on surface clasts, (2) development of desert pavement, and (3) smoothing of depositional bar and swale microtopography. Smoothing over time of depositional alluvial landforms such as bars and channels is especially apparent in comparisons of differently aged surfaces with high resolution topography (e.g., Frankel and Dolan, 2007). In the Mojave Desert region, recognizable bar and swale morphology is generally only present in active washes, but can be preserved in very young alluvial surfaces and is useful for identifying Holocene alluvial fans (Bull, 1991). Dissection also serves to differentiate alluvial surfaces. Generally, the more highly dissected fans are older (Bull, 1991). However, the smoothing effects of soil and pavement development can counteract formation of channels. Based on these criteria, three generations of older alluvial fan deposits are differentiated along the Lenwood fault. The oldest deposit, $Q2_a$, is characterized by a continuous, smooth, well-interlocked desert pavement with angular, darkly varnished and rubified surface clasts. The intermediate deposit, $Q2_b$, has less well-developed pavement and clast coatings. $Q2_b$ can also be differentiated from $Q2_a$ by the presence of well-defined, but shallow incised channels and by the degree of soil development. The youngest deposit, Q3, preserves relict bar and swale topog-

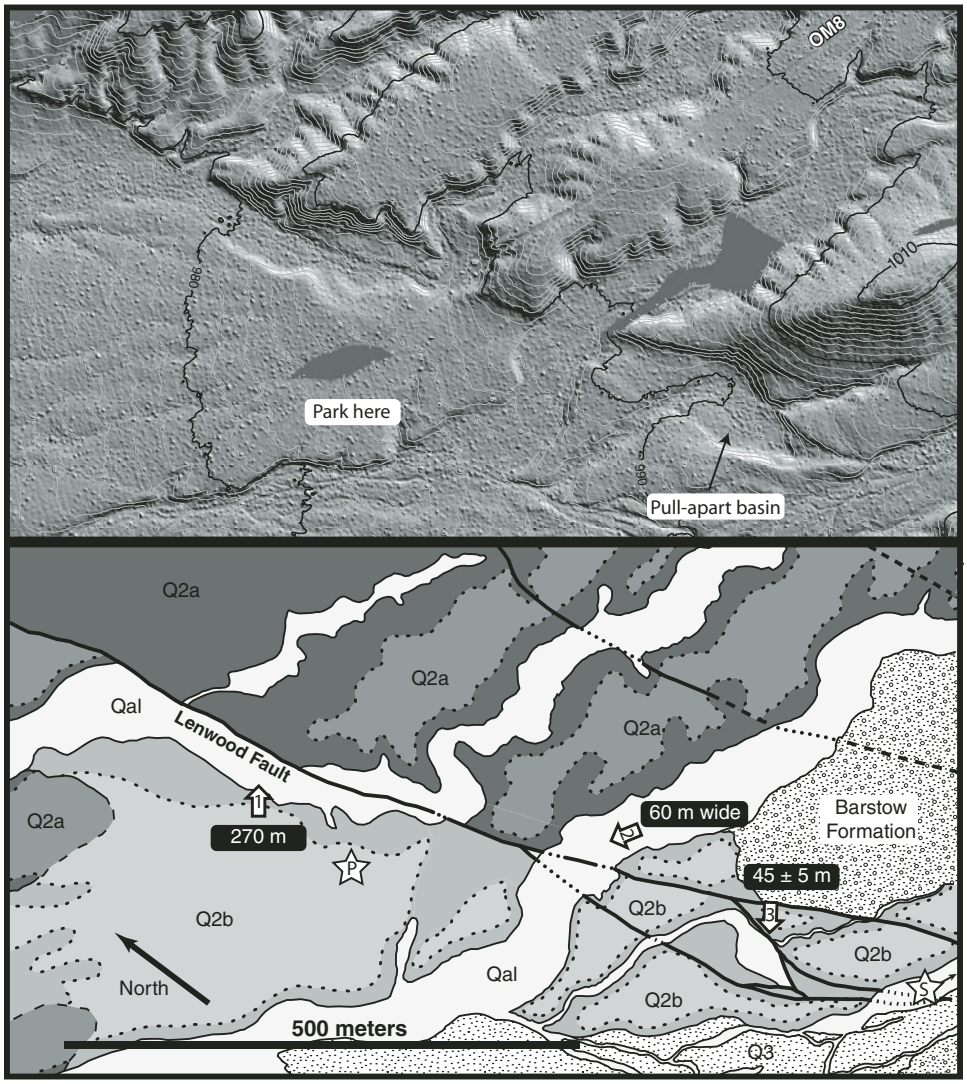

Figure 2. Hillshaded airborne laser swath mapping (ALSM) topography, illuminated from the west (top) and geologic interpretation (bottom) near Stop 1 (Fig. 1), showing stream deflections along the Lenwood fault. Gray patches are gaps in ALSM data. One-meter contours (light gray lines) with 10-m index contours (dark lines, elevations labeled). Middle to late Miocene Barstow Formation consists of poorly consolidated conglomerate at this locality. Arrows: 1—deflection of stream by ~270 m around $Q2_b$ fan. Though modified by faulting, this deflection is interpreted as primarily a result of aggradation of fans derived from the southeast; 2—~60-m-wide stream apparently undeflected by faulting. Slip since emplacement of $Q2_b$ probably does not exceed the width of this stream; 3—Pull-apart basin in $Q2_b$ hosts a small channel that is deflected 45 ± 5 m. Star symbols show locations of ^{10}Be sample pit (P) and modern stream samples (upstream of S).

raphy. Clast coatings are very light and pavement development is mostly absent except for some winnowing of fine materials from relict channels.

Cosmogenic dating using in situ accumulation of ^{10}Be in quartz (e.g., Gosse and Phillips, 2001) yielded a very well-defined age for the $Q2_b$ surface (Fig. 4). Samples of both small quartz pebbles and sand-sized bulk sediments were extracted from a 1.8-m-deep hand-excavated pit located in a large, well-preserved $Q2_b$ alluvial fan. The sample site is situated within the southern field stop (Stop 1; Figs. 1 and 2), where topographic relationships indicated a thick accumulation of $Q2_b$ deposits. This site was found to be characterized by very high ^{10}Be inheritance, equivalent to >60 k.y. of surface-exposure. Interestingly, it was also found that this inheritance varied with grain size (Fig. 4). Despite the high inheritance, the depth-profile approach yielded a very well constrained date of 37 ± 7 ka for the abandonment of the $Q2_b$ alluvial fan depositional surface.

Fault Offsets and Along-Strike Slip Rate Gradients

Offsets of $Q2_b$ alluvial fans and related inset channels are apparent in both the southern and northern field stops (Stops 1 and 2; Figs. 1, 2, and 3), though the northern set of offsets is better defined. Here, combined constraints from a pair of inset channels and a shutter ridge yield an offset of 30 ± 5 m (Fig. 3). Channel deflections in the southern field stop (Stop 1) are complicated by multiple fault strands and fan emplacement along the fault scarp (Fig. 2). Offsets of the larger channels proved difficult to constrain, but must be <60 m. One small channel that crosses a pull-apart basin appears offset 45 ± 5 m. However, it is possible that the channel flowed parallel to the Lenwood fault as the pull-apart basin formed, reducing the amount of slip required. If this amount of slip accrued here since abandonment of the $Q2_b$ alluvial fan, then the slip rate along this portion of the Lenwood fault would be 1.2 ± 0.2 mm/yr, which

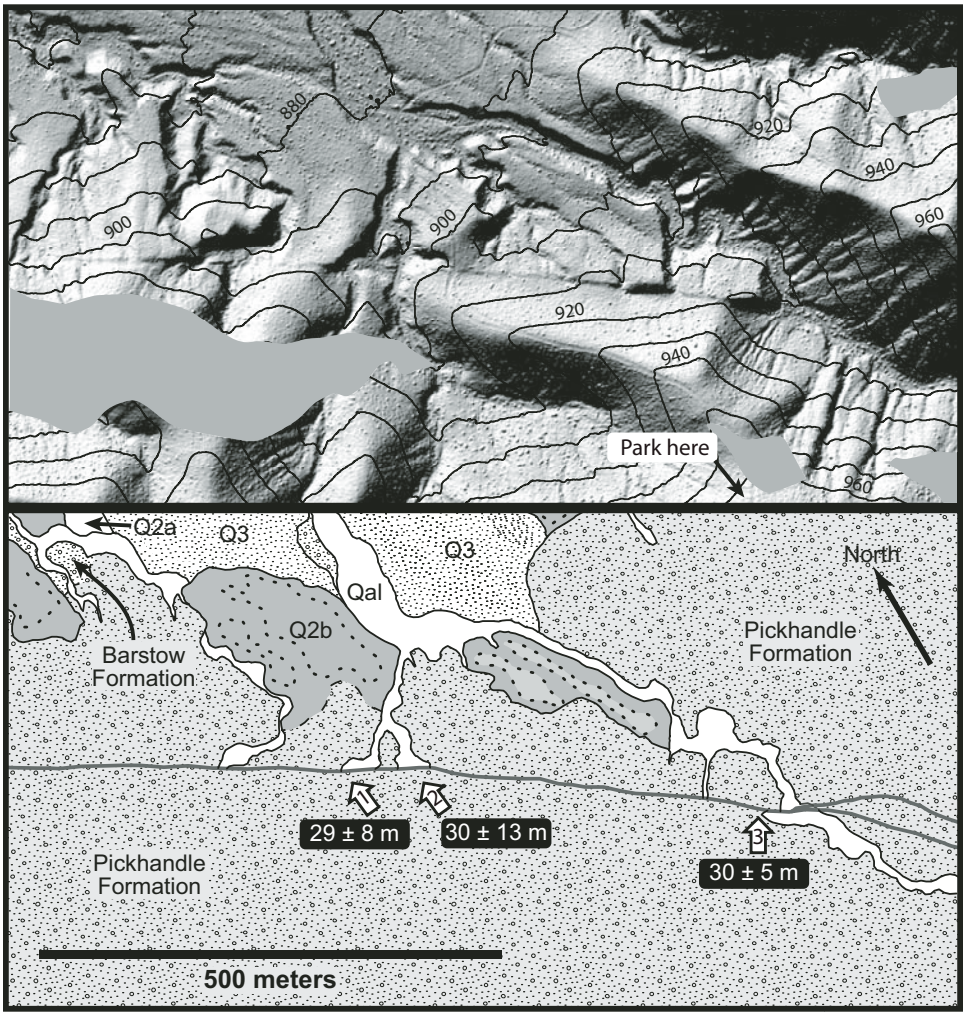

Figure 3. Hillshaded airborne laser swath mapping (ALSM) topography, illuminated from the west (top) and geologic interpretation (bottom) near Stop 2 (Fig. 1), showing stream deflections along the Lenwood fault. Gray patches are gaps in ALSM data. Ten-meter index contours shown as dark lines with elevations labeled. Early Miocene Pickhandle Formation here consists of consolidated conglomerate with poorly exposed bedding except for occasional, 2–25-m-thick lenses of monolithologic megabreccia. Mid- to late Miocene Barstow Formation consists of well-bedded sandstone and conglomerate at this locality. Arrows: 1 and 2—locations of a pair of channels deflected by dextral slip along the Lenwood fault; 3—shutter ridge formed by dextral offset of channel wall and adjacent hillslopes. Combining all of these constraints yields a best-fit offset of 30 ± 5 m since incision of $Q2_b$.

is 50% higher than the rate of 0.8 ± 0.2 mm/yr calculated from the better constrained northern site. Such along-strike gradients in slip rate have become increasingly recognized in the eastern California shear zone (e.g., Frankel et al., 2007a, 2007b; Oskin et al., 2007) and represent an important source of potential error that needs to be addressed when compiling geologic rate budgets.

Summary

The Lenwood fault is a typical example of the rather slow-moving (~1 mm/yr) dextral faults that comprise the eastern California shear zone across the central Mojave Desert. Displaced $Q2_b$ alluvial fans and related inset channels document well-constrained offset of 30 ± 5 m and a less well-constrained offset of 45 ± 5 m at two sites along the northern Lenwood fault. A cosmogenic depth-profile age of 37 ± 7 ka for a $Q2_b$ alluvial fan results in slip rates of 0.8 ± 0.2 mm/yr and 1.2 ± 0.2 mm/yr for these respective sites.

MIDDLE TO LATE MIOCENE STRATIGRAPHY OF THE SUMMIT RANGE AND RED ROCK CANYON: IMPLICATIONS FOR TEMPORAL VARIATIONS IN SLIP RATE ON THE GARLOCK FAULT

The Summit Range, or Summit Diggings as it is labeled on some maps, is located west of the Trona–Red Mountain Road, ~20 km south of Ridgecrest on the south side of the Garlock Fault (Stop 3, Fig. 1). It covers a relatively small ~20 km^2 area with the western half consisting of late middle Miocene to earliest Pliocene volcanic, volcaniclastic, and sedimentary rocks that rest nonconformably on Cretaceous (86 Ma) quartz monzonite basement (ages given above and in the rest of the sections for the Summit Range and Red Rock Canyon areas are from Monastero and Walker, unpublished data). Dibblee (1967) included the Summit Range in his discussion of the Lava Mountains although the latter area extends significantly farther south and east and is generally underlain by younger rocks than in the Summit Range (Smith et al., 2002). Recent work indicates that the Summit Range

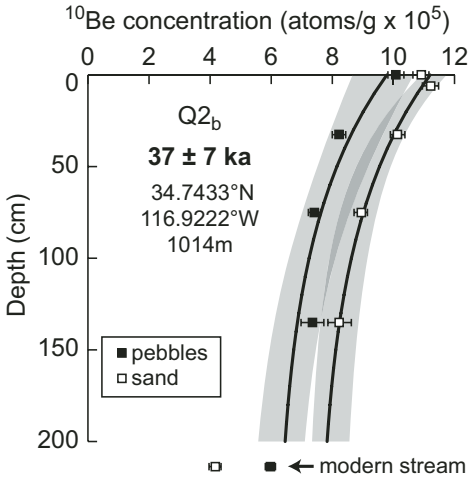

Figure 4. Plot of ^{10}Be concentration versus depth for quartz-bearing sediment from $Q2_b$ fan surface adjacent to the Lenwood fault (P in Fig. 2). Both 1–3-cm-sized pebbles and sand-sized material were measured. Beryllium-10 concentrations from these different grain sizes showed a consistent offset from one another, with higher inheritance for sand-sized grains. The order switches for the modern stream sample site (S on Fig. 2), where sand-sized grains have significantly lower concentration than shielded samples from a 150 cm depth. Gray bands show 95% confidence of mean concentration of ^{10}Be with depth for independent age models for each grain size. Both models yielded an identical mean age of 37 ka. Normalizing all pit samples to a common inheritance value, and including the sample of pebbles from the modern stream sample, yields an age of 37 ± 7 ka (95% confidence) for $Q2_b$.

rocks constitute a separate volcanic center that can be directly correlated with middle to late Miocene Dove Spring Formation rocks that crop out in the Red Rock Canyon area on the north side of the Garlock fault, ~30 km west-southwest of the Summit Range (Stop 4, Fig. 1).

Middle to Late Miocene Stratigraphy of the Summit Range

The stratigraphy in the Summit Range is shown in Figure 5. Locally overlying the crystalline basement is gray andesite porphyry. This fine-grained rock has phenocrysts of plagioclase that have altered rims and hornblende that has been completely replaced by limonite. The age for this rock is 15.6 ± 0.5 Ma (from (U-Th)/He on zircon), which makes it equivalent to the early middle Miocene Cudahy Camp unit 5 (Tc_5) of the Red Rock Canyon area. Above this unit is a series of deep red to tan arkosic sandstones, conglomerates, olive-drab–brown mudstones, limestones, and cherts. Most of these rocks appear to be water-lain sedimentary rocks with varying amounts of ash, lithic clasts, and pumice. Some of the rocks appear to be lahars with crystals of feldspar and biotite scattered throughout a dense red matrix. Many of the mineral grains are hydrothermally altered (e.g., reaction rims on feldspars and limonite replacement of mafics). These rocks are probably equivalent to the lower Dove Spring Formation of Red Rock Canyon (Loomis and Burbank, 1988).

Overlying and locally interbedded with the sedimentary units is a series of tuffs, lahars, and debris flows that display a wide range of compositions, colors, thicknesses, and degrees of induration. The base of this sequence consists of gray to dark reddish brown to light purple-brown, ash-rich debris flows and lahars (Fig. 5). Some contain volcanic bombs that range in size from 20 cm to 30 cm and are fractured in-place, indicating they were hot when emplaced.

The next overlying unit consists of a series of tuffs that vary widely in color and degree of induration (Fig. 5). Most are white, cream, green, or gray-green, probably representing varying amounts of alteration. Some are clearly air-fall tuffs that conform to irregularities, while others appear to be small ash-flow events. There are also instances where apparent epiclastic units occur within the tuff sequence as denoted by the occurrence of rounded grains of quartz and other accessory minerals. This entire unit attains a thickness of >15 m in the Summit Digging location, but the total thickness and inclusion of all tuffs in the sequence at correlative outcrops varies widely.

A distinctive pink to orange-pink ash-flow tuff lies within this unit and crops out prominently in the middle of the Summit Range area. This pumiceous lapilli tuff is rich in lithic clasts with compositions including propylitically altered porphyritic extrusive volcanic rocks, plutonic rocks of varying composition, quartz, and banded rhyolite (Fig. 5). It also has a large percentage by volume of pumice clasts. It reaches a thickness of several meters in outcrop in the Summit Digging area, and crops out widely on the floor of the valley, where it can be found overlying the tan and deep red lahars, debris flows, and sandstones, and in other places be found beneath them. The age of this unit is 11.8 ± 0.9 Ma (from (U-Th)/He on zircon).

The next highest stratigraphic unit consists of a series of dacite domes, flows, and tuffs clustered in a 5 km^2 area situated on the western and southern margins of the Summit Range. These units overlie the white tuffs that form the valley floor between the westernmost flows and the easternmost domes and overlie the tuffs on a small, elliptical, NE-trending hill 2 km south of the main diggings. Units in the domes are quite distinctive because of their coarse phenocrysts of twinned (Carlsbad habit) orthoclase that reach lengths of several centimeters. These are embedded in a fine-grained, reddish-brown matrix with biotite and small quartz grains. On the easternmost dome, there is a vertical fabric to the rock. The dome is surrounded on two sides by outcrops of lava flows with the same, only finer-grained, mineral composition as the dome. These flows exhibit abundant flow features, such as alignment of phenocrysts in flow bands, and contorted, brecciated flow fronts. Flows at the southeast corner of the dome dip 30–40° outward and show well-developed cooling column structure. The radiometric age of this dome is 11.0 ± 0.2 Ma (^{40}Ar/^{39}Ar).

A second dome, located ~1 km southwest of the dome just described, is petrologically similar although it is highly altered,

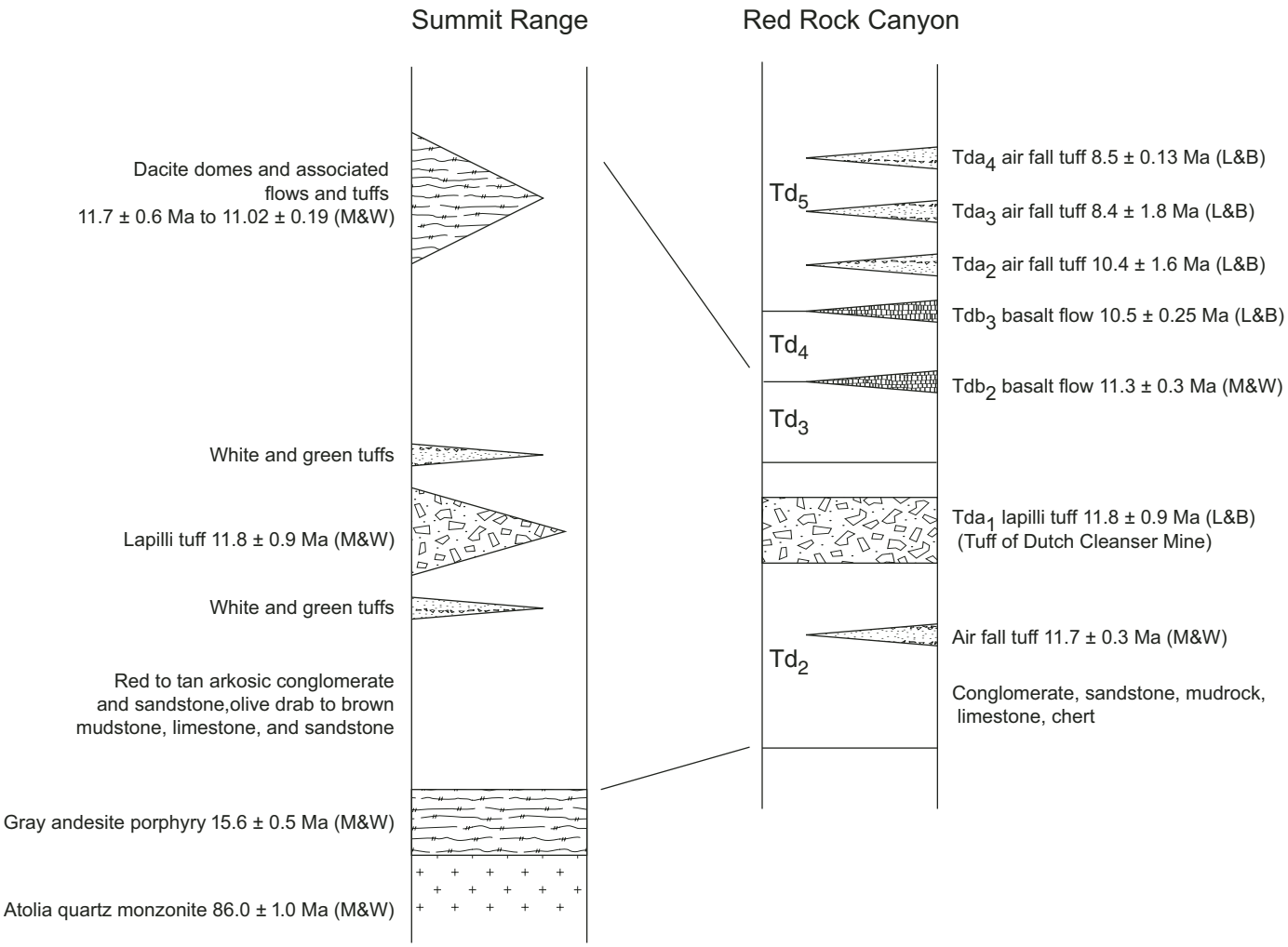

Figure 5. Schematic stratigraphic sections for the Summit Range and Red Rock Canyon areas. Important and/or dated units shown in pattern; unpatterned rocks consist of conglomerate, sandstone, mudstone, limestone, and chert. Ages are from Monastero and Walker (unpublished data), denoted M&W, and from Loomis and Burbank (1988) and Whistler and Burbank (1992), denoted L&B. Units and descriptions for the Red Rock Canyon area are from Loomis and Burbank (1988).

mostly massive, coarsely porphyritic dacite. There is pervasive argillic alteration of orthoclase and biotite phenocrysts and a general vertical fabric, which suggests flow within a vent. The heavily altered area covers ~75–100 m^2 and stands 8–10 m high. Numerous examples of monolithologic breccias reminiscent of vent structures can be found on the top of the dome. Flows extend to the south and west of the dome complex and thin rapidly to 1–3 m within 1 km. The age of this dome is determined to be 11.7 ± 0.6 Ma ($^{40}Ar/^{39}Ar$).

Middle to Late Miocene Stratigraphy of the Red Rock Canyon Area

Approximately 30 km west-southwest of the Summit Range is the Red Rock Canyon area (Stop 4, Fig. 1). Situated at the southwest end of the El Paso Mountains, this area is the type section for the middle to late Miocene Dove Springs Formation (Loomis, 1984). The stratigraphic succession for this interval is shown in Figure 5. Loomis (1984) divided the rocks into six units, ranging in age from 13.5 Ma to ca. 7 Ma; the Dove Springs rests disconformably on the early to middle Miocene Cudahy Camp Formation. The hiatus between the Cudahy Camp and Dove Springs Formations was determined by Loomis and Burbank (1988) to be 15.1–13.5 m.y. based on magnetostratigraphy, K-Ar, and fission track dates.

The lowest part of the Dove Springs section contains conglomerate and sandstone consisting of poorly sorted, massive to crudely stratified units dominated by volcanic and plutonic clasts in an ash-rich matrix. The unit grades continuously upward into massive, dirty arkosic sandstones. The top of this unit is

arbitrarily defined as the point where the sandstones and conglomerates become less massive and more stratified. There are no age-specific geochronology markers in this unit.

Member 2 of the Dove Spring Formation (Td_2) crops out extensively in the south-central part of Red Rock Canyon State Park where it is dominated by conglomerates, sandstones, and volcanic tuffs (Fig. 5). Loomis (1984) determined that the provenance of these rocks was from a source located to the south and east. The sedimentary and epiclastic rocks consist of grains of quartz, feldspars, and biotite, with varying degrees of rounding, and ash, pumice, and lithic clasts from volcanic and plutonic sources. They vary in color from deep red to tan, are intimately interleaved, and constitute between 200 and 400 m of section.

In the middle of Td_2, there is a pink lapilli ash-flow tuff (Tda) that is a prominent ridge-former in the Red Rock Canyon area (Fig. 5). The unit is made up of two separate flows, with a cooling break between them. The rock is rich in pumice clasts (0.5–2.0 cm) and lithics (propylitically altered volcanics, banded rhyolites, and plutonic fragments) in an ash- and crystal-rich matrix. This unit grades northeastward to a white to light gray air-fall tuff dated at 11.8 ± 0.9 Ma (Whistler and Burbank, 1992). There are several thin (tens of centimeters) white air-fall and pumice-rich tuffs below this unit that have been dated at 11.7 ± 0.6 Ma ($^{40}Ar/^{39}Ar$). Overlying the pink tuff is a continuation of the Td_2-type rocks described in the foregoing paragraph.

Higher in the section there are two basalt flows (Tdb_2 and Tdb_3 of Loomis, 1984), the lower of which have been dated at 11.3 ± 0.3 Ma ($^{40}Ar/^{39}Ar$; Monastero and Walker, unpublished data). These flows are interleaved with more of the Td_2 type rocks although they are grouped into higher units of the Dove Spring.

Implications of Unit Correlation at Red Rock Canyon and the Summit Range

Although the relative positions of the Summit Range volcanic center and the southern Red Rock Canyon stratigraphic sequences at the time of emplacement cannot be determined with absolute certainty, it is clear that they correlate in age and lithology over a wide range of time. It is suggested that the Summit Range location was the source area for most of the volcanic components of the lower Dove Spring Formation in Red Rock Canyon. Based on thickness of the pink lapilli tuff and the fact that the Tda unit makes a transition to a pure white air-fall tuff in a north-northeasterly direction, we interpret that the two sites were more or less juxtaposed across what is now the Garlock fault when the volcanic center was active between 12 and 11 Ma. The notion of the Garlock being an intracontinental transform (Davis and Burchfiel, 1973) that acts as an accommodation zone for extension north of the fault from a relatively unextended area south of the fault, implies that movement on the Garlock could not have initiated before the onset of extension in the southwest Basin and Range. Wernicke et al. (1988) report the onset of extension in the Las Vegas Valley shear zone–Lake Mead area ca. 16 Ma, and McKenna and Hodges (1990) cite 15 Ma as the time of initiation of extension in Death Valley. This would mark the beginning of movement on the Garlock fault inasmuch as there would have been no need for such a structure prior to this time. The assumption is, therefore, that initial movement on the eastern part of the Garlock fault began ca. 15 Ma, which means that there was ~30 km of sinistral offset on the Garlock from inception of movement until 12–11 Ma. This translates to a rate of offset of between 7 and 10 mm/yr. Since that time, an additional ~35 km of offset has resulted in the present spatial relationship of the two sites, which calculates to a slip rate of 2.75–3.0 mm/yr—much slower than the rate of the earlier period.

The specific cause of this dramatic decrease in offset rate on the Garlock fault is not known with certainty at present. Lonsdale (1991) and Atwater (1989) document a change in the configuration of the Pacific and North America plates ca. 12.5 Ma. Lonsdale (1991) contends that the plate offshore Baja California stopped spreading at this time, subduction ceased, and the Rivera triple junction jumped southward to the tip of the Baja peninsula. Atwater (1989) found that at this same time there was simultaneous formation of a continuous boundary between these two plates from central California to the tip of Baja. There are numerous examples of volcanic outbursts during this time in the nearby Owlshead Mountains (Calzia and Ramo, 2000), Death Valley (Thompson et al., 1993; Troxel, 1994), and Eagle Crags volcanic field (Monastero et al., 1994). It is possible, and actually highly probable, that the rate of sinistral offset on the Garlock fault varied considerably from 12 to 11 Ma until present, but such correlations are left to a more detailed understanding of the stratigraphy of the middle to upper Dove Spring Formation and the volcanic units found in the Lava Mountains (Smith et al., 2002).

Summary

The rocks exposed in the Summit Range and Red Rock Canyon demonstrate that at 12–11 Ma the two areas, which are now separated by ~35 km of sinistral offset on the Garlock fault, were directly opposite one another across that structure. This implies that initial motion on the Garlock fault was on the order of 10 mm/yr from ca. 15–12 Ma. If this is correct, then the later offset rate is a factor of three to four times slower, averaged over the past 11 Ma.

BEDROCK EVIDENCE FOR 65 km OF DEXTRAL OFFSET ACROSS OWENS VALLEY, CALIFORNIA, SINCE 83 Ma

Historic earthquakes (Beanland and Clark, 1994), paleoseismology (Bacon and Pezzopane, 2007; Lee et al., 2001b), and geodesy (Dixon et al., 2003) indicate that the modern tectonic regime of Owens Valley is dominated by right slip that accommodates a significant fraction of the relative motion between the North America and Pacific plates. However, the total magnitude and the timing of lateral slip across Owens Valley have been uncertain. Conventional wisdom has long been that net lateral

slip across the valley is no more than 10 km (Moore and Hopson, 1961; Ross, 1962) and that right slip in Owens Valley began in Plio-Pleistocene time (Lee et al., 2001b).

However, recently identified offsets of several bedrock geologic markers indicate dextral displacement of 65 ± 5 km (Fig. 6), including, from youngest to oldest: (1) the Golden Bear dike in the Sierra Nevada and the Coso dike swarm in the northern Coso Range; (2) 102–103 Ma leucogranite and mafic granodiorite plutons into which the Golden Bear and Coso dikes were intruded; (3) the axis of maximum dilation of the 148 Ma Independence dike swarm; and (4) a Devonian submarine channel complex and other geologic features identified in the Mount Morrison roof pendant in the Sierra Nevada and east of Tinemaha Reservoir at the base of the Inyo Range (Fig. 6). The offsets are interpreted to record the same displacement that must have accumulated since 83 Ma, when the Golden Bear–Coso dikes were emplaced.

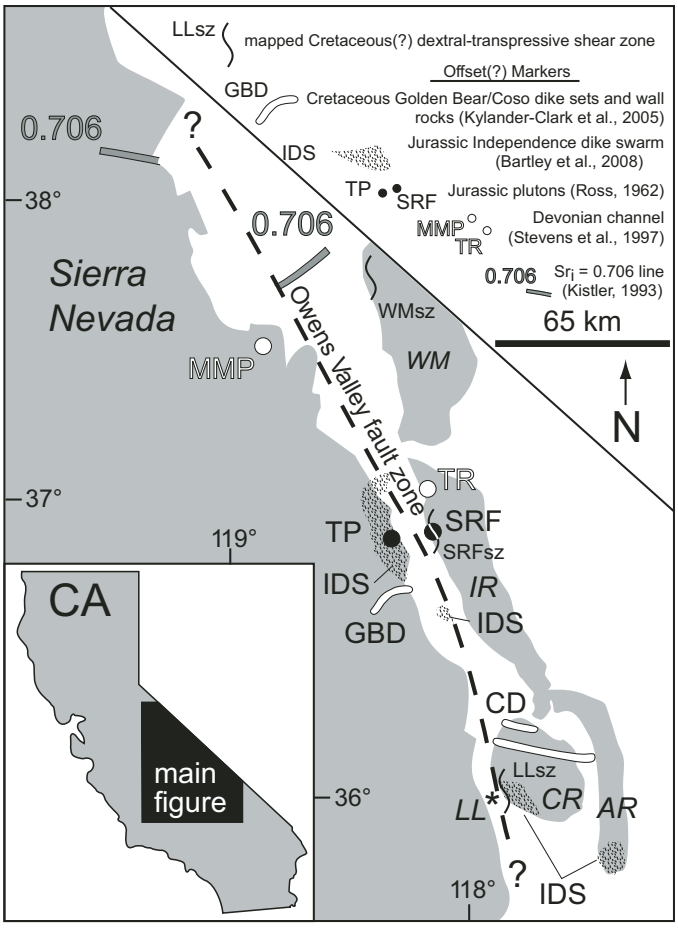

Figure 6. Locations of markers that support 65+ km of dextral offset across Owens Valley. Although correlation of the Tinemaha (TP) and Santa Rita Flat (SRF) plutons suggested little lateral offset (Ross, 1962), plutons of similar age and lithology are widespread on both sides of Owens Valley. Offset markers include (1) the densest part of the Independence dike swarm (Bartley et al., 2008); (2) the Sr 0.706 isopleth (Kistler, 1993); (3) a Devonian submarine channel at Tinemaha Reservoir and in the Mount Morrison pendant (Stevens et al., 1997); (4) the 83 Ma Golden Bear (GBD; Stop 8, Fig. 1) and Coso dike sets (CD; Stop 6, Fig. 1; Kylander-Clark et al., 2005); and (5) the 102–103 Ma plutons that the Golden Bear and Coso dikes intrude (Kylander-Clark et al., 2005). AR—Argus Range; CR—Coso Range; IDS—Independence dike swarm; IR—Inyo Range; LL—Little Lake; LLsz—Little Lake shear zone of Bartley et al. (2008; Stop 5, Fig. 1); MMP—Mount Morrison pendant; SRFsz—Santa Rita Flat shear zone of Vines (1999); TR—Tinemaha Reservoir; WM—White Mountains; WMsz—White Mountain shear zone of Sullivan and Law (2007).

Offset Geologic Markers

Golden Bear and Coso Dikes

Moore (1963, 1981) first recognized the Golden Bear dike and mapped it for ~15 km, from its western termination in the northern Mount Whitney quadrangle to where it disappears under Owens Valley near Independence (Fig. 6). The dike actually comprises from one to three branching granitic dikes that range from 5 to 30 m thick, and locally have thick (50 cm) cataclastic margins. The Coso dike swarm includes two groups of steeply dipping E-striking dikes that are separated by ~6 km across strike (Duffield et al., 1980; Whitmarsh, 1998). Major dikes of the Coso swarm are from 5 to 25 m thick, commonly accompanied by thinner (<2 m) subparallel dikes.

The Golden Bear and Coso dikes (Stops 6 and 8; Figs. 1 and 6) are porphyritic quartz monzonite with <5 vol% mafic minerals, 2–4 cm K-feldspar phenocrysts (25–30 vol%), and equant, euhedral, bipyramidal quartz crystals (~15 vol%) up to 1 cm across. Zircon U-Pb analyses by Kylander-Clark et al. (2005) of two Golden Bear dike samples defined an emplacement age of 83.4 ± 0.4 Ma. Whitmarsh (1998) reported a U-Pb zircon date of ca. 88 Ma (later interpreted as 84 ± 1 Ma; J.D. Walker, 2003, personal commun.) from one Coso dike, and Kylander-Clark et al. (2005) obtained several concordant, or nearly concordant, zircon fractions that cluster between 82 and 86 Ma from two other Coso dike samples. In addition, major-element, trace-element, and isotopic geochemistry of the dikes are compatible with correlation of the Golden Bear and Coso dikes (Kylander-Clark et al., 2005).

Although the Coso and Golden Bear dikes range up to 30 m thick, neither continues on strike across Owens Valley (Fig. 6). The Inyo Range east of the Golden Bear dike (Ross, 1965) exposes latest Precambrian through early Paleozoic sedimentary rocks that are intruded by Jurassic and Cretaceous plutons and sparse dikes of the Independence swarm, but none of the dikes resembles the Golden Bear dike in either petrology or dimensions. Similarly, on strike westward from the Coso dikes in the Olancha Peak area of the Sierra Nevada, various Mesozoic plutons are present, but no thick granite porphyry dikes (Diggles, 1987; Diggles et al., 1987).

Early Cretaceous Plutons

The Golden Bear dike intrudes Cretaceous plutons and minor Mesozoic metavolcanic and metasedimentary rocks (Moore, 1963, 1981; Chen and Moore, 1982; Kylander-Clark et al., 2005; Saleeby et al., 1990). Except near its western terminus, the dike

mainly intrudes coarse leucogranite of the 102 Ma Bullfrog and Independence plutons and granodiorite of the 103 Ma Dragon pluton (Saleeby et al., 1990; Kylander-Clark et al., 2005). Granitic plutons dated ca. 102 Ma are common farther west in the Sierra Nevada (e.g., intrusive suite of Yosemite Valley; Ratajeski et al., 2001), but the Bullfrog, Independence, and Dragon are the only plutons of this age known at the eastern range front of the Sierra Nevada.

The Coso dikes intrude Sierran-like Mesozoic plutons and minor Mesozoic metasedimentary and metavolcanic rocks. Plutonic wall rocks include the leucogranite of Cactus Flat, which yielded a U-Pb zircon date of 101.6 ± 0.8 Ma (Kylander-Clark et al., 2005), making it the only pluton east of Owens Valley to yield an Early Cretaceous age. The leucogranite of Cactus Flat is commingled with undated granodiorite that resembles the Dragon pluton.

Independence Dike Swarm

Dikes of the Independence swarm vary widely in abundance, and some parts of the swarm are compositionally diverse, whereas others are uniformly mafic (e.g., Carl and Glazner, 2002; Fig. 7). The internal anatomy of the swarm thus was mapped in search of previously unrecognized tectonic offsets. Dike thicknesses and orientations were recorded along 84 cross-strike traverses in areas of good to excellent exposure on both sides of Owens Valley (Bartley et al., 2008; Fig. 7).

Dilation by intrusion of the Independence dike swarm ranges from 0 to 44%, but dilation values >5% are restricted to distinct, relatively narrow zones in the eastern Sierra Nevada near Independence, the northern Alabama Hills, and the southern Coso and Argus ranges and Spangler Hills (Fig. 7). In high-dilation areas, the swarm is also lithologically diverse, including mafic, intermediate, and felsic dikes. Elsewhere in the swarm where dilation is less (mainly <1%), only mafic dikes generally are present. The most southerly high dilation values on the western side of Owens Valley were found in the northern Alabama Hills. The nearest high dilation area on the eastern side of the valley is ~75 km to the southeast in the southwestern Coso Range. This offset is uncertain by at least ±10 km because the dike swarm is diffuse and intersects the valley at a low angle (~30°).

Devonian Submarine Channel and Other Geologic Features

On McGee Mountain in the Mount Morrison pendant, a distinctive facies of the Middle Devonian Mount Morrison Sandstone consists of quartz sandstone and coarse conglomerate containing clasts of chert and limestone with fragments of tabulate coral (Greene and Stevens, 2002; Stevens and Greene, 1999). The unit fills a channel cut deeply into older rocks and is interpreted as the feeder channel of a major submarine fan complex. A lithologically identical conglomerate, also of Middle Devonian age and containing fragments of tabulate corals, is exposed east of Tinemaha Reservoir at the base of the northern Inyo Mountains, 65 km to the southeast of McGee Mountain. The lithologic and structural similarities between these areas led Stevens et al. (1998) to propose that rocks in these two areas are remnants of a major Devonian submarine channel that has been dextrally offset ~65 km on a cryptic fault, termed the Tinemaha fault, in northern Owens Valley (Fig. 7). This interpretation is also compatible with ~65 km of dextral offset of the initial $^{87}Sr/^{86}Sr = 0.706$ isotopic isopleth proposed by Kistler (1993) in the Mono Lake area.

The Tinemaha fault was originally considered to be Middle Triassic in age, based on the supposition that the fault was intruded by the Late Triassic Wheeler Crest Granodiorite (Stevens et al., 1998). However, given the present evidence for 65 km of well-dated Late Cretaceous or younger dextral displacement in the southern Owens Valley, it now seems clear that the fault in the northern Owens Valley must also be Cretaceous or younger in age (Stevens et al., 2003).

Discussion

Net Offset

Each of the above correlations requires right-lateral displacement of a similar magnitude. The displacement required by the Golden Bear–Coso dike correlation is insensitive to the precise location of the fault(s) that accommodated it because the dikes dip steeply and strike at high angles to the valley. Restoring the easternmost Golden Bear outcrops to a position adjacent to the westernmost Coso dike outcrops yields ~65 km of right slip (Fig. 6). Aligning the Golden Bear dike with the northernmost mapped exposures of the Coso dikes reduces the estimate to ~60 km. Correlations of the 102–103 Ma plutons, the maximum dilation axis of the Independence dike swarm, and the Devonian channel deposits are also compatible with 60–65 km of right-lateral offset.

Timing of Offset

Correlation of the Golden Bear and Coso dikes requires that the 65 km offset accumulated since ca. 83 Ma. At current estimates of long-term slip rate across Owens Valley of 2–3 mm/yr, 65 km of offset could accumulate in ~20–30 m.y. This is compatible with the late Cenozoic right-oblique subduction setting of California (Atwater and Stock, 1998), and slip could have commenced when the San Andreas system started to form in the late Oligocene. Indeed, there is evidence that dextral slip began in the Mojave Desert in the early Miocene (Glazner et al., 2002).

However, most stratigraphic, structural, and thermochronologic data suggest that the modern dextral slip regime commenced in the Pliocene (Lee et al., 2001b; Monastero et al., 2002; Stockli et al., 2003). To accumulate 65 km of offset since then would require a slip rate of >20 mm/yr, which is more than half of the total Pacific–North America plate motion and almost certainly is incompatible with regional constraints. Among the problems with this hypothesis is that the Garlock fault shows little evidence for disruption by N- to NW-striking faults. Many dextral faults in the Mojave Desert do, indeed, die out before reaching the Garlock fault, and it is not clear how ongoing dextral slip south of the

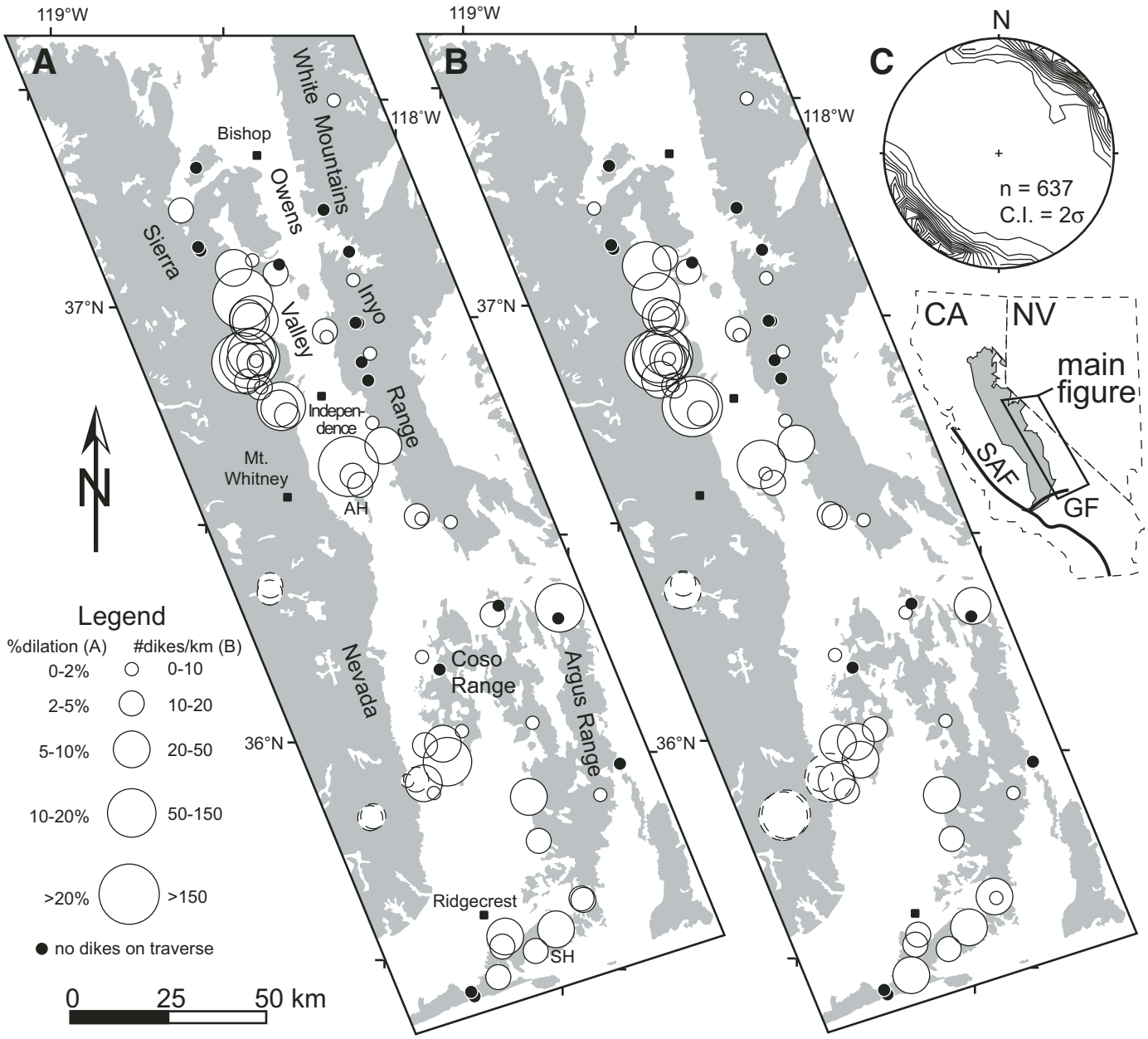

Figure 7. Map of quantitative properties of the Jurassic Independence dike swarm, modified from Bartley et al. (2008). Shaded areas are pre-Cenozoic bedrock. Symbols are centered on midpoints of traverses. Dashed symbols indicate traverses where observed dikes may be Cretaceous and therefore not part of the Independence swarm (see Bartley et al., 2008, for further discussion). (A) Percent dilation by diking. Note offset of high-dilation zone between the Alabama Hills (AH) and Coso Range and the distinct northern boundary on both sides of Owens Valley where high dilations drop to zero. SH—Spangler Hills. (B) Number of dikes crossed per kilometer. The pattern resembles that in (A), but traverses in the southeastern Sierra Nevada (dashed) appear more prominent owing to much higher abundances of thin (5–30 cm) mafic dikes. Such a high proportion of thin mafic dikes is atypical of the Independence swarm and more characteristic of Cretaceous dikes in the region. (C) Kamb contour plot of poles to dikes measured on traverses. GF—Garlock fault; SAF—San Andreas fault; CA—California; NV—Nevada.

Garlock fault is transmitted to the north (e.g., Oskin and Iriondo, 2004).

Thus, it seems most likely that a significant fraction of the total 65 km of slip—perhaps as much as 50–60 km—is significantly older, possibly Late Cretaceous (Bartley et al., 2008). Laramide-age right slip along the eastern margin of the Sierra Nevada may have been linked to a south-directed extensional detachment system in the southern Sierra Nevada (Wood and Saleeby, 1997) that unroofed high-pressure rocks in latest Cretaceous–early Tertiary time. Dextral shear of this age would predate formation of the Garlock fault (Monastero et al., 1997) and thus eliminate that conflict.

Locus of Slip

The fault zone responsible for offset of the various markers lies between the Sierra Nevada and White-Inyo-Coso Ranges (Fig. 6). Although mostly buried by alluvium, it can be located within 100 m at Little Lake on the west side of the Coso Range, where Jurassic plutonic rocks with abundant Independence dikes are juxtaposed against a distinctive Jurassic orthogneiss that lacks such dikes (Stop 5; Figs. 1 and 8; Bartley et al., 2008). Cretaceous and Jurassic intrusive rocks on both sides of the fault in this area are cut by transpressive ductile-brittle shear zones with a persistent dextral component of shear. These shear zones, and similar Late Cretaceous dextral transpressive shear zones exposed in the Inyo (Vines, 1999) and White (Sullivan and Law, 2007) Mountains, probably belong to a family of structures that accommodated 50+ km of dextral offset in Late Cretaceous–early Tertiary time. Approaching the main fault contact at Little Lake, cataclastic microstructures increasingly overprint the ductile microstructures in the shear zones. This spatial pattern may reflect the reactivation of a Late Cretaceous shear system by the modern right-slip fault zone.

Summary

Several independent geologic markers indicate 65 ± 5 km of net dextral shear across Owens Valley since 83 Ma. On the order of 10 km of this displacement accumulated in the modern dextral transtension regime, and the remainder probably accumulated in Late Cretaceous–early Tertiary time. The modern tectonic regime therefore appears to reflect reactivation of a long-lived throughgoing crustal boundary.

QUATERNARY TECTONISM OF THE NORTHWESTERN COSO RANGE

The Coso Range is a tectonically and volcanically active region along the southeastern margin of the Sierra Nevada ("Sierran") microplate, which moves ~13 mm/yr northwest with respect to stable North America (Argus and Gordon, 1991, 2001; Dixon et al., 1995, 2000). Northwest motion of the Sierran microplate is accommodated by distributed strike-slip and normal faulting in a 100-km-wide zone of active deformation bordering the eastern Sierra Nevada (Fig. 1; Dokka and Travis, 1990; Unruh et al., 2003).

Active crustal extension in the Coso Range primarily is driven by a releasing transfer of dextral motion from the Airport Lake fault to the Owens Valley fault, two major right-lateral strike-slip faults that form the eastern tectonic boundaries of the Sierran microplate south and north, respectively, of the Coso Range (Fig. 1; Monastero et al., 2005; Unruh et al., 2002). In detail, the Airport Lake fault zone splits into several branches at the southern end of the step-over region (Fig. 9). An eastern branch, consisting of N- to NNE-striking normal faults in northeastern Indian Wells Valley, extends northward across eastern Coso Basin and into the southern end of Wild Horse Mesa, where it continues northward and forms a dramatic series of scarps in Pliocene volcanic flows. The faults with the largest scarps in Wild Horse Mesa exhibit a distinct left-stepping pattern (Fig. 9). A central branch, consisting of a zone of short NNE-striking, left-stepping surface traces, crosses the White Hills anticline south of Airport Lake playa and becomes the Coso Wash fault, which is characterized by a single trace along the southeastern flank of the Coso Range. A western branch of the Airport Lake fault zone crosses the southern Coso Range and joins the Little Lake fault zone in southern Rose Valley (Fig. 9).

Slip Transfer across the Central Coso Range

Based on the geomorphic expression of faults in late Quaternary deposits, the bulk of Holocene deformation in the Coso Range appears to be associated with the central branch of the Airport Lake fault zone (Fig. 9). The most significant structure in this branch is the Coso Wash fault, which consists of a series of NNE-striking normal faults that dip both to the SSE and the WNW. This fault zone extends from the White Hills anticline northward to Haiwee Spring in northern Coso Wash (Fig. 9) and is interpreted to be the principal locus for transferring active dextral shear through the Coso Range (Unruh et al., 2008).

The Coso Wash fault zone can be traced ~9 km north of Airport Lake playa as a single SE-dipping trace that has excellent geomorphic expression as scarps in Holocene alluvial fan deposits. The fault along this reach consists of a series of alternating short NNE- and NW-striking reaches. At the southern margin of the Coso geothermal field (GF; Fig. 9), the fault splays out into a series of WNW-dipping traces that step northwest (left) into the bedrock of the Coso Range and dip toward the main geothermal production zones. The WNW-dipping fault segments are geomorphically well-expressed by NW-facing scarps in bedrock and alluvium, and the faults locally pond alluvium in their downdropped hanging wall blocks upstream of the scarps.

At the latitude of the geothermal field, the E-dipping Coso Wash fault and the WNW-dipping normal faults collectively bound a prominent NNE-trending basement ridge that separates Coso Wash from the main production area of the Coso geothermal field (Walker and Whitmarsh, 1998). The basement ridge is at least 10 km long (Fig. 9), locally exhibits up to 550 m of relief,

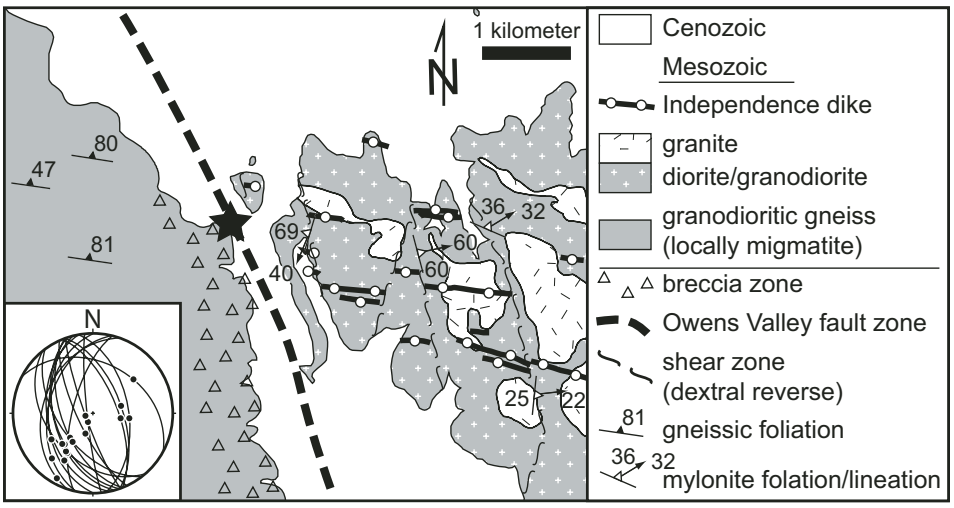

Figure 8. Simplified geologic map of the Little Lake area (modified from Bartley et al., 2008). Distribution of granite and diorite-granodiorite units east of the Owens Valley fault zone from Whitmarsh (1998). Stereoplot shows foliation (great circles) and lineation (dots) in shear zones east of the fault zone.

Figure 9. Northward branching of the Holocene-active Airport Lake fault zone in northern Indian Wells Valley, Rose Valley, the Coso Range, and Wild Horse Mesa. AL—Airport Lake playa; BR—basement ridge; CB—Central branch; CWF—Coso Wash fault; EB—Eastern branch; GF—geothermal field; HS—Haiwee Spring; LCF—Lower Cactus Flat; MF—McCloud Flat; UCF—Upper Centennial Flat; WB—Western branch; WHA—White Hills anticline; WHM—Wild Horse Mesa; WHMFZ—Wild Horse Mesa fault zone. Faults with especially prominent scarps in Wild Horse Mesa are highlighted in bold. Late Quaternary faults modified from Duffield and Bacon (1981) and Whitmarsh (1998), with additional original mapping. A and B indicate two faults that display evidence for late Quaternary dextral offset (please see text for discussion).

and is best expressed between the geothermal field and Haiwee Spring. The basement ridge is essentially a horst block and may be analogous to the "central ridge" that Dooley et al. (2004) observed in scaled analog models of transtensional releasing stepovers that include a ductile substratum beneath a simulated brittle upper crust (quartz sand).

North of the geothermal field, the Coso Wash fault dips consistently ESE and can be traced as a series of E-facing scarps in Holocene alluvium northward to the area around Haiwee Springs, where it loses its surface expression (Fig. 9). North of Haiwee Springs, Coso Wash terminates as a Quaternary basin and narrows to a steep canyon cut in Cretaceous bedrock and Pliocene basalts of Wild House Mesa. Analysis of stereo aerial photography of this segment of the fault indicates E-facing bedrock scarps and possibly fault-related E-facing bedrock slopes. These features probably represent Quaternary faulting, as recognized earlier by Walker and Whitmarsh (1998). The step-faulted terrain associated with the eastern branch of the Airport Lake fault and the Coso Wash fault appear to merge at this location to form a rhombic array of faults at the southern end of Upper Centennial Flat (Fig. 9), north of the termination of the basement ridge.

At the latitude of Haiwee Spring, the locus of active deformation steps west from Coso Wash to a series of NNE-striking, left-stepping normal faults that bound the western margins of Quaternary basins in the northwestern Coso Range such as McCloud Flat and Lower Cactus Flat (Fig. 10). The geomorphic expression and relative activity of these structures appear to increase northward as slip dies out on the Coso Wash fault and basement ridge to the east. The left step in the locus of deformation across the Coso Range is associated with an elongated, NW-trending zone of low P-wave and S-wave velocities in the depth range of ~5–12 km (Hauksson and Unruh, 2007; Reasenberg et al., 1980; Wilson et al., 2003). The base of seismicity is distinctly elevated above the low velocity zone (Monastero and Unruh, 2002), suggesting that hot fluids (brines and/or magma) are present below ~5 km (Hauksson and Unruh, 2007; Wilson et al., 2003).

At least two faults that display evidence for late Quaternary dextral offset can be traced north from Lower Cactus Flat into the northwestern Coso Range piedmont (faults A and B; Figs. 9 and 10). The easternmost of the two faults (A) transfers slip in a restraining stepover across NW-plunging, basement-involved anticlines to the Red Ridge fault zone, a zone of short NNE-striking, en echelon normal faults that extends from Red Ridge northward to the margin of Owens Lake basin (Fig. 10). The westernmost of the two faults (B) is part of a zone of short, discontinuous NW-striking fault segments that trend toward the southern end of the Owens Valley fault (Fig. 10). Slemmons et al. (2008) documented dextral offset of Holocene beach ridges of Owens Lake along this fault trend, which they attribute to surface rupture during the 1872 Owens Valley earthquake. A Pleistocene pediment that fringes the northern Coso Range is deformed by WNW-trending folds in the triangular region between faults A and B (Fig. 10). The coeval NNE-SSW shortening and WNW-ESE extension of the pediment surface in the triangular region between fault trends A and B is consistent with northwest dextral shear passing through the northwestern Coso Range.

The Red Ridge fault zone, which is mapped in detail by Slemmons et al. (2008), may transfer slip to the Central Valley fault zone, a NW-striking fault in Owens Lake basin interpreted by Neponset Geophysical Corporation and Aquila Geosciences (1997) from analysis of seismic reflection data (Fig. 10). The "Central block" bounded by this structure and the Owens Valley fault to the west has subsided episodically during the Quaternary (Neponset Geophysical Corporation and Aquila Geosciences, 1997), possibly during large earthquakes. The NW-trending folds in the pediment surface may be the surface expression of reverse slip on blind, WNW-striking splays of the southern Owens Valley fault, also mapped by Neponset Geophysical Corporation and Aquila Geosciences (1997) from interpretation of reflection data (Fig. 10).

Southern Owens Valley Fault, Northwest Coso Range

The field trip stop along CA-190 (Stop 7; Fig. 1) affords an excellent opportunity to look at, stand on, and walk around evidence of surface rupture during the 1872 Owens Valley earthquake. Figure 11 is a slightly oblique aerial view of the field trip stop, looking toward the southeast. The highway parallels an abandoned shoreline of Owens Lake, and a series of gravelly late Holocene beach ridges are present on the north side of the highway. The photo shows a series of NW-trending lineaments south of the highway that project to the broad bend in the road. These features are the surface expression of the zone of discontinuous fault segments that can be traced northwest of fault A in Figure 10, and they trend toward the southern end of the Owens Valley fault zone mapped by Neponset Geophysical Corporation and Aquila Geosciences (1997) in southeastern Owens Lake basin (Fig. 10). D.B. Slemmons and his colleagues discovered that the Holocene beach ridges north of the highway are offset in a right-lateral sense along the trend of the lineaments. Slemmons et al. (2008) argue that the offset beach ridges represent surface rupture during the 1872 earthquake on the Owens Valley fault zone. If this is correct, then the 1872 rupture extended at least to the southern end of Owens Lake basin and probably south into the Coso Range piedmont (Slemmons et al., 2008).

This stop is a good location to observe other tectonic-geomorphic evidence that northwest dextral shear extends from the southern end of the Owens Valley fault into the northwest Coso Range. There is a large hill ~3 km south of CA-190, on trend with the lineaments in Figure 11, where the associated fault segment terminates or makes a poorly expressed left step (Fig. 10). The hill is cut by a series of left-stepping, W-facing scarps (Fig. 12). About 3–4 km south of CA-190, there is a prominent N-facing wave-cut scarp at ~1160 m (3800 ft) elevation bordering the northern Coso Range piedmont. The shoreline of Owens Lake last reached the elevation of this escarpment ca. 24 ka during a Tioga-age pluvial highstand (Bacon et al., 2006). The shoreline

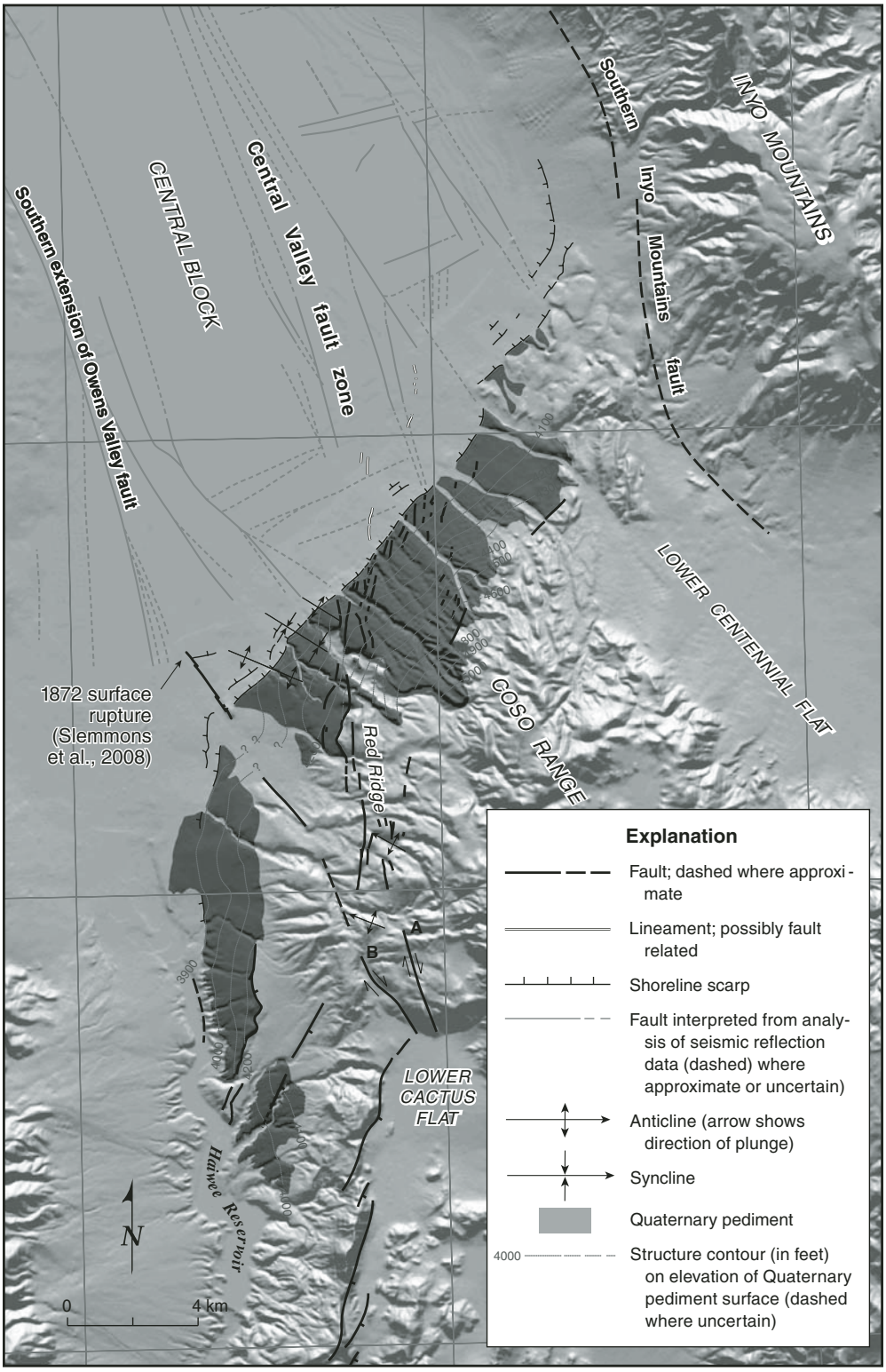

Figure 10. Hillshade map showing extent of a Quaternary pediment surface that fringes the northern and northwestern Coso Range. The pediment is crossed by two zones of faulting that can be traced northward from Lower Cactus flat (i.e., faults A and B). The easternmost of the fault zones (A) strikes N to NNE and joins the Red Ridge fault zone in the northern Coso Range piedmont, which in turn may merge with the "Central Valley fault zone" in southern Owens Lake basin (faults in Owens Lake basin from Neponset Geophysical Corporation and Aquila Geosciences, 1997). Fault B to the west is part of a discontinuous NW-striking zone that can be traced to the southern end of the Owens Valley fault and that experienced surface rupture during the 1872 Owens Valley earthquake (Slemmons et al., 2008). The pediment surface is folded into a series of anticlines about WNW-trending axes west of the Red Ridge fault zone.

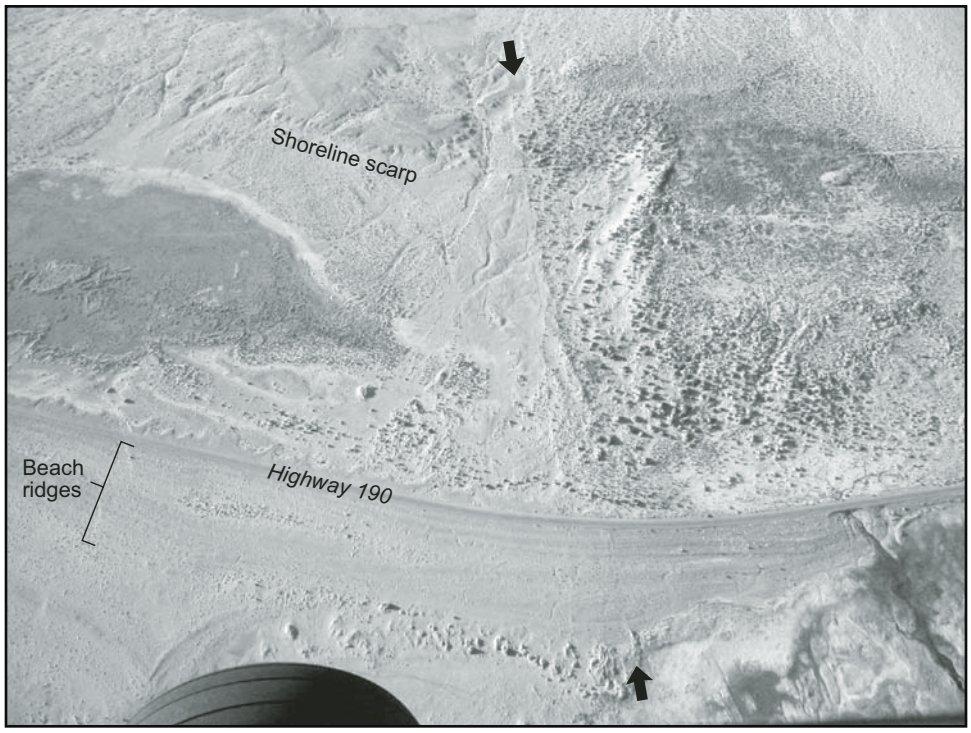

Figure 11. Slightly oblique aerial view to the southeast of lineaments (arrows) associated with the southern Owens Valley fault zone (distance between arrows is ~1.1 km; see Fig. 10 for location). The field trip stop is along CA-190 at the curve in the road (Stop 7, Fig. 1). Beach ridges on the north side of the highway associated with an older Holocene shoreline of Owens Lake are offset in a right-lateral sense by the Owens Valley fault (the displacement is not visible at this scale). Slemmons et al. (2008) interpret that the displacement occurred during the 1872 Owens Valley earthquake, indicating that coseismic rupture on the Owens Valley fault extended at least as far south as the Coso Range piedmont.

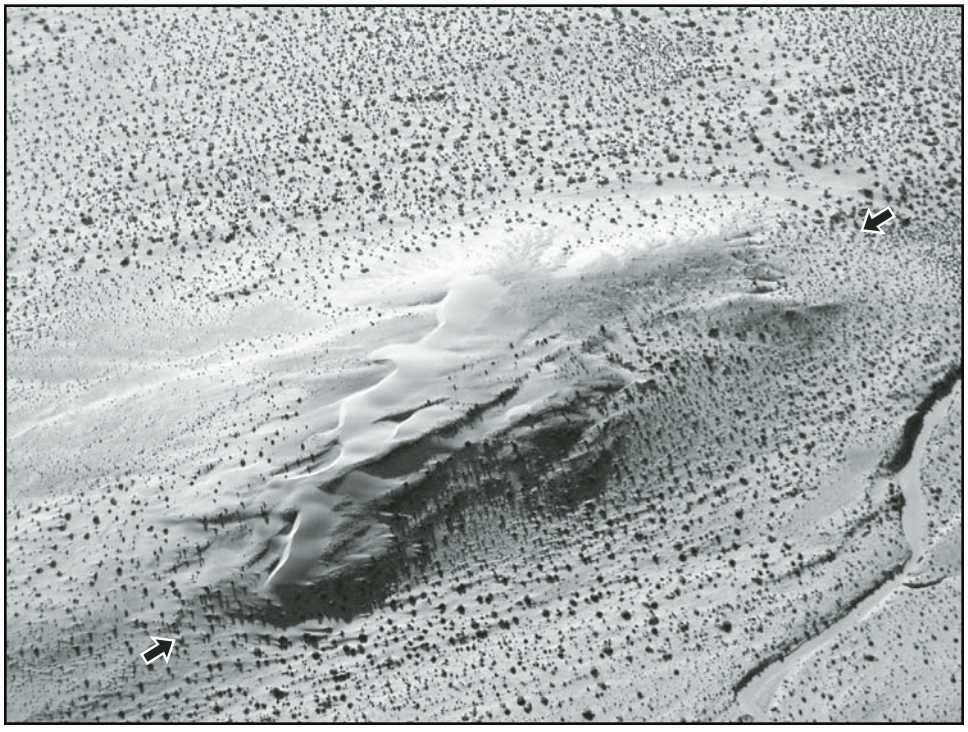

Figure 12. Oblique aerial view to the east of a hill located ~3 km southeast of field trip Stop 7 on CA-190. The west flank of the hill is cut by a series of left-stepping splays of the fault shown in Figure 11. The fault splays are expressed as W-facing scarps (shadowed). Distance between the arrows is ~600 m.

scarp is visibly warped by a series of low-amplitude folds west of the Red Ridge fault zone (Fig. 10); the fold deformation is best observed from CA-190 in low-angle, early morning light when the escarpment is shadowed (Fig. 13). Although not readily visible from the field trip stop, the Red Ridge fault zone is expressed as a series of horst and graben in a middle (?) to late Pleistocene pediment surface south of the 1160 m shoreline escarpment (Figs. 13 and 14).

Summary

Northwest-directed dextral shear along the southeastern margin of the Sierran microplate is transferred from the Airport Lake fault to the Owens Valley fault across a discontinuous series of active structures in the central and northwestern Coso Range. Holocene surface faults in this region locally are separated by en echelon steps, and by short restraining stepovers characterized by uplift and folding. Observations by Slemmons et al. (2008) indicate that surface rupture during the 1872 earthquake on the Owens Valley fault extended at least as far south as the late Holocene shoreline of Owens Lake, and possibly southward into the Coso Range piedmont.

PLEISTOCENE DEFORMATION IN NORTHERN OWENS VALLEY

Several of the broad, outstanding issues concerning the pace and tempo of active deformation throughout the eastern California shear zone–Walker Lane region exist in microcosm within the Owens Valley (Fig. 1). Chief among these is how one interprets differences between modern strain fields, typically measured with space geodesy (e.g., Dixon et al., 2000), and fault slip rates measured over millennia (e.g., Beanland and Clark, 1994). It has long been recognized that geodetic strain rates across the Owens Valley fault are rapid (Savage and Lisowski, 1980, 1995), and simple models of elastic strain accumulation require ~6–7 mm/yr of shear at depth to explain these observations (Gan et al., 2000). These results are in conflict with paleoseismic estimates of late Pleistocene to Holocene slip along the Owens Valley fault zone of 1–3 mm/yr (Bacon and Pezzopane, 2007; Beanland and Clark, 1994; Bierman et al., 1995; Lee et al., 2001b; Lubetkin and Clark, 1988). Recent studies explain this discrepancy as a consequence of transient post-seismic velocities induced by the 1872 Owens Valley earthquake (Dixon et al., 2003; Malservisi et al., 2001). However, long-term slip rates derived from paleoseismic data are subject to numerous epistemic uncertainties regarding the ratio of vertical to horizontal slip, uniform or non-uniform recurrence intervals, and the characteristic size of rupture events. Thus, such data are most useful when combined with geologic estimates of slip rate that average displacement over multiple seismic cycles.

Active deformation across Owens Valley has also engendered considerable debate regarding longer-timescale variability of fault slip. At issue here is the question of whether coeval normal faulting along the Sierra Nevada range front and strike-slip faulting along the Owens Valley fault reflect changes in the regional stress field (Bellier and Zoback, 1995) or simply slip partitioning along a transtensional fault system (Wesnousky and Jones, 1994). Although sites where multiple, well-dated markers

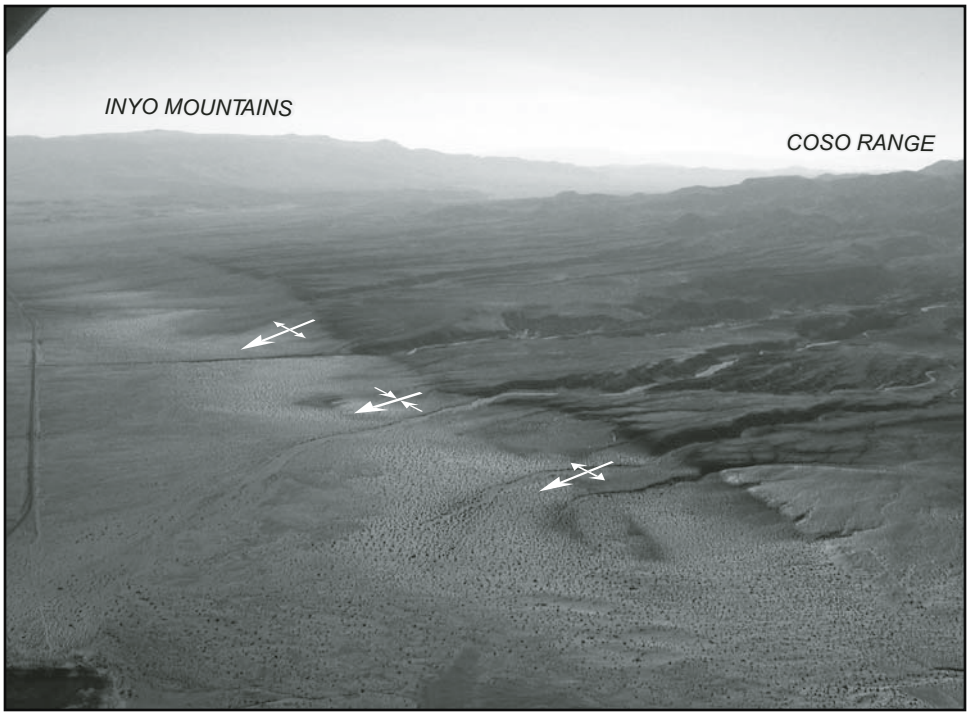

Figure 13. Oblique aerial view to the east of the northern Coso Range piedmont and southern Owens Valley. The darker, more eroded surface to the south (right) is a pediment surface cut across tilted strata of the Pliocene Coso Formation. The pediment terminates to the north against a wave-cut escarpment associated with one or more Pleistocene high stands of pluvial Owens Lake. The pediment and wave-cut scarp are noticeably folded about WNW-trending axes into a series of broad, low amplitude anticlines (distance between anticline axes is ~3.2 km). As demonstrated by the varying width of the shadowed escarpment, the scarp is higher across the axes of the anticlines and lower through the syncline. See Figure 10 for location of folds relative to faults cutting the pediment surface.

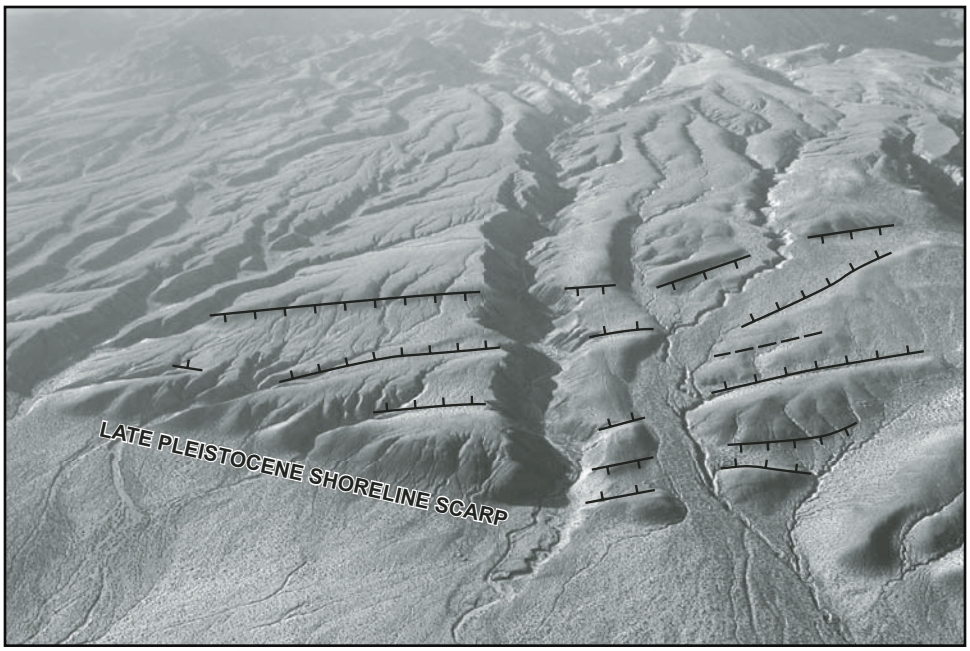

Figure 14. Oblique aerial view to the southeast of the northern Coso Range pediment surface broken up in a series of horst and graben by the Red Ridge fault zone (see Fig. 10 for location). The distance along the labeled shoreline scarp is ~1 km.

are displaced across a single fault are rare, several exist within the northern part of Owens Valley. Along the Fish Springs fault, a normal fault that splays from the Owens Valley fault south of the town of Big Pine (Fig. 15), throw appears to have been steady at rates of 0.2–0.3 mm/yr over the past ~300 k.y. (Martel et al., 1987; Zehfuss et al., 2001). Likewise, normal faulting along the Sierra Nevada frontal fault appears to have been steady (throw rates of 0.2–0.3 mm/yr) when averaged over the past ~120 k.y. but may have accelerated in the late Holocene (Le et al., 2007). On longer timescales, Gillespie (1991) argued that extension along the Sierra Nevada range front underwent a period of rapid slip in the middle Pleistocene, near the time of eruption of the Bishop Tuff (ca. 760 ka; Sarna-Wojcicki et al., 2000). Similarly, coordinated variations in oblique slip rate during the middle and late Pleistocene are argued to have occurred on the White Mountains fault zone and Fish Lake Valley faults (Kirby et al., 2006; Reheis and Sawyer, 1997). Resolution of the timescales over which such variations may have occurred, and the processes driving such behavior, requires increasingly precise chronology of fault slip over multiple temporal intervals.

The final insight that active deformation within Owens Valley can provide with regard to the eastern California shear zone as a whole is the question of the role played by distributed arrays of faults in accommodating active deformation. Although active extension across the southern Owens Valley appears to be concentrated on the Sierra Nevada frontal fault (Le et al., 2007), numerous subsidiary faults occur throughout the northern valley (Fig. 15), suggesting the possibility that extension rates vary from south to north.

Recent work in northern Owens Valley addresses aspects of each of these three issues. The key to surmounting uncertainties in paleoseismic estimates of slip rate, and to assessing spatial and temporal variations in fault slip, is to quantify fault slip over millennial timescales, long enough to average multiple seismic cycles yet short enough to capture potential variations in fault slip. Direct dating of landscape features, enabled by cosmogenic isotopic methods (Gosse and Phillips, 2001), affords this opportunity (e.g., Frankel et al., 2007a; Kirby et al., 2006; Oskin et al., 2007). In the following, new geologic estimates of fault slip along the primary strand of the northern Owens Valley fault are presented using displaced lava flows along the eastern flank of the Crater Mountain volcanic complex (Kirby et al., 2008). Preliminary results of ongoing efforts to develop a budget of late Quaternary extension across the valley are also presented, along with a brief discussion of the regional implications of this new work.

Slip Rate along the Northern Owens Valley Fault

For most of its length, the trace of the 1872 rupture along the Owens Valley fault runs near or within the floodplain of the Owens River, and long-term markers of fault displacement are rare (Beanland and Clark, 1994). South of the town of Big Pine (Stop 10; Figs. 1 and 15), the fault displaces basaltic lava flows along the eastern flank of Crater Mountain (Beanland and Clark, 1994), one of the largest vent complexes in the Big Pine volcanic field. Although the similarity in composition between flows makes correlation of individual flows across the fault difficult, an apparent right-lateral separation of the contact between the flow complex and alluvial fans is present at the northeastern corner of the cone (Fig. 16). The fault geometry defines a small releasing step at this site, and the pull-apart is filled with fine-grained, young alluvium. Potential uncertainties regarding the degree of burial and

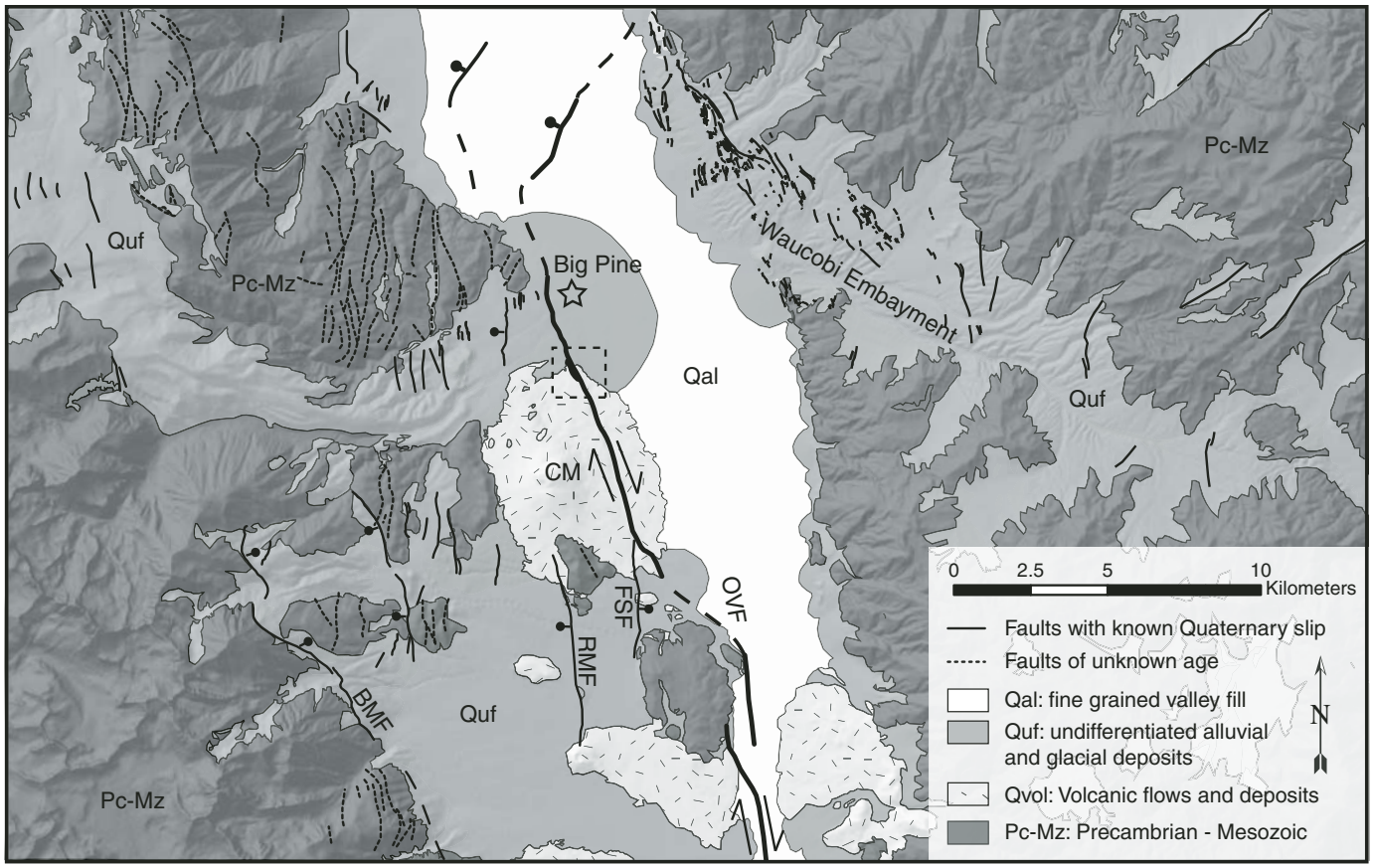

Figure 15. Simplified tectonic map of the Owens Valley region, near the town of Big Pine (star). Map modified from Bateman (1965). Faults shown as solid lines are known to displace late Quaternary surficial deposits, whereas those shown as dashed lines are inferred to have Quaternary slip. Box shows the location of Figure 16. CM—Crater Mountain; FSF—Fish Springs fault; OVF—Owens Valley fault; RMF—Red Mountain fault.

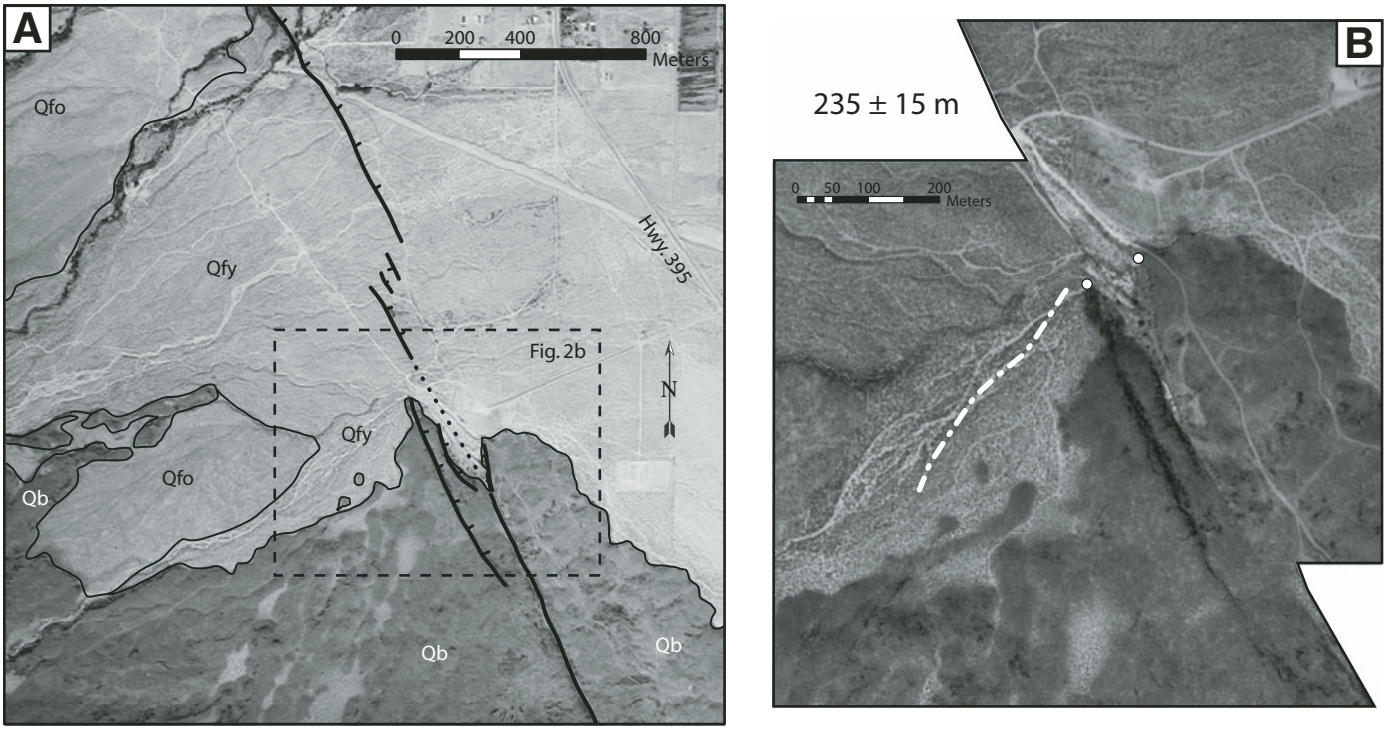

Figure 16. Displaced margin of the Crater Mountain flow complex near the Big Pine town dump (Stop 10, Fig. 1). (A) Geologic map of Owens Valley fault zone and Quaternary deposits overlain on air photo. Qb—Quaternary basalt; Qfo—older fan, likely equivalent to ca. 130 ka surface of Zehfuss et al. (2001); Qfy—young to active fan. (B) Retrodeformed displacement of ~235 m restores flow margin (circles). Dashed white line shows the approximate position of the buried flow margin west of the Owens Valley fault zone (after Kirby et al., 2008).

the subsurface geometry of the flow margin required assessment before this site could provide a robust constraint on fault slip.

To test the hypothesis that dextral separation of the flow margin observed at the surface (235 ± 15 m) is a reliable estimate of lateral slip along this segment of the Owens Valley fault, a ground-penetrating radar survey of the site was conducted (Kirby et al., 2008). The results of this survey confirm the presence of a shallowly buried flow margin to the west of the fault (Fig. 16), but do not reveal any basalt beneath the pull-apart itself. Rather, the flow margin appears to end abruptly against alluvium. Thus, Kirby et al. (2008) concluded that the horizontal component of fault slip at this site is ~235 m.

The age of the flow surface was estimated using the concentrations of cosmogenic ^{36}Cl in samples taken from well-preserved remnants of the flow surface. Samples were selected to minimize the chance of burial by eolian or alluvial material and were collected from outcrops that exhibited glassy surfaces representative of minimal surface lowering during weathering. Three samples were collected locally, on the west side of the fault, and three additional samples were collected from flows on the southwestern side of the vent complex, near the Red Mountain fault (Fig. 15). Because perfect surface preservation in this environment is extremely unlikely, exposure ages were modeled for a range of possible lowering rates (Kirby et al., 2008), and the resultant age ranges are taken as a best estimate of the age of the flow. Ages from both sample localities overlap within uncertainty, and indicate that the flow is 70 ± 14 ka (Kirby et al., 2008).

When combined with the displacement of the flow margin, these results imply that slip rates on the Owens Valley fault during this time period have been 3.6 ± 1.0 mm/yr. Notably, this range is consistent with, but at the high end of, previous estimates (Beanland and Clark, 1994; Lee et al., 2001b), and it is 2–3 times greater than Holocene estimates of Bacon and Pezzopane (2007). Whether these differences reflect spatial differences in slip between the northern and southern segments of the fault zone, or whether they represent a period of rapid slip prior to ca. 20–25 ka remains unknown (Kirby et al., 2008).

Distributed Extension across Northern Owens Valley

Ongoing work is focused on developing a budget for late Pleistocene extension across the northern part of Owens Valley. Here, a limited portion of this effort is discussed, focused on new estimates of the slip rate along the Red Mountain and Birch Mountain faults (Fig. 15).

The Red Mountain fault is a 10-km-long normal fault that extends south from the southwestern flank of Crater Mountain, subparallel to and ~2 km west of the Fish Springs fault (Stop 9; Figs. 1 and 15). It is marked along much of its trace by W-facing scarps that pond young alluvium in the hanging wall block. Despite its length and proximity to the Fish Springs fault, the Red Mountain structure has received considerably less attention, and the role of this fault in the extension budget across northern Owens Valley is essentially unknown.

At the northern end of the fault, lava flows from Crater Mountain are displaced in a W-side–down sense and have been subsequently buried by young alluvial fans emanating from Birch Creek. The flow itself buries an older alluvial fan surface with a moderately well-developed soil profile; surface characteristics of this fan suggest that it is likely equivalent to surfaces dated 2 km to the east at ca. 135 ka (Zehfuss et al., 2001), whereas the younger fan appears continuous with surfaces dated at 13–15 ka (Zehfuss et al., 2001). Chlorine-36 ages from the footwall exposures of the flow cluster at 70 ± 14 ka (Kirby et al., 2008) and are consistent with the regional chronology of Zehfuss et al. (2001). The flow surface has been offset vertically by 14.5 ± 1.5 m, and two small scarps are present in the youngest late Pleistocene surface that exhibit a combined throw of 2.5 ± 0.2 m. Both of these displacements are consistent with long-term vertical displacement rates along the Red Mountain fault of 0.2–0.3 mm/yr (Greene et al., 2007). Thus, this structure appears to play as great a role in the regional deformation field, as does the Fish Springs fault.

Significant slip is also present along the Sierra Nevada frontal fault at this latitude, as indicated by prominent scarps high on the range front (Fig. 17). The fault displaces sharp, triangular moraine crests in both the Tinemaha and Birch Creek drainages; moraines appear fresh, with minimal soil development and little to no weathering of boulder surfaces. Vertical displacements in both drainages are similar, ranging from 7 to 9 m (Fig. 17). Exposure ages derived from cosmogenic ^{36}Cl concentrations in five samples taken from boulders atop the northern lateral moraine in Tinemaha Creek cluster between 14–15 ka (Greene et al., 2007). Thus, vertical displacement rates on this segment of the Sierra Nevada frontal fault system appear to be relatively high, at 0.5–0.7 mm/yr. These rates may reflect relatively recent breaching of the relay between the northern tip of the southern Sierra Nevada frontal fault system and the southern tip of the Round Valley fault.

Regional Implications

From a regional perspective, these results contribute to an emerging picture of spatial variations in slip rate along the eastern California shear zone. Recent estimates of late Pleistocene slip rates along the Death Valley–Fish Lake Valley fault system suggest that slip rates decrease northward, from 4 to 5 mm/yr along the central section (Frankel et al., 2007a) to 2–3 mm/yr along the northern sections (Frankel et al., 2007b). In a similar fashion, right-lateral slip rates in the Owens Valley appear to decrease northward, from 3 to 4 mm/yr along the Owens Valley fault to ~0.5 mm/yr along the White Mountain fault zone (Kirby et al., 2006). These apparently systematic patterns suggest that simple approaches to reconciling geologic slip and geodetic strain by summing geologic slip along a two-dimensional transect are likely to be misleading. Although strain accumulation and release may reconcile across a given transect (e.g., Frankel et al., 2007a), the spatial distribution of strain in this young, evolving fault system appears be quite variable along strike.

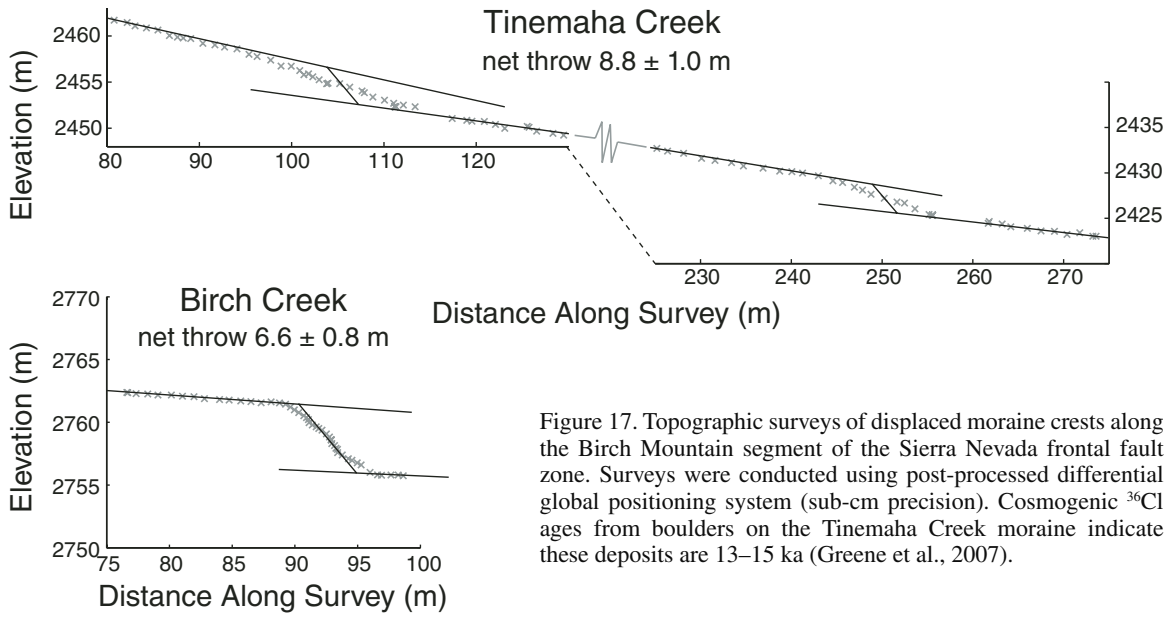

Figure 17. Topographic surveys of displaced moraine crests along the Birch Mountain segment of the Sierra Nevada frontal fault zone. Surveys were conducted using post-processed differential global positioning system (sub-cm precision). Cosmogenic ^{36}Cl ages from boulders on the Tinemaha Creek moraine indicate these deposits are 13–15 ka (Greene et al., 2007).

Summary

New estimates of late Quaternary deformation rates in the vicinity of Big Pine, California suggest that (1) slip rates along the northern Owens Valley fault zone over the past 55–85 k.y. are 3.6 ± 1.0 mm/yr, significantly higher than recent estimates along the southern portion of the fault zone, but similar to geodetic data, and (2) that extension rates associated with distributed fault arrays in the northern Owens Valley also appear to be higher than recent estimates in the southern Owens Valley. These results highlight spatial variations in late Quaternary slip rates throughout the eastern California shear zone and suggest caution in comparison of geologic slip rates with geodetic data along 2-D transects.

SPATIAL VARIATIONS IN LATE PLEISTOCENE SLIP RATE ALONG THE DEATH VALLEY–FISH LAKE VALLEY FAULT ZONE

The Death Valley–Fish Lake Valley fault zone is the largest and most continuous fault system in the eastern California shear zone, extending some 300 km northward from its intersection with the Garlock fault (Fig. 1). Both geologic and geodetic observations suggest that the Death Valley–Fish Lake Valley fault zone accommodates the majority of slip in the northern eastern California shear zone. Specifically, several space-based geodetic surveys show that, over the past ~15 yr, the Death Valley–Fish Lake Valley fault zone has been taking up 3–8 mm/yr of the measured 9.3 ± 0.2 mm/yr of Pacific–North America plate motion in the northern eastern California shear zone and Walker Lane (Bennett et al., 1997, 2003; Dixon et al., 1995, 2000, 2003; Humphreys and Weldon, 1994; McClusky et al., 2001; Savage et al., 1990; Wernicke et al., 2004). Along the northern part of the Death Valley–Fish Lake Valley fault zone in Fish Lake Valley, modeling of geodetic data shows the fault system is storing strain at 4–10 mm/yr and that the White Mountains fault zone, the other major strike-slip structure at this latitude, stores strain at 1–5 mm/yr (Dixon et al., 1995, 2000). The geodetic data, therefore, suggest that at latitude ~37.5°N, essentially all plate boundary strain in the eastern California shear zone is accommodated on these two structures.

Although numerous geodetic data are available from the region, only a few field-based studies have attempted to measure intermediate- and long-term (1,000–1,000,000 yr) geologic slip rates on the Death Valley–Fish Lake Valley fault zone (Brogan et al., 1991; Frankel, 2007; Frankel et al., 2007a, 2007b; Klinger, 2001; Reheis and Sawyer, 1997). A lack of geochronologic constraints on the age of offset alluvial landforms has thus made it difficult to compare rates of deformation over multiple time scales along this part of the plate boundary. Previous estimates of the late Pleistocene slip rate for the Death Valley–Fish Lake Valley fault zone in Fish Lake Valley range from 1 to 9 mm/yr (Reheis and Dixon, 1996; Reheis and Sawyer, 1997). However, recent work combining high-resolution ALSM digital topographic data with cosmogenic nuclide geochronology to investigate fault offsets and slip rates has helped refine the long-term slip rates in this region (Frankel, 2007; Frankel et al., 2007a, 2007b). These new results reveal spatial variations in the slip rate along the Death Valley–Fish Lake Valley fault zone and have important implications for eastern California shear zone and Pacific–North America plate boundary kinematics.

Faulting in Fish Lake Valley

The Death Valley–Fish Lake Valley fault zone bounds the east side of the White Mountains in Fish Lake Valley (Fig. 1).

This region makes up the northern 80 km of the Death Valley–Fish Lake Valley fault zone. Estimates of total dextral displacement along the northern Death Valley–Fish Lake Valley fault zone are thought to range from ~50 to 80 km since Cambrian to Middle Jurassic time (McKee, 1968; Stewart, 1967). More recent right lateral–oblique fault activity in Fish Lake Valley is characterized by numerous deformed geomorphic features, including fault scarps, displaced alluvial fans, offset drainage channels, shutter-ridges, and sag ponds (e.g., Brogan et al., 1991). An ALSM survey was recently conducted along the Death Valley–Fish Lake Valley fault zone in northern Death Valley and Fish Lake Valley to precisely map displacement on late Pleistocene and Holocene fault-related landforms (please see Frankel, 2007, and Frankel et al., 2007b for details about ALSM data collection and processing parameters). Results from two of the survey locations, the offset Furnace Creek and Indian Creek alluvial fans in Fish Lake Valley, are discussed below.

Furnace Creek Offset

The Furnace Creek alluvial fan in central Fish Lake Valley is located along the Oasis section of the Death Valley–Fish Lake Valley fault zone (Stop 11, Fig. 1; Brogan et al., 1991; Reheis and Sawyer, 1997). At this location, alluvial fans are offset along two parallel strands of the fault (Fig. 18). Previous work established a number of possible late Pleistocene channel displacements at Furnace Creek, ranging from 111 to >550 m (Brogan et al., 1991; Reheis et al., 1995; Reheis and Sawyer, 1997). ALSM data were used to determine more precise offset measurements. These high-resolution topographic data helped reveal subtle topographic features with hillshade, topographic, and slope aspect maps, topographic profiles, and thalweg positions to reconstruct a prominent drainage channel and the overall fan morphology (Fig. 18). Based on these data, Frankel et al. (2007b) revised the late Pleistocene strike-parallel displacement for the Furnace Creek alluvial fan to 290 ± 20 m (Fig. 18).

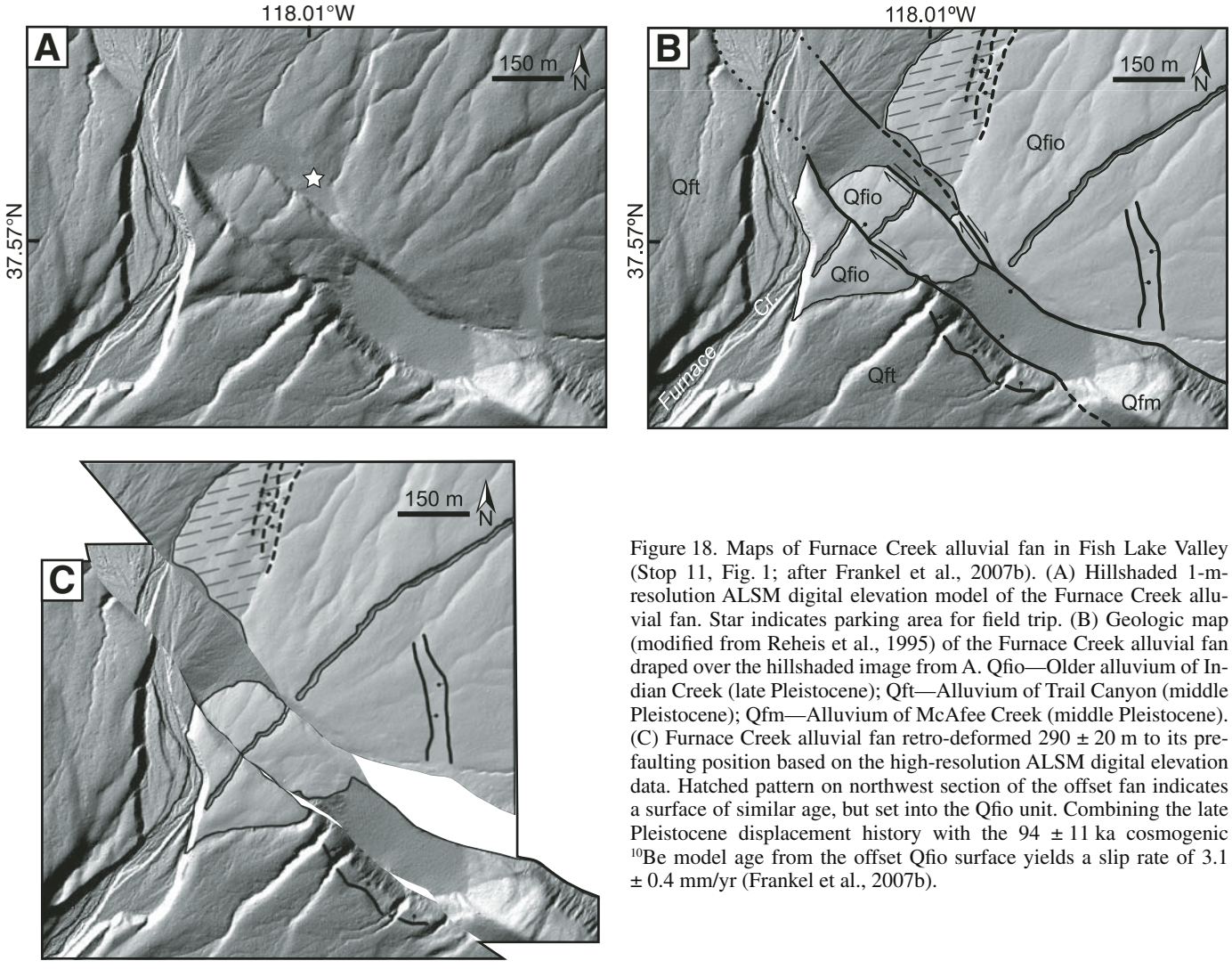

Figure 18. Maps of Furnace Creek alluvial fan in Fish Lake Valley (Stop 11, Fig. 1; after Frankel et al., 2007b). (A) Hillshaded 1-m-resolution ALSM digital elevation model of the Furnace Creek alluvial fan. Star indicates parking area for field trip. (B) Geologic map (modified from Reheis et al., 1995) of the Furnace Creek alluvial fan draped over the hillshaded image from A. Qfio—Older alluvium of Indian Creek (late Pleistocene); Qft—Alluvium of Trail Canyon (middle Pleistocene); Qfm—Alluvium of McAfee Creek (middle Pleistocene). (C) Furnace Creek alluvial fan retro-deformed 290 ± 20 m to its pre-faulting position based on the high-resolution ALSM digital elevation data. Hatched pattern on northwest section of the offset fan indicates a surface of similar age, but set into the Qfio unit. Combining the late Pleistocene displacement history with the 94 ± 11 ka cosmogenic ^{10}Be model age from the offset Qfio surface yields a slip rate of 3.1 ± 0.4 mm/yr (Frankel et al., 2007b).

Indian Creek Offset

The Indian Creek alluvial fan is located at the north end of Fish Lake Valley, near the northern termination of the Death Valley–Fish Lake Valley fault zone (Stop 12, Fig. 1). The fan is part of the Chiatovich Creek section of the Death Valley–Fish Lake Valley fault zone (Brogan et al., 1991; Reheis and Sawyer, 1997). Here, the fault zone splays into numerous normal faults, and the strike-slip component of deformation is localized along a single strand that displaces both late Pleistocene and Holocene alluvium (Fig. 19). Reheis et al. (1993) and Reheis and Sawyer (1997) estimated 83–165 m of late Pleistocene right-lateral deformation at this location based on a single offset debris flow channel. Hillshade, slope aspect, and topographic maps and channel thalwegs derived from ALSM data were used to revise the late Pleistocene displacement at Indian Creek to 178 ± 20 m by retrodeforming at least four, and possibly six, offset channels incised through the alluvial fan (Fig. 19; Frankel et al., 2007b).

Alluvial Fan Ages

Ages of the offset alluvial fans in Fish Lake Valley were previously estimated on the basis of soil development and surface morphology (e.g., Reheis et al., 1993, 1995; Reheis and Sawyer, 1997). Both the Furnace Creek and Indian Creek fans have similar soil and morphologic characteristics. The offset late Pleistocene fans have well-developed soils with a 5–10-cm-thick silty vesicular A horizon and an argillic B horizon with moderate clay-films and stage II to III carbonate development (Reheis and Sawyer, 1997). The fan surfaces are characterized by a moderately to well-developed desert pavement, moderate to dark desert varnish coatings on clasts ranging in size from pebbles to boulders, and subdued to moderately incised channels (Fig. 20).

Ages of the offset alluvial fans at Furnace Creek and Indian Creek were quantified by cosmogenic nuclide ^{10}Be geochronology (Frankel et al., 2007b; Gosse and Phillips, 2001). Geochronology samples were collected from the top 2–5 cm of large

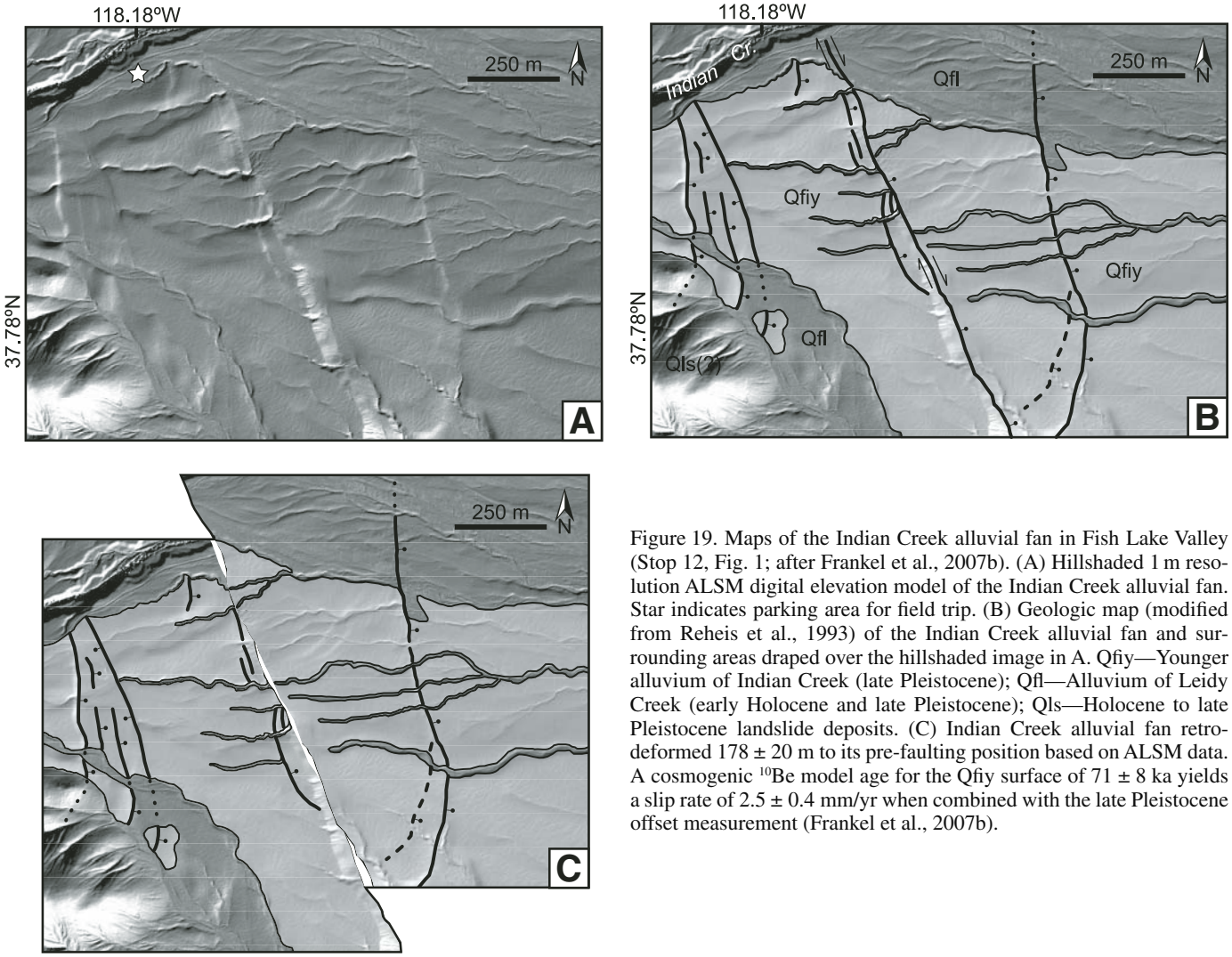

Figure 19. Maps of the Indian Creek alluvial fan in Fish Lake Valley (Stop 12, Fig. 1; after Frankel et al., 2007b). (A) Hillshaded 1 m resolution ALSM digital elevation model of the Indian Creek alluvial fan. Star indicates parking area for field trip. (B) Geologic map (modified from Reheis et al., 1993) of the Indian Creek alluvial fan and surrounding areas draped over the hillshaded image in A. Qfiy—Younger alluvium of Indian Creek (late Pleistocene); Qfl—Alluvium of Leidy Creek (early Holocene and late Pleistocene); Qls—Holocene to late Pleistocene landslide deposits. (C) Indian Creek alluvial fan retrodeformed 178 ± 20 m to its pre-faulting position based on ALSM data. A cosmogenic ^{10}Be model age for the Qfiy surface of 71 ± 8 ka yields a slip rate of 2.5 ± 0.4 mm/yr when combined with the late Pleistocene offset measurement (Frankel et al., 2007b).

Figure 20. Photograph looking west across the Furnace Creek alluvial fan. The White Mountains make up the distant skyline ridge. Boulder in the foreground is representative of locations from which samples were collected on the Furnace Creek and Indian Creek alluvial fans. Note the high degree of varnish development on the boulder surface. Boulders averaged ~115 × 90 × 85 cm at Furnace Creek and ~65 × 55 × 50 cm at Indian Creek.

boulders on the stable parts of offset fan surfaces mapped as Qfi by Reheis et al. (1993, 1995; Fig. 20) and analyzed by accelerator mass spectrometry at Lawrence Livermore National Laboratory (please see Frankel, 2007, and Frankel et al., 2007b, for geochronology methods and data).

Furnace Creek Fan Age

Eight cosmogenic ^{10}Be samples from the Qfio surface at Furnace Creek (Fig. 18; unit Qfi of Reheis et al., 1995) range in age from 79 ± 8 ka to 112 ± 8 ka (Frankel et al., 2007b). The relatively tight cluster of dates suggests that the Qfio surface has remained stable, with samples having been exposed to cosmic rays in their current configuration, since deposition. The age of the fan is taken to be the mean and standard deviation of the eight samples, which yields a date of 94 ± 11 ka (Frankel et al., 2007b). This age falls within the broad age range of 50–130 ka estimated for the Furnace Creek fan on the basis of soil development and surface morphology by Reheis and Sawyer (1997).

Indian Creek Fan Age

Eight cosmogenic ^{10}Be samples were also collected from the Qfiy surface (Fig. 19; unit Qfi of Reheis et al., 1993) at Indian Creek. These samples range in age from 59 ± 4 ka to 81 ± 6 ka (Frankel et al., 2007b). The samples from Indian Creek are somewhat younger than those from Furnace Creek, yet they display a similarly tight cluster, which is also interpreted to indicate the stability of the Qfiy surface since deposition. The mean and standard deviation of the eight ^{10}Be dates yields an age of 71 ± 8 ka for the Qfiy surface at Indian Creek, which is in agreement with the previously estimated range of 50–130 ka (Frankel et al., 2007b; Reheis and Sawyer, 1997).

Late Pleistocene Slip Rates in Fish Lake Valley

The cosmogenic ^{10}Be surface exposure dates from the Furnace Creek and Indian Creek fans are interpreted as maximum ages for the deposits because the channels used as piercing points must have formed at some undetermined time following fan deposition. The slip rates reported here should therefore be interpreted as minima, though it appears that most, if not all, of the right-lateral deformation accommodated on faults has been accounted for. The pervasive normal faulting observed on the eastern White Mountains piedmont is not considered in these rates.

Combining the displacement of 290 ± 20 m with the age of 94 ± 11 ka for the offset Qfio surface at Furnace Creek yields a late Pleistocene slip rate for the Oasis section of the Death Valley–Fish Lake Valley fault zone of 3.1 ± 0.4 mm/yr. Previous slip rate estimates at this location ranged from 1.5 to 9.3 mm/yr (Reheis and Sawyer, 1997). The 178 ± 20 m of displacement and 71 ± 8 ka age of the offset Qfiy surface at Indian Creek results in a slightly slower slip rate of 2.5 ± 0.4 mm/yr along the northern Chiatovich Creek section of the Death Valley–Fish Lake Valley fault zone. This rate falls within the bounds of the previous slip rate estimate of 1.1–3.3 mm/yr for this site (Reheis and Sawyer, 1997).

Spatial Variations in Slip Rate and Northern Eastern California Shear Zone Strain Distribution

Previous studies in the northern eastern California shear zone suggest that the down-to-the-NW faults located between the major strike-slip faults of the region transfer slip from the Owens Valley and Panamint Valley–Hunter Mountain–Saline Valley faults to the northern part of the Death Valley–Fish Lake Valley fault zone (Fig. 1; Dixon et al., 1995; Lee et al., 2001a; Reheis and Dixon, 1996). However, recent results from three slip rate sites along the Death Valley–Fish Lake Valley fault zone show that this may not be the case (Frankel et al., 2007a, 2007b).

The late Pleistocene slip rate along the Death Valley–Fish Lake Valley fault zone in northern Death Valley is ~4.5 mm/yr (Frankel et al., 2007a). The rates determined at the offset Furnace Creek and Indian Creek alluvial fans show that this rate decreases to ~2.5–3 mm/yr on the northern part of the Death Valley–Fish Lake Valley fault zone in Fish Lake Valley (Frankel et al., 2007b). The late Pleistocene slip rate on the White Mountains fault zone is 0.3–0.4 mm/yr (Kirby et al., 2006). Taken together, the late Pleistocene slip rates on the two major faults at latitude ~37.5°N are less than half the 9.3 ± 0.2 mm/yr region-wide rate of dextral shear determined from geodetic data (Bennett et al., 2003). This result suggests either that deformation at the latitude of Fish Lake Valley is accommodated on structures other than the White Mountains fault zone and Death Valley–Fish Lake Valley fault zone or that a strain transient exists in the northern eastern California shear zone, similar to that proposed for the Mojave Desert (Oskin and Iriondo, 2004; Oskin et al., 2006, 2007).

Strain rates appear to have remained constant in the northern eastern California shear zone over the past ~70 k.y. at the

latitude of northern Death Valley (Frankel et al., 2007a). If true, this implies that strain must be accommodated off the White Mountains and Death Valley–Fish Lake Valley fault zones, either to the west through Long Valley caldera (e.g., Kirby et al., 2006) or to the east from the Emigrant Peak fault zone through the Silver Peak–Lone Mountain extensional complex (Fig. 1; Oldow et al., 1994). If the faults to the east are indeed accommodating this additional strain, then the eastern California shear zone–Walker Lane transition must occur farther south, in a broader, more diffuse zone than previously recognized.

Summary

The late Pleistocene slip rate on the Death Valley–Fish Lake Valley fault zone decreases from ~4.5 mm/yr in northern Death Valley to ~3 mm/yr at Furnace Creek in central Fish Lake Valley and ~2.5 mm/yr at Indian Creek in northern Fish Lake Valley. Combining slip rates from the northern Death Valley–Fish Lake Valley and White Mountains fault zones, the two major faults at latitude ~37.5°N, indicates that the late Pleistocene rate of dextral shear is less than half that determined from geodetic data. This suggests either the existence of a strain transient in the northern eastern California shear zone or that deformation is distributed across other structures in the region.

SUMMARY

The eastern California shear zone accommodates the majority of Pacific–North America plate boundary motion east of the San Andreas fault. Therefore, deformation in this region is critical to our understanding of plate boundary kinematics, in addition to the behavior and evolution of fault systems. The studies presented in this guidebook are some of the most recent investigations undertaken in the region. We have highlighted new late Pleistocene slip rates in Owens Valley, Fish Lake Valley, and the Mojave Desert; discussed the timing and rates of offset along the Garlock fault; provided evidence for ~65 km of total cumulative right-lateral displacement across Owens Valley; and observed recent deformation associated with southern Owens Valley fault in the northwestern Coso Range. Together, the topics in this guidebook span the Cretaceous to late Holocene tectonic history of the eastern California shear zone.

As is often the case, much of this recent research, while generating a wealth of new data on slip rates, displacement histories, and fault kinematics, has brought about even more questions regarding spatial and temporal patterns of deformation in the eastern California shear zone. The eastern California shear zone provides a unique opportunity to study the kinematics of an evolving plate boundary. Continued work in the region, focused on defining rates of deformation across broad temporal (tens to millions of years) and spatial (tens to hundreds of kilometers) scales, will help fill gaps in our understanding of the role the eastern California shear zone plays in accommodating Pacific–North America plate boundary deformation.

FIELD GUIDE

This guide provides directions to field trip stops relative to nearby towns, landmarks, and major roads. It does not provide distances between individual stops. All field trip stop locations are keyed to the map in Figure 1. In addition, Universal Transverse Mercator (UTM) coordinates of all stops are provided in NAD83 datum, zone 11. It is preferable to have a high-clearance vehicle (and possibly 4WD, depending on road conditions) for many of the stops.

Day 1: Mojave Desert, Summit Range, and Red Rock Canyon

Stop 1: Lenwood Fault (Southern Offset)

Directions. This stop is located at UTM 507142E, 3844558N in Stoddard Valley, east of highway 247, ~10 mi south of Barstow, California. To reach the site from Interstate 15, exit at CA-247 (Barstow Road). Turn south on CA-247 and drive ~10 mi. The field site is located on Bureau of Land Management (BLM) route OM8, which is ~1 mi south of the Slash X Ranch Café, on the left. To locate the road, look for the end of barbed wire fence and a "Call Box" sign. Turn left on to BLM route OM8 immediately after the "Call Box" sign. There are several homesteads on OM8 on the way to the site, so please drive slowly to keep the dust down and watch for oncoming traffic. Take OM8 for ~4.5 mi. You will pass over a cattle guard. If you drive through a creek bed, then up a steep rocky section of the road ~4 m high, you've probably just passed it. Park in the flat area just before this rocky slope (Fig. 2).

Description. Figure 2 shows a hillshade map of this stop generated from a portion of the Lenwood fault ALSM survey (also see Fig. 21). A feature of particular interest at this location is a 100-m-wide pull-apart basin with slip partitioned onto several strands. A channel that crosses this basin appears offset ~45 m. Northwest of the pull-apart basin, fault displacement

Figure 21. Low-relief scarps of the Lenwood fault (in mid-ground; Stop 1). Photograph taken looking to the northeast.

formed a prominent SW-facing scarp cutting both $Q2_a$ and $Q2_b$ alluvial fans. Inset into the fans are younger channel-fill deposits also cut by low, SW-facing scarps in several localities. One of the larger channels crossing the fault is deflected ~270 m. Most of this deflection is due to construction of a $Q2_b$ alluvial fan in front of the channel. Two secondary faults form scarps in the late Pleistocene fans east of the main fault trace.

Stop 2: Lenwood Fault (Northern Offset)

Directions. This stop is located at UTM 501464E, 3851618N. The stop is ~3.5 mi from the highway. From Stop 1, return to CA-247 and turn right to go north. Approximately 1.5 mi north of the Slash X Ranch Café, bear right onto Stoddard Valley Road. The intersection is located 0.2 mi past the power lines with towers shaped like a Π symbol. Take this road straight back with no turns until you are past the first set of hills. Here, look for a dirt track cutting southeast, up the valley, to join the power-line road. Turn left onto the power-line road and ascend the hills. Note that it is also possible to drive the power-line road from CA-247; however, this route requires a very steep descent of the first set of hills. Once on the power-line road, stay left at the next three forks. Park at the fourth and final fork, located at the crest of the hills (Fig. 3). The Lenwood fault runs along the hillside, ~80 m below. Walk down the road to reach the fault. It is not recommended to drive down the hill, as the descent is dangerously steep and may require 4WD to ascend.

Description. Stop 2 features an ~600 m length section where the Lenwood fault is spectacularly exposed as a set of uphill-facing scarps and shutter ridges (Figs. 3 and 22). Southward, the fault crosses a wash and runs up the northeast side of a fault-line valley. The slip rate of the Lenwood fault was estimated here from deflection of a pair of channels located immediately NW of the road, and from a shutter ridge forming in front of the larger channel descending the fault-line valley. These channels are inset into outcrops of conglomerate and $Q2_b$ alluvial fan surfaces. Based on the 37 ± 7 ka age of $Q2_b$ determined from the southern site, the slip rate here is 0.8 ± 0.2 mm/yr.

Stop 3: Garlock Fault in Summit Range

Directions. This stop is located at UTM 445564E, 3924572N. This location is between Barstow and Ridgecrest, near the small town of Johannesburg. From Barstow, head east on CA-58 until it intersects with US-395. Go north on US-395 for ~27 mi to Trona Road. Turn east on Trona Road and continue for ~7.75 mi to the dirt road leading off to the west; park there.

Description. This stop is to introduce the main units in the Summit Range. This will be the basis for correlation/comparison with rocks in the Red Rock Canyon area (Stop 4). We will walk through the stratigraphy here to examine the various units (Figs. 5 and 23). First stops will be in the lower sedimentary sequence. We will then examine the lapilli tuff and its relation to underlying and overlying units. Lastly, we will look at the various tuffs overlying the lapilli tuff.

Stop 4: Garlock Fault in Red Rock Canyon

Directions. This stop is located at UTM 411017E, 3913555N. Red Rock Canyon is located 25 mi north of Mojave on CA-14, near Cantil. Signs on CA-14 clearly indicate the turnoff on Abbott Road. Go west on Abbott Road to the visitor center parking lot and park. From there, walk ~0.2 mi northeast to the outcrop.

Figure 22. View looking to the northwest at fault scarps and shutter-ridges along the Lenwood fault (Stop 2). Note truck on right side of photograph for scale.

Description. This stop will emphasize units of the Dove Spring Formation (Figs. 5 and 24). We start at the parking area east of the road and proceed up section. Our first stops are in the sedimentary and volcanic units below the lapilli tuff. First outcrops are the conglomerates in the Td_2 sequence. We will then work our way up-section into white tuffs below the thick lapilli tuff. Proceed then through the tuff looking at the possible cooling break in the middle of this massive unit. We will then look at (or hike westward to) the rocks above the tuff, including the basalt flows in the higher parts of the section.

Day 2: Little Lake, Cactus Flat, Coso Range, Independence Creek, and Birch Creek

Stop 5: Independence Dike Swarm at Little Lake

Directions. This stop is located at UTM 417369E, 3977338N, just west of Little Lake. Heading north on US-395, exit at the southernmost Little Lake Road exit. (NOTE: if approaching this stop from the north, this will be the second Little Lake Road exit; if approaching from the south, this will be the first Little Lake Road exit.) Cross to the west side of the highway and drive 0.1 mi for a view stop.

Description. This is stop 13 of Glazner et al. (2005). The Little Lake structural block (Fig. 8) exposed at this stop and in the mountains directly to the east is composed of Jurassic (165 Ma; Whitmarsh, 1998) plutonic rocks that vary in composition from diorite to leucogranite (mainly as a result of pervasive magma mingling) and lack a penetrative fabric. The heterogeneous plutonic complex is intruded by Jurassic (148 Ma; Whitmarsh, 1998) Independence dikes that vary in composition roughly as much as their wall rocks do. Because the dikes are more erosion-resistant than their wall rocks, most of the craggy outcrops on the hills to the east are dikes. A traverse of the skyline to the southeast of the stop yielded 9.1% dilation by dike intrusion (Fig. 8; Bartley et al., 2008).

Individual dikes in the Little Lake block range up to >10 m thick, yet any individual dike cannot be traced for more than 200 m because the dikes are transected by numerous NW- to N-striking ductile-brittle shear zones. The complete mismatch of dikes across each shear zone suggests that displacements across individual zones may be large. Shear zones commonly are exposed in numerous prospect pits that dot the area, and consist of greenschist-facies (white mica–chlorite–albite–epidote ± biotite) phyllonite. Most of the shear zones dip steeply to moderately westward (Fig. 9), and lineation and shear-sense indicators (S-C composite foliations, asymmetric porphyroclasts, mica fish)

Figure 23. Photograph looking southeast across the Summit Diggings volcanic field (Stop 3). The prominent ridge in the center of the photo is a N80E-striking, SSE-dipping sequence of tuffs capped by a distinctive pink lapilli ash-flow tuff. This outcrop is surrounded by a patchwork of tuffs, epiclastic rocks, and sedimentary rocks of the Bedrock Springs Formation. The photo is taken from the side of a dacite dome (dark-colored rocks in left foreground) which is part of a larger 12–11 Ma dome-flow-tuff complex. The tuffs occur in a topographically low valley that is likely related to formation of a small caldera resulting from the extrusion of the pink ash-flow tuff.

Figure 24. An ~125 m sequence of tuffs, epiclastic, and clastic units of the lower Dove Spring Formation, Ricardo Group, located on the north side of the Garlock Fault in the Red Rock Canyon State Park (Stop 4). The E-dipping normal fault through the sequence displaces the units ~25 m. The prominent white air fall tuffs are dated at older than 11 Ma. The capping pink lapilli ash-flow tuff correlates with the pink tuff found at the Summit Range, 34 km to the east on the south side of the Garlock Fault. The red and tan clastic units are also identical in lithology to those found in the Summit Range area that are attributed to the Bedrock Springs Formation.

indicate varying proportions of dextral and reverse displacement (Bartley et al., 2008). Shear zones decrease in abundance eastward toward the main axis of the Coso Range. Timing relations, kinematics, and spatial distribution of the shear zones suggest that they may be representative of structures that accommodated significant offset across Owens Valley.

Roadcuts along the microwave tower access road south of this stop expose rocks of the Sierran block, including granodiorite and granodiorite gneiss, variably intruded by 10–20-cm-thick mafic dikes, all of which are thoroughly shattered. Like plutonic rocks of the Little Lake block, the granodiorite yielded a U-Pb age near 165 Ma (Bartley et al., 2008), but geologic similarities between the Little Lake block and adjacent Sierra rocks end there. The granodiorite varies much less in composition than Little Lake plutonic rocks, contains a pervasive gneissic fabric that is locally migmatitic, and contains quartzite and calc-silicate rock xenoliths not seen in the Coso Range. Dikes in the granodiorite are uniformly mafic, rarely as thick as 1 m, vary widely in orientation, and account for only 1%–2% dilation. In areas where geochronology and cross-cutting relations distinguish Jurassic Independence dikes from associated Cretaceous dikes (Coleman et al., 2000; Mahan et al., 2003), all of these characteristics correspond to Cretaceous dikes.

Note that rocks of the Little Lake block are exposed on the west side of US-395 in low outcrops along the west side of Little Lake Road immediately north of here (on and around hill at UTM 417979E, 3977298N). There is an almost complete geologic mismatch between the Little Lake block and the adjacent Sierra Nevada, and it is inferred that the boundary in between, which is concealed by alluvium, is a locus of major tectonic offset.

Stop 6: Coso Dike at Cactus Flat

Directions. This stop is located at UTM 418900E, 4008439N, ~5 mi southeast of Olancha. From Olancha, drive south on US-395 ~1.5 mi to Cactus Flat Road (opposite the fire station). Turn east and drive past the pumice mine (mine is 4.2 mi from intersection of Cactus Flat Road and US-395). Two and a half miles beyond the mine, make a left turn on a narrow dirt road, and 0.4 mi beyond this, turn left at a side road at UTM 419210E, 4007018N. Continue down this road ~0.5 mi and park at UTM 419490E, 4007610N. An outcrop of the Coso dike is obvious in the hillside north-northwest of the parking area.

Description. This is Stop 11 of Glazner et al. (2005). Cretaceous dikes in the Coso Range were first described by Duffield et al. (1980) as steeply dipping, W-striking, conspicuously K-feldspar and quartz-phyric granitic dikes that are up to 10 m thick. Whitmarsh (1998) named these dikes the Coso dike swarm, mapped the dikes in significant detail, and obtained a preliminary U-Pb zircon date of ca. 84 Ma from a thick dike in the swarm exposed near Upper Centennial Flat. One of us (Glazner) made a reconnaissance trip into the Coso Range in 1996 and noted the strong similarity between the Coso and Golden Bear dikes and proposed that the two areas might once have been contiguous. Kylander-Clark (2003) tested this correlation and found identical ages of 83.5 Ma for the two swarms, overlapping geochemistry, and similar, unique wall rocks (102 Ma leucogranite) that strongly support correlation of the two areas and ~65 km of dextral displacement.

At this locality, the Coso dike (Fig. 25) is >20 m wide, strikes 281°, and dips ~80°N. The quartz monzonite porphyry contains 1–5-cm-long euhedral K-feldspar phenocrysts that locally contain Carlsbad twins. Plagioclase occurs as small (2–4 mm) subhedral, subequant grains. Quartz occurs in euhedral

Figure 25. Westernmost outcrop of Coso dike swarm in the Coso Range (Stop 6). View is to the northwest from Cactus Flat. The dike is ~20 m thick, strikes W, and forms the prominent crags on skyline; the skyline behind is underlain by Pliocene mafic volcanic rocks that overlap the dike.

bipyramids that range from 2 to 8 mm in diameter. Biotite is the major mafic mineral, occurring as small (typically 1 mm) subhedral to euhedral grains. Looking east, the dike continues on strike, but is difficult to follow from a distance.

Stop 7: Northern Coso Range Piedmont

Directions. This stop is located at UTM 413630E, 4019852N. From Olancha, head east on CA-190, ~3.5 mi from the intersection with US-395 (~1 mi west of the well-marked road to Dirty Sock Corporation Yard) and park on the side of the road along the broad shoulder.

Description. The thing to look at, stand on, and walk around here is evidence for surface rupture during the 1872 Owens Valley earthquake. With a little searching, you will find a series of right-laterally displaced Holocene beach ridges on the north side of the highway that were discovered by Burt Slemmons and his colleagues ~30 years ago and that are on trend with the Owens Valley fault to the north where it heads into the playa from Bartlett Point (Fig. 11). Slemmons et al. (2008) argue that the offset beach ridges indicate that surface rupture during the 1872 earthquake extended all the way to the Coso Range piedmont, rather than dying out at Bartlett Point as suggested by Beanland and Clark (1994).

Once you find the offset beach ridges, look to the southeast to view tectonic-geomorphic evidence for dextral shear extending from the southern end of the Owens Valley fault into the northwest Coso Range. There is a large push-up ridge ~3 km south of the road where the fault zone that offsets the beach ridges terminates or makes a left step. About 3–4 km south of the road is a high, N-facing wave-cut scarp at ~1160 m (3800 ft) elevation along the northern Coso Range piedmont. This scarp was last inundated ca. 24 ka during a Tioga-age pluvial highstand of Owens Lake. The wave-cut scarp is visibly warped into a series of low-amplitude folds associated with a fault zone that transfers slip from Owens Valley southward through the Coso Range to the Airport Lake fault zone in Indian Wells Valley. These structures comprise the eastern tectonic margin of the Sierra Nevada microplate at this latitude.

Stop 8: Golden Bear Dike Near Independence Creek

Directions. This stop is located at UTM 387410E, 4068329N along the Sierra Nevada range front southeast of Independence. From the center of Independence, drive 4.5 mi west on Onion Valley Road. Turn south on Foothill Road and continue for 1.5 mi to the foot of the boulder-covered hill and park on the side of the road.

Description. This is Stop 6 of Glazner et al. (2005). The Golden Bear dike crops out from the valley floor to the range crest and beyond, crossing the crest north of Forester Pass to eventually peter out in the headwaters of the Kern River (Fig. 6). Looking west from this locality, it is possible to trace the dike from the foothills up the range front to the crest of the Sierra Nevada (Fig. 26). Here, in the foothills, the dike is shattered and dismembered due to range-front faulting and landsliding. However, most of the large boulders mantling the slope are distinctive porphyritic Golden Bear dike. West of the Independence fault (Moore, 1963), the dike is intact, strikes nearly E-W, dips steeply, and is 10–15 m wide. Here we will see large float boulders of the dike and gain an appreciation for its width the last time it is exposed passing east into Owens Valley.

The Golden Bear dike is a K-feldspar quartz monzonite porphyry with euhedral zoned phenocrysts of K-feldspar that range 2–4 cm in length and commonly display Carlsbad twins.

Figure 26. Golden Bear dike on the south side of Pinyon Creek drainage, eastern flank of Sierra Nevada, viewed looking west from Onion Valley Road. Dashed lines follow the outcrop trace of the dike. The prominent peak, Mount Bradley (13,289 ft, 4050 m), is carved in the 102 Ma Bullfrog leucogranite, another tie point across Owens Valley. Stop 8 is along the range front just left (south) of photo.

Plagioclase is subhedral, subequant, and typically 1–4 mm in diameter. Quartz typically occurs as distinctive equant, euhedral, and bipyramidal crystals 2–5 mm in diameter. Mafic minerals include both biotite and rare hornblende.

Stop 9: Red Mountain Fault at Birch Creek

Directions. This stop is located at UTM 384884E, 4103959N. From Big Pine, head south on US-395 ~5 mi to North Fish Springs Road. Turn west (right) on North Fish Springs Road and continue until it begins to bend back to the east (toward US-395). At the bend (a large triangular intersection), head west on Tinemaha Road. Bear to the right after 300 m, at the base of the Poverty Hills. Birch Creek Road will appear as a dirt road on the right on a very gentle right-hand turn (almost straight) parallel to the creek. This road passes through a cluster of homes, crosses Birch Creek, and then turns back to the west to parallel the creek again. Continue up the switchbacks onto the alluvial fan surface. Stay to the left (straight) at the intersection with a power-line road. The road then veers to the northwest away from Birch Creek toward the granitic Fish Springs Hills. Take the first left, following Birch Creek Road back to the southwest (toward Birch Creek). In ~0.6 mi, the road descends at a W-facing scarp. Park just west of the scarp at UTM 384964E, 4103425N. Walk ~400 m north along the scarp to the large gully.

Description. Although recent extension across the southern Owens Valley, near the town of Lone Pine, is primarily accomplished by slip on the Sierra Nevada frontal fault (Le et al., 2007), the geometry and distribution of recent faulting changes markedly in the northern part of the valley (Fig. 1). North-striking normal faults occur in distributed arrays that extend from the foot of the range across the western piedmont to the Owens Valley fault. The best known of these structures is the Fish Springs fault, a W-side-down normal fault that forms the large scarp ~2 km east of this location. Slip on this structure appears to have been dip and relatively steady at throw rates of 0.2–0.3 mm/yr (Martel et al., 1987; Zehfuss et al., 2001) since ca. 330 ka. The association of this structure with the surface trace of the Owens Valley fault has led most workers to consider them part of the same fault zone. However, the broad array of normal faults of similar orientation north and west of this location suggests that the Fish Springs fault may be simply one of a distributed array of normal faults that accommodate extension across the Owens Valley at this latitude. The goal of this stop is to examine evidence for the rates of displacement along a couple of these structures.

This stop begins at the W-facing scarp of the Red Mountain fault where it displaces alluvial fan deposits of Birch Creek (presently deeply incised to the south of the parking spot; Fig. 27). The topographic expression of the fault is not particularly impressive (a few meters), due to the fact that fan aggradation during and shortly after the last glacial maximum (Zehfuss et al., 2001) on the downthrown hanging-wall block has largely filled the accommodation space. Just north of the road, bouldery surfaces of this fan spill over the scarp and are continuous with sites to the east, dated by Zehfuss et al. (2001) at 13–15 ka (Fig. 27). Approximately 100 m north of the Birch Creek road, two small (~1 m) scarps are present within this alluvial surface. These likely represent the most recent rupture along the Red Mountain fault, and, if representative of average slip, would imply single event throw rates of ~0.2 mm/yr.

The Red Mountain fault also displaces lava flows along the southwestern flank of Crater Mountain. Continue northward along the fault scarp, until you reach a large gully draining through the Fish Springs Hills (~300 m). East of this gully, flows are exposed capping a fan deposit with a moderately well-developed soil profile. West of the gully, the flow has been displaced vertically ~12–14 m and buried by younger alluvium. Cosmogenic ^{36}Cl

Figure 27. Field photograph taken looking toward the northeast at a scarp of the Owens Valley fault zone at Birch Creek in Owens Valley (Stop 9). Ridges in the background are the Fish Springs Hills.

ages from the flow surface indicate that the flow is 70 ± 14 ka (Kirby et al., 2008) and suggest late Pleistocene throw rates of ~0.2 mm/yr. Thus, the Red Mountain fault appears to exhibit similar slip rates to the Fish Springs fault.

From this vantage, one can see the Birch Mountain fault, the northernmost segment of the Sierra Nevada frontal fault system. The scarp is apparent south of Tinemaha Creek, where it displaces steep talus and debris-cones at the base of the range, and north of the creek, as it trends upslope toward the prominent cliff at the base of Birch Mountain. The fault displaces Tioga-age moraines in both the Tinemaha and Birch Creek drainages (Fig. 17). Total throw on the structure in these localities varies from 7 to 9 m, and ^{36}Cl ages of boulders from the moraine crest in Tinemaha Creek indicate an age of 13–15 ka (Greene et al., 2007). Thus, throw rates on this segment of the Sierra Nevada frontal fault are ~0.5–0.7 mm/yr Notably, these rates are two to three times greater than those measured along the southern segments of this fault system (Le et al., 2007).

Day 3: Big Pine, Furnace Creek, Indian Creek

Stop 10: Owens Valley Fault at Big Pine Dump

Directions. This stop is located at UTM 385102E, 4111923N. Just before entering Big Pine from the south on US-395, turn west (left) on Big Pine Dump Road. At the trash/recycling facility, stay to the left onto the dirt road. Stay straight (west) until the intersection with a power-line road. From here, you will see the old town dump. Drive just past the old dump and park under the power lines (~0.3 mi from start of dirt road). Watch out for old nails.

Description. At this stop, we will examine evidence for long-term lateral displacement along the Owens Valley fault. From the parking lot near the recycling center, walk west along the dirt road for ~300 m. The high-tension power lines visible to the west mark the approximate trace of the Owens Valley fault through this locality. The E-facing scarp of the fault within basalt flows from Crater Mountain is visible as a ~5–7 m high, broken cliff (Fig. 28). At the base of this scarp, fine-grained alluvium has filled a small extensional step in the fault zone. Anthropogenic activity (the historic town dump) has obliterated any trace of the 1872 rupture through this alluvium, although a strand of the fault is visible as a small scarp ~300 m north of this locality (Beanland and Clark, 1994).

The apparent right-lateral separation of the flow margin with the modern alluvium is interpreted to reflect dextral displacement across the fault (Kirby et al., 2008). Subsurface surveys using ground-penetrating radar do not reveal any shallow reflectors associated with a buried flow margin on the east side of the fault. Rather, the flow margin visible on the surface appears to represent the former extent of the flow (Kirby et al., 2008). West of the fault, however, young alluvial material did bury the flow margin; prominent islands of basalt are visible above alluvium (Fig. 16). Surveys in this region suggest that the flow margin extends to a position near the prominent protrusion of basalt along the fault scarp (Fig. 16). Restoration of this margin with the exposed flow on the east side of the fault suggests ~235 ± 15 m of lateral displacement along the Owens Valley fault in the past 70 ± 14 k.y. Thus, right-lateral slip rates along the northern Owens Valley fault appear to have been 3.6 ± 1.0 mm/yr over the past 56–80 k.y. (Kirby et al., 2008).

Stop 11: Fish Lake Valley Fault at Furnace Creek

Directions. This stop is located at UTM 410935E, 4158364N. From Big Pine, take CA-168 east over Westgaard Pass. Continue on CA-168 through Deep Springs Valley to Fish Lake Valley. At the intersection of CA-168 and CA-266 in Oasis, turn north on

Figure 28. Photograph taken looking to the west at fault scarps of the Owens Valley fault zone cutting basalt on the northeast side of Crater Mountain near the Big Pine town dump (Stop 10). Peaks along the eastern Sierra Nevada are visible beyond the scarps.

Figure 29. View to the northwest along the Death Valley–Fish Lake Valley fault zone at Furnace Creek in central Fish Lake Valley (Stop 11). Note the two prominent fault scarps cutting the Furnace Creek alluvial fan. White Mountain Peak is the prominent summit along the skyline ridge.

CA-266 and go ~7.1 mi to a dirt track leading off to the west (just north of White Wolf Canyon Road to the east). Go ~1.5 mi toward the large shutter-ridge. Continue on the dirt track, bearing to the northwest and paralleling the fault, for another 0.3 mi and park near the incised channel (Fig. 18). Walk ~0.1 mi west up the westernmost fault scarp to the apex of the fan.

Description. Just south of the canyon mouth at Furnace Creek, the Fish Lake Valley fault is exposed as two parallel NW-striking strands displacing a late Pleistocene alluvial fan complex (Fig. 29; Frankel et al., 2007b; Reheis et al., 1995; Reheis and Sawyer, 1997). Prominent scarps are exposed in the alluvial fans with the western strand dipping to the NE and the eastern strand dipping to the SW, and with other small normal fault scarps scattered across the fan surfaces (Reheis et al., 1995). The area between the two fault strands is down-dropped in a small pull-apart basin (parking area is at the northern end of this pull-apart structure). Just south of the offset late Pleistocene fan is a large NW-SE–striking shutter-ridge, which is bounded on its northeast and southwest sides by the two fault strands (Reheis et al., 1995).

Although a number of alluvial fan surfaces are mapped in this location (Reheis et al., 1995), the primary surface of interest is the late Pleistocene Qfio deposit (Qfi of Reheis et al., 1995), which is displaced by the fault (Fig. 18). Cosmogenic nuclide ^{10}Be dates from the Qfio surface yield an age of 94 ± 11 ka (Frankel et al., 2007b).

A recent reexamination of offset channels at this location using ALSM data revised the late Pleistocene offset to 290 ± 20 m (Fig. 18; Frankel et al., 2007b). Combining the 290 ± 20 m of displacement determined from ALSM topography with the cosmogenic ^{10}Be age of 94 ± 11 ka for the Qfio surface yields a minimum late Pleistocene, right-lateral slip rate of 3.1 ± 0.4 mm/yr for the Fish Lake Valley fault zone at Furnace Creek (Frankel et al., 2007b).

Stop 12: Fish Lake Valley Fault at Indian Creek

Directions. This stop is located at UTM 396137E, 4182771N. From Dyer, Nevada, head ~8.5 mi north on NV-264 (~16.8 mi north of the California-Nevada border). Turn west on Indian Creek Road (dirt) and continue for ~5 mi until you reach the prominent E-facing scarp near the canyon mouth at UTM 395992E, 4183225N. Park just west of the scarp on the south side of the road (Fig. 19). Walk ~0.3 mi south along the base of the scarp to the third deeply incised channel cutting the footwall. Climb up to the top of the scarp at this location for a good view of the fault zone.

Description. The fault scarps at Indian Creek are located at the northern end of the northern Death Valley–Fish Lake Valley fault system. The fault zone splays into numerous normal faults in this location (Reheis et al., 1993), however, a significant strike-slip component is still present (Fig. 19; Frankel et al., 2007b; Reheis et al., 1993; Reheis and Sawyer, 1997). Most of the faulting at this site displaces the late Pleistocene Qfiy surface (Figs. 19 and 30; Qfi of Reheis et al., 1993). The dextral component of slip at this location is restricted to a single strand of the fault near the eastern range-front of the White Mountains (Fig. 19). The strike-slip component of the fault zone is expressed as a prominent scarp cutting the Qfiy and Qfl surfaces (Frankel et al., 2007b; Reheis et al. 1993; Reheis and Sawyer, 1997).

The Qfiy surface at Indian Creek has a similar set of soil and morphologic characteristics as the Qfio surface at Furnace Creek. Eight tightly clustered cosmogenic nuclide ^{10}Be surface exposure dates from boulders on the Qfiy fan surface have a mean age and standard deviation of 71 ± 8 ka (Frankel et al., 2007b). Frankel et al. (2007b) used ALSM data to revise the late Pleistocene displacement history to 178 ± 20 m on the basis of six offset channels (Fig. 19). A late Pleistocene slip rate of 2.5 ± 0.4 mm/yr results from the offset determined with ALSM

Figure 30. Photograph looking southwest along the right-lateral oblique fault scarp at Indian Creek in Fish Lake Valley at the northern end of the Death Valley–Fish Lake Valley fault zone (Stop 12). The eastern White Mountains range front is visible beyond the scarp. Numerous normal faults displace the distal portion of the Indian Creek; all dextral deformation at this location is accommodated on the pictured fault.

data combined with the 71 ± 8 ka ^{10}Be age of the Qfiy surface at Indian Creek (Frankel et al., 2007b).

ACKNOWLEDGMENTS

Research presented in this guidebook was supported by the National Science Foundation (NSF), the Geothermal Program Office of the China Lake Naval Air Warfare Center, the Southern California Earthquake Center (SCEC), the National Aeronautics and Space Administration, Lawrence Livermore National Laboratory, The Geological Society of America, and the University of California White Mountain Research Station. SCEC is funded by NSF Cooperative Agreement EAR-0106924 and U.S. Geological Survey Cooperative Agreement 02HQAG0008. This is SCEC contribution 1131. ALSM data were collected by the National Center for Airborne Laser Mapping at the University of Florida. A number of people contributed to the work presented in this field guide, including S. Briggs, D. Burbank, N. Dawers, J. Helms, E. Hauksson, J. Hoeft, B. Miller, M. Reheis, M. Rogers, G. Roquemore, T. Sheehan, D. Slemmons, and R. Whitmarsh. Thoughtful reviews by Ernie Duebendorfer and Nathan Niemi helped improve the clarity and presentation of this field trip guidebook.

REFERENCES CITED

Argus, D.F., and Gordon, R.G., 1991, Current Sierra Nevada–North America motion from very long baseline interferometry: implications for the kinematics of the western United States: Geology, v. 19, p. 1085–1088, doi: 10.1130/0091-7613(1991)019<1085:CSNNAM>2.3.CO;2.

Argus, D.F., and Gordon, R.G., 2001, Present tectonic motion across the Coast Ranges and San Andreas fault system in central California: Geological Society of America Bulletin, v. 113, p. 1580–1592, doi: 10.1130/0016-7606(2001)113<1580:PTMATC>2.0.CO;2.

Atwater, T., 1989, Plate tectonic history of the northeast Pacific and western North America, *in* Winterer, E.L., Hussong, D.M., and Decker, R.W., eds., The eastern Pacific Ocean and Hawaii: Boulder, Colorado, Geological Society of America, The Geology of North America, v. N, p. 21–72.

Atwater, T., and Stock, J., 1998, Pacific–North America plate tectonics of the Neogene southwestern United States: An update: International Geology Review, v. 40, p. 375–402.

Bacon, S.N., and Pezzopane, S.K., 2007, A 25,000-year record of earthquakes on the Owens Valley fault near Lone Pine, California: Implications for recurrence intervals, slip rates, and segmentation models: Geological Society of America Bulletin, v. 119, p. 823–847, doi: 10.1130/B25879.1

Bacon, S.N., Burke, R.M., Pezzopane, S.K., and Jayko, A.S., 2006, Last glacial maximum and Holocene lake levels of Owens Lake, eastern California, USA: Quaternary Science Reviews, v. 25, p. 1264–1282, doi: 10.1016/j.quascirev.2005.10.014.

Bartley, J.M., Glazner, A.F., Coleman, D.S., Kylander-Clark, A.R.C., Mapes, R., and Friedrich, A.M., 2008, Large Laramide dextral offset across Owens Valley, California, and its possible relation to tectonic unroofing of the southern Sierra Nevada, *in* Till, A.B., Roeske, S.M., Foster, D.A. and Sample, J.C., eds., Exhumation Processes along Major Continental Strike-slip Fault Systems: Geological Society of America Special Paper 434, p. 129–148, doi: 10.1130/2007.2343(07).

Bateman, P.C., 1965, Geology and Tungsten Mineralization of the Bishop District California: Washington, D.C., U.S. Geological Survey Professional Paper 470, 208 p.

Beanland, S., and Clark, M.M., 1994, The Owens Valley fault zone, eastern California, and surface rupture associated with the 1872 earthquake: U.S. Geological Survey Bulletin 1982, 29 p.

Bellier, O., and Zoback, M.L., 1995, Recent state of stress change in the Walker Lane zone, western Basin and Range province, United States: Tectonics, v. 14, no. 3, p. 564–593, doi: 10.1029/94TC00596.

Bennett, R.A., Wernicke, B.P., Davis, J.L., Elosegui, P., Snow, J.K., Abolins, M., House, M.A., Stirewalt, G.L., and Ferrill, D.A., 1997, Global positioning system constraints on fault slip rates in the Death Valley region, California and Nevada: Geophysical Research Letters, v. 24, p. 3073–3076, doi: 10.1029/97GL02951.

Bennett, R., Wernicke, B.P., Niemi, N.A., Friedrich, A.M., and Davis, J.L., 2003, Contemporary strain rates in the northern Basin and Range province from GPS data: Tectonics, v. 22, doi: 10.1029/2001TC001355

Bennett, R.A., Friedrich, A.M., and Furlong, K.P., 2004, Codependent histories of the San Andreas and San Jacinto fault zones from inversion of fault displacement rates: Geology, v. 32, p. 961–964, doi: 10.1130/G20806.1.

Bierman, P.R., Gillespie, A.R., and Caffee, M.W., 1995, Cosmogenic ages for earthquake recurrence intervals and debris flow fan deposition, Owens Valley, California: Science, v. 270, p. 447–449, doi: 10.1126/science.270.5235.447.

Brogan, G.E., Kellog, K.S., Slemmons, D.B., and Terhune, C.L., 1991, Late Quaternary faulting along the Death Valley-Furnace Creek fault system, California and Nevada: U.S. Geological Survey Bulletin 1991, 23 p.

Bull, W.B., 1991, Geomorphic responses to climatic change: New York, Oxford University Press, 326 p.

Burbank, D.W., and Whistler, D.P., 1987, Temporally constrained tectonic relations derived from magnetostratigraphic data: Implications for the initiation of the Garlock fault, California: Geology, v. 15, p. 1172–1175, doi: 10.1130/0091-7613(1987)15<1172:TCTRDF>2.0.CO;2.

Burchfiel, B.C., Hodges, K.V., and Royden, L.H., 1987, Geology of Panamint Valley–Saline Valley pull-apart system, California-Palinspastic evidence for low-angle geometry of a Neogene range-bounding fault: Journal of Geophysical Research, v. 92, p. 10,422–10,426.

Carl, B.S., and Glazner, A.F., 2002, Extent and significance of the Independence dike swarm, eastern California, *in* Glazner, A.F., Walker, J.D., and Bartley, J.M., eds., Geologic evolution of the Mojave Desert and Southwestern Basin and Range: Geological Society of America Memoir 195, p. 117–130.

Carleton, C.F., 1988, Tectonic Significance of Late Miocene Deposits in the Southern Fry Mountains, Mojave Desert, California [M.S. Thesis]: Riverside, University of California, 130 p.

Carter, B.A., 1980, Quaternary displacement on the Garlock fault, California, *in* Fife, D.L., and Brown, A.R., eds., Geology and mineral wealth of the California desert: Santa Ana, California, South Coast Geological Society Guidebook, Dibblee Volume, p. 457–466.

Calzia, J.P., and Ramo, O.T., 2000, Late Cenozoic crustal extension and magmatism, southern Death Valley region, California, *in* Lageson, D.R., Peters, S.G., and Lahren, M.M., eds., Great Basin and Sierra Nevada: Geological Society of America Field Guide 2, p. 135–164.

Chen, J.H., and Moore, J.G., 1982, Uranium-lead isotopic ages from the Sierra Nevada batholith, California: Journal of Geophysical Research, v. 87, p. 4761–4784.

Coleman, D.S., Glazner, A.F., Bartley, J.M., and Carl, B.S., 2000, Cretaceous dikes within the Jurassic Independence dike swarm in eastern California: Geological Society of America Bulletin, v. 112, p. 504–511, doi: 10.1130/0016-7606(2000)112<0504:CDWTJI>2.3.CO;2.

Davis, G.A., and Burchfiel, B.C., 1973, Garlock fault: An intracontinental transform structure, southern California: Geological Society of America Bulletin, v. 84, p. 1407–1422, doi: 10.1130/0016-7606(1973)84<1407:GFAITS>2.0.CO;2.

Dawson, T.E., McGill, S.F., and Rockwell, T.K., 2003, Irregular recurrence of paleoearthquakes along the central Garlock fault near El Paso Peaks, California: Journal of Geophysical Research, v. 108, doi: 10.1029/2001JB001744

Dibblee, T.W., Jr., 1967, Areal geology of the western Mojave Desert, California: U.S. Geological Survey Professional Paper 522, 153 p.

Dibblee, T.W., 1970, Geologic map of the Daggett quadrangle, San Bernardino County, California: U.S. Geological Survey Miscellaneous Geologic Investigations Map I-592, scale 1:62,500.

Diggles, M.F., 1987, Mineral resource potential map of the South Sierra Wilderness and the South Sierra Roadless Area, Inyo and Tulare Counties, California: U.S. Geological Survey Map MF-1913-A, scale 1:48,000.

Diggles, M.F., Dellinger, D., and Conrad, J., 1987, Geologic map of the Owens Peak and Little Lake Canyon Wilderness Study areas, Inyo and Kern Counties, California: U.S. Geological Survey Map MF-1927-A, scale 1:48,000.

Dixon, T.H., Robaudo, S., Lee, J., and Reheis, M.C., 1995, Constraints on present-day Basin and Range deformation from space geodesy: Tectonics, v. 14, p. 755–772, doi: 10.1029/95TC00931.

Dixon, T.H., Miller, M., Farina, F., Wang, H., and Johnson, D., 2000, Present-day motion of the Sierra Nevada block and some tectonic implications for the basin and Range province: North American Cordillera: Tectonics, v. 19, p. 1–24, doi: 10.1029/1998TC001088.

Dixon, T.H., Norabuena, E., and Hotaling, L., 2003, Paleoseismology and Global Positioning System: Earthquake-cycle effects and geodetic versus geologic fault slip rates in the Eastern California shear zone: Geology, v. 31, p. 55–58, doi: 10.1130/0091-7613(2003)031<0055:PAGPSE>2.0.CO;2.

Dokka, R.K., and Travis, C.J., 1990, Late-Cenozoic strike-slip faulting in the Mojave Desert, California: Tectonics, v. 9, p. 311–340.

Dolan, J.F., Bowman, D.D., and Sammis, C.G., 2007, Long-range and long-term fault interactions in southern California: Geology, v. 35, p. 855–858, doi: 10.1130/G23789A.1.

Dooley, T., Monastero, F.C., Hall, B., McClay, K., and Whitehouse, P., 2004, Scaled sandbox modeling of transtensional pull-apart basin—Applications to the Coso geothermal system: Geothermal Resources Council Transactions, v. 28, p. 637–641.

Duffield, W.A., and Bacon, C.R., 1981, Geologic map of the Coso Volcanic field and adjacent areas, Inyo County, California: U.S. Geological Survey Miscellaneous Investigations Series Map I-1200, scale 1:50,000.

Duffield, W.A., Bacon, C.R., and Dalrymple, G.B., 1980, Late Cenozoic volcanism, geochronology, and structure of the Coso Range, Inyo County, California: Journal of Geophysical Research, v. 85, p. 2381–2404.

Faulds, J.E., Henry, C.D., and Heinz, N.H., 2005, Kinematics of the northern Walker Lane: An incipient transform fault along the Pacific–North America plate boundary: Geology, v. 33, p. 505–508, doi: 10.1130/G21274.1.

Frankel, K.L., 2007, Fault slip rates, constancy of seismic strain release, and landscape evolution in the eastern California shear zone [Ph.D. dissertation]: Los Angeles, University of Southern California, 179 p.

Frankel, K.L., and Dolan, J.F., 2007, Characterizing arid region alluvial fan surface roughness with airborne laser swath mapping digital topographic data: Journal of Geophysical Research, v. 112, F02025, doi: 10.1029/2006JF000644.

Frankel, K.L., Brantley, K.S., Dolan, J.F., Finkel, R.C., Klinger, R., Knott, J., Machette, M., Owen, L.A., Phillips, F.M., Slate, J.L., and Wernicke, B.P., 2007a, Cosmogenic ^{10}Be and ^{36}Cl geochronology of offset alluvial fans along the northern Death Valley fault zone: Implications for transient strain in the eastern California shear zone: Journal of Geophysical Research, v. 112, B06407, doi: 10.1029/2006JB004350.

Frankel, K.L., Dolan, J.F., Owen, L.A., Finkel, R.C., and Hoeft, J.S., 2007b, Spatial variations in slip rate along the Death Valley–Fish Lake Valley fault system from LiDAR topographic data and cosmogenic ^{10}Be geochronology: Geophysical Research Letters, v. 34, L18303, doi: 10.1029/2007GL030549.

Friedrich, A.M., Wernicke, B.P., and Niemi, N.A., 2003, Comparison of geodetic and geologic data from the Wasatch region, Utah, and implications for the spectral character of Earth deformation at periods of 10 to 10 million years: Journal of Geophysical Research, v. 108, doi: 10.1029/2001JB000682.

Gan, W., Svarc, J.L., Savage, J.C., and Prescott, W.H., 2000, Strain accumulation across the eastern California shear zone at latitude 36°30′N: Journal of Geophysical Research, v. 105, p. 16,229–16,236, doi: 10.1029/2000JB900105.

Gillespie, A.R., 1991, Quaternary subsidence of Owens Valley, California, *in* Hall, C.A., ed., Natural History of eastern California and high-altitude research: Los Angeles, White Mountain Research Station Proceedings, p. 356–382.

Glazner, A.F., Walker, J.D., Bartley, J.M., and Fletcher, J.M., 2002, Cenozoic evolution of the Mojave block of southern California, *in* Glazner, A.F., Walker, J.D., and Bartley, J.M., eds., Geologic evolution of the Mojave Desert and Southwestern Basin and Range: Geological Society of America Memoir 195, p. 19–41.

Glazner, A.F., Lee, J., Bartley, J.M., Coleman, D.S., Kylander-Clark, A., Greene, D.C., and Le, K., 2005, Large dextral offset across Owens Valley, California from 148 Ma to 1872 A.D., *in* Stevens, C., and Cooper, J., eds., Western great basin geology: Fieldtrip guidebook and volume for the joint meeting of the Cordilleran section–GSA and Pacific Section–AAPG, April 29–May 1, 2005, San José, California: Fullerton, California, Pacific Section SEPM (Society for Sedimentary Geology), Book 99, p. 1–35.

Gosse, J.C., and Phillips, F.M., 2001, Terrestrial in situ cosmogenic nuclides: theory and application: Quaternary Science Reviews, v. 20, p. 1475–1560, doi: 10.1016/S0277-3791(00)00171-2.

Greene, D.C., and Stevens, C.H., 2002, Geologic map of Paleozoic rocks in the Mount Morrison pendant, eastern Sierra Nevada, California: California Division of Mines and Geology Map Sheet 53, scale 1:24,000.

Greene, D., Kirby, E., Dawers, N., Phillips, F., McGee, S., and Burbank, D., 2007, Quantifying accommodation of active strain along distributed fault arrays in Owens Valley, California: Geological Society of America Abstracts with Programs, v. 39, no. 6, p. 441.

Guest, B., Niemi, N., and Wernicke, B., 2007, Stateline fault system: A new component of the Miocene-Quaternary Eastern California shear zone: Geological Society of America Bulletin, v. 119, p. 1337–1346, doi: 10.1130B26138.1.

Hauksson, E., and Unruh, J., 2007, Regional tectonics of the Coso geothermal area along the intra-continental plate boundary in central-eastern California: Three-dimensional V_p and V_p/V_S models, spatial-temporal seismicity patterns, and seismogenic strain deformation: Journal of Geophysical Research, v. 112, doi: 10.1029/2006JB004721.

Hearn, E.H., and Humphreys, E.D., 1998, Kinematics of the southern Walker Lane Belt and motion of the Sierra Nevada block, California: Journal of Geophysical Research, v. 103, p. 27,033–27,049, doi: 10.1029/98JB01390.

Humphreys, E.D., and Weldon, R.J., 1994, Deformation across the western United States: A local estimate of Pacific–North America transform deformation: Journal of Geophysical Research, v. 99, p. 19,975–20,010, doi: 10.1029/94JB00899.

Kirby, E., Anandakrishnan, S., Phillips, F., and Marrero, S., 2008, Millennial-scale slip rate along the Owens Valley fault, eastern California: Geophysical Research Letters, v. 35, L01304, doi:10.1029/2007GL031970..

Kirby, E., Burbank, D.W., Reheis, M., and Phillips, F., 2006, Temporal variations in slip rate of the White Mountain Fault Zone: Eastern California: Earth and Planetary Science Letters. v. 248, p. 153–170, doi: 10.1016/j.epsl.2006.05.026

Kistler, R.W., 1993, Mesozoic intrabatholithic faulting, Sierra Nevada, California, *in* Dunne, G.C., and McDougall, K.A., eds., Mesozoic Paleogeography of the Western United States–II: Society for Sedimentary Geology (SEPM), Pacific Section Book 71, p. 247–261.

Klinger, R.E., 2001, Stop A3: Evidence for large dextral offset near Red Wall Canyon, *in* Machette, M.N., Johnson, M.L., and Slate, J.L., eds., Quaternary and late Pliocene geology of the Death Valley region: Recent observations on tectonic, stratigraphic, and lake cycles: U.S. Geological Survey Open-File Report 01-51, p. A32–A37.

Kylander-Clark, A.R.C., 2003, Correlation of Golden Bear and Coso dike sets: Implications for post-Cretaceous offset across Owens Valley, California [M.S. Thesis]: Chapel Hill, University of North Carolina, 105 p.

Kylander-Clark, A.R.C., Coleman, D.S., Glazner, A.F., and Bartley, J.M., 2005, Evidence for 65 km of dextral slip across Owens Valley, California since 83 Ma: Geological Society of America Bulletin, v. 117, p. 962–968, doi: 10.1130/B25624.1.

Le, K., Lee, J., Owen, L.A., and Finkel, R., 2007, Late Quaternary slip rates along the Sierra Nevada frontal fault zone, California: Slip partitioning across the western margin of the Eastern California Shear Zone–Basin and Range Province: Geological Society of America Bulletin, v. 119, p. 240–256, doi: 10.1130/B25960.1.

Lee, J., Rubin, C.M., and Calvert, A., 2001a, Quaternary faulting history along the Deep Springs fault, California: Geological Society of America Bulletin, v. 113, p. 855–869, doi: 10.1130/0016-7606(2001)113<0855:QFHATD>2.0.CO;2.

Lee, J., Spencer, J., and Owen, L., 2001b, Holocene slip rates along the Owens Valley fault, California: Implications for the recent evolution of the eastern California shear zone: Geology, v. 29, p. 819–822, doi: 10.1130/0091-7613(2001)029<0819:HSRATO>2.0.CO;2.

Lonsdale, P., 1991, Structural patterns of the Pacific floor offshore of Peninsular California, *in* Dauphin, J.P., and Simoneit, B.R.T., eds., The Gulf and Peninsular Province of California: AAPG Memoir, v. 47, p. 87-125.

Loomis, D.P., 1984, Miocene stratigraphy and tectonic evolution of the El Paso Basin, California: [M.S. Thesis]: Chapel Hill, University of North Carolina, 172 p.

Loomis, D.P., and Burbank, D.W., 1988, The stratigraphic evolution of the El Paso basin, southern California: Implications for the Miocene development of the Garlock fault and uplift of the Sierra Nevada: Geological Society of America Bulletin, v. 100, p. 12–28, doi: 10.1130/0016-7606(1988)100<0012:TSEOTE>2.3.CO;2.

Lubetkin, L.K.C., and Clark, M.M., 1988, Late Quaternary activity along the Lone Pine fault, eastern California: Geological Society of America Bulletin, v. 100, p. 755–766, doi: 10.1130/0016-7606(1988)100<0755:LQAATL>2.3.CO;2.

Mahan, K.H., Bartley, J.M., Coleman, D.S., Glazner, A.F., and Carl, B.S., 2003, Sheeted intrusion of the synkinematic McDoogle pluton, Sierra Nevada, California: Geological Society of America Bulletin, v. 115, p. 1570–1582, doi: 10.1130/B22083.1.

Malservisi, R., Furlong, K.P., and Dixon, T.H., 2001, Influence of the earthquake cycle and lithospheric rheology on the dynamics of the Eastern California shear zone: Geophysical Research Letters, v. 28, p. 2731–2734, doi: 10.1029/2001GL013311.

Martel, S.J., Harrison, T.M., and Gillespie, A.R., 1987, Late Quaternary vertical displacement across the Fish Springs fault, Owens Valley fault zone, California: Quaternary Research, v. 27, p. 113–129, doi: 10.1016/0033-5894(87)90071-8.

McClusky, S.C., Bjornstad, S.C., Hager, B.H., King, R.W., Meade, B.J., Miller, M.M., Monastero, F.C., and Souter, B.J., 2001, Present day kinematics of the eastern California shear zone from a geodetically constrained block model: Geophysical Research Letters, v. 28, p. 3369–3372, doi: 10.1029/2001GL013091.

McGill, S.F., and Sieh, K., 1991, Surficial offsets on the central and eastern Garlock fault associated with prehistoric earthquakes: Journal of Geophysical Research, v. 96, p. 21,597–21,621.

McGill, S.F., and Sieh, K., 1993, Holocene slip rate of the central Garlock fault in southeastern Searles Valley, California: Journal of Geophysical Research, v. 98, p. 14,217–14,231.

McKee, E.H., 1968, Age and rate of movement of the northern part of the Death Valley–Furnace Creek fault zone: Geological Society of America Bulletin, v. 79, p. 509–512, doi: 10.1130/0016-7606(1968)79[509:AAROMO]2.0.CO;2.

McKenna, L.W., and Hodges, K.V., 1990, Constraints on the kinematics and timing of late Miocene–Recent extension between the Panamint and Black Mountains, southeastern California, *in* Wernicke, B.P., ed., Tertiary extensional tectonics near the latitude of Las Vegas: Geological Society of America Memoir 176, p. 363–376.

Miller, M.M., Johnson, D.J., Dixon, T.H., and Dokka, R.K., 2001, Refined kinematics of the eastern California shear zone from GPS observations, 1993–1994: Journal of Geophysical Research, v. 106, p. 2245–2263, doi: 10.1029/2000JB900328.

Monastero, F.C., and Unruh, J.R., 2002, Definition of the brittle-plastic transition in the Coso geothermal field, east-central California, USA: EAGE 64th Conference and Exhibition, Florence, Italy, May 27–30.

Monastero, F.C., Sabin, A.E., and Katzenstein, A.M., 1994, Middle to late Miocene age stratovolcano on the South Ranges, Naval Air Weapons Station, San Bernardino County, California: Geological Society of America Cordilleran Section Guidebook 27, p. 293–301.

Monastero, F.C., Sabin, A.E., and Walker, J.D., 1997, Evidence for post-early Miocene initiation of movement on the Garlock fault from offset of the Cudahy Camp Formation, east-central California: Geology, v. 25, p. 247–250, doi: 10.1130/0091-7613(1997)025<0247:EFPEMI>2.3.CO;2.

Monastero, F.C., Walker, J.D., Katzenstein, A.K., and Sabin, A.E., 2002, Neogene evolution of the Indian Wells Valley, east-central California, *in* Glazner, A.F., Walker, J.D., and Bartley, J.M., eds., Geologic evolution of the Mojave Desert and Southwestern Basin and Range: Geological Society of America Memoir 195, p. 199–228.

Monastero, F.C., Katzenstein, A.M., Miller, J.S., Unruh, J.R., Adams, M.C., and Richards-Dinger, K., 2005, The Coso geothermal field: a nascent metamorphic core complex: Geological Society of America Bulletin, v. 117, p. 1534–1553, doi: 10.1130/B25600.1.

Moore, J.G., 1963, Geology of the Mount Pinchot quadrangle, southern Sierra Nevada, California: U.S. Geological Survey Bulletin 1130, 152 p.

Moore, J.G., 1981, Geologic map of the Mount Whitney quadrangle, Inyo and Tulare Counties, California: U.S. Geological Survey Map GQ-1012, scale 1:62,500.

Moore, J.G., and Hopson, C.A., 1961, The Independence dike swarm in eastern California: American Journal of Science, v. 259, p. 241–259.

Neponset Geophysical Corporation and Aquila Geosciences, 1997, Phase 3 and Phase 4 Seismic Program, Owens Lake, Inyo County, California: Bishop, California, Final Report prepared for Great Basin Unified Air Pollution Control District, 146 p.

Niemi, N.A., Wernicke, B.P., Brady, R.J., Saleeby, J.B., and Dunne, G.C., 2001, Distribution and provenance of the middle Miocene Eagle Mountain Formation, and implication for regional kinematic analysis of the Basin and Range province: Geological Society of America Bulletin, v. 113, p. 419–442, doi: 10.1130/0016-7606(2001)113<0419:DAPOTM>2.0.CO;2.

Oldow, J.S., Kohler, G., and Donelick, R.A., 1994, Late Cenozoic extensional transfer in the Walker Lane strike-slip belt, Nevada: Geology, v. 22, p. 637–640, doi: 10.1130/0091-7613(1994)022<0637:LCETIT>2.3.CO;2.

Oskin, M., and Iriondo, A., 2004, Large-magnitude transient strain accumulation on the Blackwater fault, Eastern California shear zone: Geology, v. 32, p. 313–316, doi: 10.1130/G20223.1.

Oskin, M., Perg, L., Shelef, E., Strane, M., Gurney, E., Blumentritt, D., Mukhopadhyay, S., Iriondo, A., 2006: Geologic fault slip rates support transitory, elevated geodetic strain accumulation across the Mojave Desert, Eastern California shear zone: Eos (Transactions, American Geophysical Union), v. 87, Abstract G43B-0992.

Oskin, M., Perg, L., Blumentritt, D., Mukhopadhyay, S., and Iriondo, A., 2007, Slip rate of the Calico fault: Implications for geologic versus geodetic rate discrepancy in the eastern California shear zone: Journal of Geophysical Research, v. 112, B03402, doi: 10.1029/2006JB004451.

Oswald, J.A., and Wesnousky, S.A., 2002, Neotectonics and Quaternary geology of the Hunter Mountain fault zone and Saline Valley region, south-

eastern California: Geomorphology, v. 42, p. 255–278, doi: 10.1016/S0169-555X(01)00089-7.

Peltzer, G., Crampe, F., Hensley, S., and Rosen, P., 2001, Transient strain accumulation and fault interaction in the eastern California shear zone: Geology, v. 29, p. 975–978, doi: 10.1130/0091-7613(2001)029<0975:TSAAFI>2.0.CO;2.

Ratajeski, K., Glazner, A.F., and Miller, B.V., 2001, Geology and geochemistry of mafic and felsic plutonic rocks in the Cretaceous intrusive suite of Yosemite Valley, California: Geological Society of America Bulletin, v. 113, p. 1486–1502, doi: 10.1130/0016-7606(2001)113<1486:GAGOMT>2.0.CO;2.

Reasenberg, P., Ellsworth, W., and Walter, A., 1980, Teleseismic evidence for a low-velocity body under the Coso geothermal resource area: Journal of Geophysical Research, v. 85, p. 2471–2483.

Reheis, M.C., and Dixon, T.H., 1996, Kinematics of the Eastern California shear zone: Evidence for slip transfer from Owens and Saline Valley fault zones to Fish Lake Valley fault zone: Geology, v. 24, p. 339–342, doi: 10.1130/0091-7613(1996)024<0339:KOTECS>2.3.CO;2.

Reheis, M.C., and Sawyer, T.L., 1997, Late Cenozoic history and slip rates of the Fish Lake Valley, Emigrant Peak, and Deep Springs fault zones, Nevada and California: Geological Society of America Bulletin, v. 109, p. 280–299, doi: 10.1130/0016-7606(1997)109<0280:LCHASR>2.3.CO;2.

Reheis, M.C., Sawyer, T.L., Slate, J.L., and Gillespie, A.R., 1993, Geologic map of late Cenozoic deposits and faults in the southern part of the Davis Mountain 15′ quadrangle, Esmeralda County, Nevada: U.S. Geological Survey Map I-2342, scale 1:24,000.

Reheis, M.C., Slate, J.L., and Sawyer, T.L., 1995, Geologic map of late Cenozoic deposits and faults in parts of the Mt. Barcroft, Piper Peak, and Soldier Pass 15′ quadrangles, Esmeralda County, Nevada, and Mono County, California: U.S. Geological Survey Map I-2464, scale 1:24,000.

Rockwell, T.K., Lindvall, S., Herzberg, M., Murbach, D., Dawson, T., and Berger, G., 2000, Paleoseismology of the Johnson Valley, Kickapoo, and Homestead Valley faults: Clustering of earthquakes in the eastern California shear zone: Bulletin of the Seismological Society of America, v. 90, p. 1200–1236, doi: 10.1785/0119990023.

Rockwell, T., Seitz, G., Dawson, T., and Young, J., 2006, The long record of San Jacinto fault paleoearthquakes at Hog Lake: Implications for regional patterns of strain release in the southern San Andreas fault system: Seismological Research Letters, v. 77, p. 270.

Ross, D.C., 1962, Correlation of granitic plutons across faulted Owens Valley, California: U.S. Geological Survey Professional Paper 450-D, p. D86–D88.

Ross, D.C., 1965, Geology of the Independence quadrangle, Inyo County, California: U.S. Geological Survey Bulletin B1181-O, p. O1–O64.

Saleeby, J.B., Kistler, R.W., Longiaru, S., Moore, J.G., and Nokleberg, W.J., 1990, Middle Cretaceous silicic metavolcanic rocks in the Kings Canyon area, central Sierra Nevada, California, *in* Anderson, J.L., ed., The nature and origin of Cordilleran magmatism: Geological Society of America Memoir 174, p. 251–270.

Sarna-Wojcicki, A.M., Pringle, M.S., and Wijbrans, J., 2000, New $^{40}Ar/^{39}Ar$ age of the Bishop Tuff from multiple sites and sediment rate calibration for the Matuyama-Brunhes boundary: Journal of Geophysical Research, v. 105, p. 21,431–21,443, doi: 10.1029/2000JB900091.

Sauber, J., Thatcher, W., Solomon, S.C., and Lisowski, M., 1994, Geodetic slip rate for the eastern California shear zone and the recurrence time of Mojave desert earthquakes: Nature, v. 367, p. 264–266, doi: 10.1038/367264a0.

Savage, J.C., and Lisowski, M., 1980, Deformation in Owens Valley, California: Bulletin of the Seismological Society of America, v. 70, p. 1225-1232.

Savage, J.C., and Lisowski, M., 1995, Strain accumulation in Owens Valley, California, 1974 to 1988: Bulletin of the Seismological Society of America, v. 85, p. 151–158.

Savage, J.C., Lisowski, M., and Prescott, W.H., 1990, An apparent shear zone trending north-northwest across the Mojave Desert into Owens Valley, California: Geophysical Research Letters, v. 17, p. 2113–2116.

Slemmons, D.B, Vittori, E., Jayko, A.S., Carver, G.A., and Bacon, S.N., 2008, Quaternary fault and lineament map of Owens Valley, Inyo County, eastern California: Geological Society of America Map and Chart 96, scale 1:100.000, 2 plates, 25 p. text.

Smith, E.I., Sanchez, A., Keenan, D.L., and Monastero, F.C., 2002, Stratigraphy and geochemistry of the volcanic rocks in the Lava Mountain, California: Implications for the Miocene development of the Garlock fault, *in* Glazner, A.F., Walker, J.D., and Bartley, J.M., eds., Geologic evolution of the Mojave Desert and Southwestern Basin and Range: Geological Society of America Memoir 195, p. 151–160.

Stevens, C.H., and Greene, D.C., 1999, Stratigraphy, depositional history, and tectonic evolution of Paleozoic continental-margin rocks in roof pendants of the eastern Sierra Nevada, California: Geological Society of America Bulletin, v. 111, p. 919–933, doi: 10.1130/0016-7606(1999)111<0919:SDHATE>2.3.CO;2.

Stevens, C.H., Stone, P., Dunne, G.C., Greene, D.C., Walker, J.D., and Swanson, B.J., 1997, Paleozoic and Mesozoic evolution of east-central California: International Geology Review, v. 39, p. 788-829.

Stevens, C.H., Stone, P., Dunne, G.C., Greene, D.C., Walker, J.D., and Swanson, B.J., 1998, Paleozoic and Mesozoic evolution of east-central California, *in* Ernst, W.G., and Nelson, C.A., eds., Integrated Earth and environmental evolution of the southwestern United States, The Clarence A. Hall, Jr., Volume: Boulder, Colorado, Geological Society of America International Book Series 1, p. 119–160.

Stevens, C.H., Stone, P., and Greene, D.C., 2003, Correlation of Permian and Triassic deformations in the western Great Basin and eastern Sierra Nevada: Evidence from the northern Inyo Mountains near Tinemaha Reservoir, east-central California: Geological Society of America Bulletin, v. 115, p. 1309–1311, doi: 10.1130/B25385D.1.

Stewart, J.H., 1967, Possible large right-lateral displacement along fault and shear zones in the Death Valley–Las Vegas area, California and Nevada: Geological Society of America Bulletin, v. 78, p. 131–142, doi: 10.1130/0016-7606(1967)78[131:PLRDAF]2.0.CO;2.

Strane, M.D., 2007, Slip rate and structure of the nascent Lenwood fault zone, Eastern California [M.S. Thesis]: Chapel Hill, University of North Carolina, 55 p.

Stockli, D.F., Dumitru, T.A., McWilliams, M.O., and Farley, K.A., 2003, Cenozoic tectonic evolution of the White Mountains, California and Nevada: Geological Society of America Bulletin, v. 115, p. 788–816, doi: 10.1130/0016-7606(2003)115<0788:CTEOTW>2.0.CO;2.

Sullivan, W.A., and Law, R.D., 2007, Deformation path partitioning within the transpressional White Mountain shear zone, California and Nevada: Journal of Structural Geology, v. 29, p. 583–599, doi: 10.1016/j.jsg.2006.11.001.

Thatcher, W., Foulger, G.R., Julian, B.R., Svarc, J., Quilty, E., and Bawden, G.W., 1999, Present-day deformation across the Basin and Range province, western United States: Science, v. 283, p. 1714–1718, doi: 10.1126/science.283.5408.1714.

Thompson, R.A., Milling, M.E., Fleck, R.J., Wright, L.A., and Roger, N.W., 1993, Temporal, spatial, and compositional constraints on volcanism associated with large-scale crustal extension in central Death Valley, California: Eos (Transactions, American Geophysical Union), v. 74, p. 624.

Troxel, B.W., 1994, Right-lateral offset of ca. 28 km along a strand of the southern Death Valley fault zone, California: Geological Society of America Abstracts with Programs, v. 26, no. 6, p. 99.

Unruh, J.R., Hauksson, E., Monastero, F.C., Twiss, R.J., and Lewis, J.C., 2002, Seismotectonics of the Coso Range–Indian Wells Valley region, California: Transtensional deformation along the southeastern margin of the Sierran microplate, *in* Glazner, A.F., Walker J.D., and Bartley, J.M., eds., Geologic evolution of the Mojave Desert and Southwestern Basin and Range: Geological Society of America Memoir 195, p. 277–294.

Unruh, J.R., Humphrey, J., and Barron, A., 2003, Transtensional model for the Sierra Nevada frontal fault system, eastern California: Geology, v. 31, p. 327–330, doi: 10.1130/0091-7613(2003)031<0327:TMFTSN>2.0.CO;2.

Unruh, J.R., Monastero, F.C., and Pullammanappallil, S.K., 2008, The nascent Coso metamorphic core complex, east-central California: Brittle upper plate structure revealed by reflection seismic data: International Geology Review (in press).

Vines, J.A., 1999, Emplacement of the Santa Rita Flat pluton and kinematic analysis of cross-cutting shear zones, eastern California [M.S. Thesis]: Blacksburg, Virginia Polytechnic Institute and State University, 89 p.

Walker, J.D., and Whitmarsh, R.W., 1998, A tectonic model for the Coso geothermal area: U.S. Department of Energy Proceedings Geothermal Program Review XVI, April 1–2, Berkeley, California, p. 2-17–2-24.

Weldon, R., Scharer, K., Fumal, T., and Biasi, G., 2004, Wrightwood and the earthquake cycle: What a long recurrence record tells us about how faults work: GSA Today, v. 14, no. 9, p. 4–10, doi: 10.1130/1052-5173(2004)014<4:WATECW>2.0.CO;2.

Wells, S.G., McFadden, L.D., and Dohrenwend, J.C., 1987, Influence of late Quaternary climatic changes on a desert piedmont, eastern Mojave desert, California: Quaternary Research, v. 27, p. 130–146, doi: 10.1016/0033-5894(87)90072-X.

Wernicke, B., Axen, G.J., and Snow, J.K., 1988, Basin and Range extensional tectonics at the latitude of Las Vegas, Nevada: Geological Society of America

Bulletin, v. 100, p. 1738–1757, doi: 10.1130/0016-7606(1988)100<1738:BARETA>2.3.CO;2.

Wernicke, B., Davis, J.L., Bennett, R.A., Normandeau, J.E., Friedrich, A.M., and Niemi, N.A., 2004, Tectonic implications of a dense continuous GPS velocity field at Yucca Mountain, Nevada: Tectonics, v. 109, doi: 10.1029/2003JB002832.

Wesnousky, S.G., 2005, The San Andreas and Walker Lane fault systems, western North America: transpression, transtension, cumulative slip and the structural evolution of a major transform plate boundary: Journal of Structural Geology, v. 27, p. 1505–1512, doi: 10.1016/j.jsg.2005.01.015.

Wesnousky, S.G., and Jones, C.H., 1994, Oblique slip, slip partitioning, spatial and temporal changes in the regional stress field, and the relative strength of active faults in the Basin and Range, western United States: Geology, v. 22, p. 1031–1034, doi: 10.1130/0091-7613(1994)022<1031:OSSPSA>2.3.CO;2.

Whistler, D.P., and Burbank, D.W., 1992, Miocene biostratigraphy and biochronology of the Dove Spring Formation, Mojave Desert, California, and characterization of the Clarendonian mammal age (late Miocene) in California: Geological Society of America Bulletin, v. 104, p. 644–658, doi: 10.1130/0016-7606(1992)104<0644:MBABOT>2.3.CO;2.

Whitmarsh, R.W., 1998, Geologic map of the Coso Range: Geological Society of America Online Map Series, scale 1:24,000, doi:10.1130/1998-whitmarsh-coso.

Wilson, C.K., Jones, C.H., and Gilbert, H.J., 2003, Single-chamber silicic magma system inferred from shear wave discontinuities of the crust and uppermost mantle, Coso geothermal area, California: Journal of Geophysical Research, v. 108, doi: 10.1029/2003.

Wood, D.J., and Saleeby, J.B., 1997, Late Cretaceous–Paleocene extensional collapse and disaggregation of the southernmost Sierra Nevada Batholith: International Geology Review, v. 39, p. 973–1009.

Zehfuss, P.H., Bierman, P.R., Gillespie, A.R., Burke, R.M., and Caffee, M.W., 2001, Slip rates on the Fish Springs Fault, Owens Valley, California, deduced from cosmogenic ^{10}Be and ^{26}Al and soil development on fan surfaces: Geological Society of America Bulletin, v. 113, no. 2, p. 241–255, doi: 10.1130/0016-7606(2001)113<0241:SROTFS>2.0.CO;2.

Manuscript Accepted by the Society 18 January 2008